IDENTIFYING A NOVEL VULNERABILITY AT THE INTERSECTION OF COPPER HOMEOSTASIS AND GLYCOLYTIC METABOLISM IN HEPATOCELLULAR CARCINOMA

Caroline Ines Davis

A DISSERTATION

in

Biochemistry and Molecular Biophysics

Presented to the Faculties of the University of Pennsylvania

in

Partial Fulfillment of the Requirements for the

Degree of Doctor of Philosophy

2020

Supervisor of Dissertation

_____

Donita C. Brady, Ph.D.

Presidential Professor of Cancer Biology

Graduate Group Chairperson

_____

Kim A. Sharp, Ph.D.

Associate Professor of Biochemistry and Biophysics

Dissertation Committee

Chi V. Dang, M.D., Ph.D., Professor of The Wistar Institute Cancer Center

Kathryn E. Wellen, Ph.D., Associate Professor of Cancer Biology

Luca Busino, Ph.D., Assistant Professor of Cancer Biology

Ronen Marmorstein, Ph.D., George W. Raiziss Professor of Biochemistry and Biophysics

I would like to dedicate this thesis to my parents, María Fernandez and Tomas Davis.

ACKNOWLEDGMENT

Firstly, I would like to thank my thesis advisor Donita C. Brady for all of her guidance, mentorship, and support throughout my graduate career. Donita has provided so much wonderful advice and feedback on my experiments, study designs, posters, presentations, and writing over the years. Most importantly, she has given me the freedom to follow my intellectual curiosity and encouraged me to “follow where the science takes you”. I am so thankful for my thesis committee members, Ronen Marmorstein, Kathryn Wellen, Luca Busino, and Chi Van Dang, who are scientific superstars that provided many guiding thoughts for my projects. Each of you was an expert in your respective field, and being able to host all of you in one room during every committee meeting really enriched my graduate experience. I would like to thank my lab mates for all of their scientific and non-scientific support through the years. I would like to acknowledge all of my dearest friends and family for being there during the ups, downs, twists, and turns of graduate school life. Lastly, I would like to thank my parents, twin sister, and fiancé, Maria, Tom, Julianne, and Ross, for all of their love, encouragement, and support during my graduate studies.

ABSTRACT

IDENTIFYING A NOVEL VULNERABILITY AT THE INTERSECTION OF COPPER HOMEOSTASIS AND GLYCOLYTIC METABOLISM IN HEPATOCELLULAR CARCINOMA

Caroline I. Davis

Dr. Donita C. Brady

Hepatocellular carcinoma (HCC), the most common primary liver cancer, of which ~800,000 new cases will be diagnosed worldwide this year, portends a five-year survival rate of merely 17% in patients with unresectable disease. This dismal prognosis is due, at least in part, from the late stage of diagnosis and the limited efficacy of systemic therapies. As a result, there is an urgent need to identify risk factors that contribute to HCC initiation and provide targetable vulnerabilities to improve patient survival. While myriad risk factors are known, elevated copper (Cu) levels in HCC patients and the incidence of hepatobiliary malignancies in Wilson disease patients, which exhibit hereditary liver Cu overload, suggests the possibility that metal accumulation promotes malignant transformation. Here we found that expression of the Cu transporter genes *ATP7A*, *ATP7B*, *SLC31A1*, and *SLC31A2* were significantly altered in liver cancer samples and were associated with elevated Cu levels in liver cancer tissue and cells. Further analysis of genomic copy number data revealed that alterations in Cu transporter gene loci correlates with poorer survival in HCC patients. Genetic loss of the Cu importer *SLC31A1* (*CTR1*) or pharmacologic suppression of Cu decreased the viability, clonogenic survival, and anchorage-independent growth of human HCC cell lines. Mechanistically, *CTR1* knockdown or Cu chelation decreased glycolytic gene expression and downstream metabolite utilization and as a result forestall tumor cell survival after exposure to hypoxia, which mimics oxygen deprivation elicited by transarterial embolization, a standard-of-care therapy used for patients with unresectable HCC. Taken together, these findings established an association between altered Cu homeostasis and HCC and suggest that limiting Cu bioavailability may provide a new treatment strategy for HCC by restricting the metabolic reprogramming necessary for cancer cell survival.

TABLE OF CONTENTS

LIST OF ILLUSTRATIONS

CHAPTER 1: INTRODUCTION TO HEPATOCELLULAR CARCINOMA AND COPPER HOMEOSTASIS

Overview

Hepatocellular carcinoma is the most prevalent type of liver cancer that is typically discovered at an advanced stage of disease. Several risk factors influence both the onset and progression of this malignancy. Importantly, the liver serves as a nexus for multiple metabolic processes, from metal homeostasis to lipid synthesis. In this chapter, we will present background information about hepatocellular carcinoma and consider the relevance of copper (Cu) homeostasis in this pathology. Accordingly, Cu chelation therapy will also be discussed as a suitable treatment modality for various disease contexts. Understanding that healthy liver generates an oxygen gradient as blood circulates from the hepatic artery to the portal vein, and that a similar oxygen gradient exists within the tumor microenvironment, the fundamentals of hypoxia and HIF signaling will also be reviewed. Building upon these principles, the Cu dependencies that arise from a lack of oxygenation will be discussed in detail. Taken together, this chapter will provide the pertinent background information critical to connecting cancer metabolism to Cu dyshomeostasis in hepatocellular carcinoma.

Introduction to Hepatocellular Carcinoma and Liver Metabolism

Hepatocellular Carcinoma (HCC) as a Liver Cancer Subtype

Approximately 43,000 Americans will receive diagnoses of liver & intrahepatic bile duct cancer this year, while nearly 30,000 Americans will succumb to this disease. Although trends indicate an improvement from recent years, the five-year relative survival rate is approximately 18%, increasing only to 33% when considering localized

cases alone (Siegel et al., 2020). Primary liver cancer is broadly defined as cancer that originates from the liver, and can be further categorized into the following distinct subtypes: angiosarcoma, hepatoblastoma, cholangiocarcinoma, and hepatocellular carcinoma. Angiosarcoma is a rare, aggressive form of liver cancer that develops from the endothelial cells that constitute the inner lining of blood vessels within the liver (Gaballah et al., 2017). Like angiosarcoma, hepatoblastoma is another rare form of liver cancer that affects mainly children and is thought to be an outcome of inherited syndromes, congenital anomalies, and uncommon risk factors (Spector & Birch, 2012). In contrast, cholangiocarcinoma, also referred to as bile duct cancer, represents between 10-20% of newly diagnosed liver cancers in the US, and arises from epithelial cells that the line bile ducts which surround the liver (Razumilava & Gores, 2014; Rizvi et al., 2018). The last subtype, hepatocellular carcinoma (HCC), constitutes the greater remainder of liver cancer cases as it accounts for nearly 75% of new diagnoses (Siegel et al., 2020). Unfortunately, most HCC cases are diagnosed at late stage due to asymptomatic progression in early stages and to a lack of surveillance for populations at risk (Sanyal et al., 2010; Simmons et al., 2019). Therefore, considering the relatively high incidence of disease, poor prognosis, and frequency of recurrence, we decided to focus our attention to this form of liver cancer.

Briefly, genetic lineage tracing suggests that HCC arises from hepatocytes (Mu et al., 2015). These cells comprise the majority, more than 70%, of all cells in the liver and carry out many intricate processes, including glycogenolysis, glycolysis, gluconeogenesis, and lipogenesis, depending on their lobular location (Linden et al., 2018; Si-Tayeb et al., 2010). Compared to other organs of the digestive tract, the liver is relatively quiescent as the turnover time for liver parenchyma is around 8-12 months (Alison & Lin, 2011; Furuyama et al., 2011). Although fully differentiated hepatocytes

maintain the ability to regenerate the liver for normal homeostatic activities, these cells may divide upon acute injury or stress stimuli (Malato et al., 2011). Interestingly, when damaged hepatocytes are unable to replicate, hepatocyte progenitor cells (HPCs) may serve as a reservoir of fresh cells. Importantly, recent studies indicate that the oncogenic status and type of stress imposed will dictate the propensity of hepatocytes to form HCCs, as well as the fate of HPCs to form benign lesions (Tummala et al., 2017). Understanding that different stressors initiate different genetic alterations that propagate tumorigenesis, it is imperative to discuss the pre-existing conditions and mutations associated with HCC.

Underlying Risk-Factors and Mutational Status in HCC

Understanding that the five-year survival rate decreases with increasing tumor size and stage, examining the underlying etiologies and subsequent changes in genetic landscape is pivotal to navigating treatment regimens (G. Wu et al., 2018). Importantly, HCC tends to develop from cirrhosis that arises due to chronic necroinflammation linked to several risk factors (**Fig 1.1**). Chronic viral hepatitis infections are the most common pre-existing conditions observed in HCC patients worldwide. Hepatitis B Virus (HBV) is most prevalent in Asian and African countries, representing nearly 70% of all HCC patients, while Hepatitis C Virus (HCV) is more common in Western nations (H. seok Kim & El-Serag, 2019; Torre et al., 2015). Interestingly, aflatoxin exposure or HBV-HCV co-infection amplify the risk of developing HCC (Qian et al., 1994; Zampino et al., 2015). Although viral etiologies are major contributors to the global incidence of HCC, the presence of alcoholic and non-alcoholic fatty liver disease (NAFLD) that prelude HCC continue to rise in the United States (D. L. White et al., 2017). Because major factors that comprise metabolic syndrome promote the progression to NAFLD, the increase in

NAFLD-associated HCC may be explained by the parallel increased prevalence of obesity and type II diabetes in adults (Palmer & Toth, 2019). While less commonly observed, Wilson Disease (WD), which is characterized by aberrant liver Cu accumulation resulting from genetic alterations in the *ATP7B* gene, constitutes an additional predisposing factor that influences HCC pathogenesis (Reyes, 2008).

To complement the etiological factors underlying HCC, the mutational landscape associated with these specific etiologies may be useful in uncovering molecular mechanisms. Notably, a gene expression profiling study revealed that G→T substitutions are the most frequently observed mutations in HCC patients (Guichard et al., 2012). However, for alterations to the telomerase reverse transcriptase (TERT) promoter observed in nearly half of analyzed HCC tissue samples- many of which have an underlying HBV infection- G→A mutations are often observed (Nault et al., 2013; Totoki et al., 2014). These nucleotide changes provide sites for E-twenty-six transcription factor binding, and thus, drive the enhancement of TERT expression. Other frequently mutated genes are the DNA-binding tumor suppressor *TP53* and the gene encoding the cell-cell adhesion protein β-catenin, *CTNNB1.* In HCC, most mutations to *TP53* are missense mutations that reduce DNA binding capabilities, while mutations to *CTNNB1* usually result in constitutive activation of β-catenin to augment tumor invasiveness (J. S. Lee, 2015). Even though these genes are often associated with HBV or HCV infection in a background of cirrhosis, their mutations are almost always mutually exclusive (Ahn et al., 2014). Lastly, loss-of-function or frame-shift mutants of *ARID1A* and *ARID2*, chromatin remodeling factors within the AT-rich interaction domain family, represent more than 10% of the HCC mutational landscape and appear in patients with a chronic HCV infection (J. S. Lee, 2015). These remodeling factors are part of an essential complex that regulates DNA accessibility through the insertion of histone

protomers, and thus, loss of function impedes activity of downstream transcriptional or DNA repair machinery (Lin et al., 2014). Although mutational status is helpful to informing therapeutic decisions, changes between the metabolism of normal liver and that in HCC must also be considered.

Glycolytic Metabolism in Healthy Liver and HCC Contexts

Since the liver serves as a central hub for several homeostatic processes, it is not surprising that metabolic rewiring occurs to favor cancer cell survival. Under physiological conditions, the liver is responsible for the catabolism and anabolism of lipids, amino acids, and carbohydrates. More specifically, *de novo* lipogenesis, cholesterol synthesis, β-oxidation, protein synthesis, gluconeogenesis, and glycolysis all occur within the liver (De Matteis et al., 2018). While lipid and amino acid metabolism are also hijacked during tumorigenesis, reprogramming of glucose metabolism is arguably the most crucial pathway in driving HCC proliferation and survival. Specifically, the breakdown of glucose through glycolysis produces pyruvate, which may be converted to lactate or channeled towards the tricarboxylic acid (TCA) cycle for ATP production and fatty acid synthesis. Furthermore, glycolytic intermediates serve as branch points to other metabolic pathways, such as the pentose phosphate pathway or serine biosynthesis pathway, that are pivotal in replenishing intracellular redox potential, providing nucleotide precursors, and generating substrates for post-translational modifications (Lewis et al., 2014; Pacold et al., 2016). In normal physiology, hepatocytes maintain a balance between glycolysis and gluconeogenesis by adjusting fluxes in response to fed or fasted states. However, to support the overall increase in metabolic demand of rapidly proliferating cells, HCCs favor a characteristic shared amongst many

cancer types: a unidirectional flux through glycolysis to result in increased glucose uptake and lactate production (De Berardinis & Chandel, 2016).

To drive flux through glycolysis, alterations in protein expression manifest and subsequently distinguish HCC from normal hepatocytes. Notably, the glucose uptake transporter, GLUT1, is the main form expressed in HCC. This expression contrasts the isoform that is typically observed in hepatocytes: the bidirectional glucose transporter GLUT2 (Karim et al., 2012). To breakdown glucose through the first commitment step, there is a concomitant upregulation in the high-affinity glucose kinase Hexokinase 2 and suppression of the low-affinity isoform Hexokinase 4 (Guzman et al., 2015). A similar shift from aldolase B to aldolase A is observed further downstream (Castaldo et al., 2000; Y. Wang et al., 2011). Lastly, a switch from the pyruvate kinase liver isoform (PKL) to the pyruvate kinase muscle isoform 2 (PKM2) and elevated LDHA expression solidify the conversion to lactate and simultaneous regeneration of NAD^+ (C. C.-L. Wong et al., 2014). Moreover, to accompany the upregulation of these glycolytic enzymes, suppression of key gluconeogenic enzymes, particularly fructose-1,6-bisphosphatase and phosphoenolpyruvate carboxykinase, further promote unidirectional flux through glycolysis by restricting the reverse flux towards gluconeogenesis (B. Wang et al., 2012). Taken together, HCC cells establish genetic adaptations that modify the flux of metabolites, particularly glycolytic metabolites, to propagate and sustain hepatocarcinogenesis.

Collectively, the mutational landscape, underlying etiologies, and metabolic alterations form a triad of factors that are imperative to generating and improving HCC therapies, as current treatments often incite an aggressive relapse or recurrence.

Current Diagnostics & Therapies for HCC Patients

In order to select the appropriate treatment modality, a clear diagnosis must be established by integrating a combination of clinical, radiological, and laboratory procedures. Since early stages of HCC malignancy are often asymptomatic, most patients display signs of disease only after progressing to advanced stage. Simple clinical presentations include erythrocytosis, thrombocytosis, dyspnea, hypoglycemia, and jaundice due to obstruction generated by the tumor (Attwa & El-Etreby, 2015). To dissect clinical symptoms, physicians must select the appropriate image-guided modality (**Fig 1.2**). Radiologically, an abdominal ultrasound is generally the first line in HCC detection, as it is used during routine surveillance for patients with a background of cirrhosis. This method has the capacity to detect suspicious lesions less than 1 cm in size (Bhosale et al., 2006). For pronounced tumors, hepatic arteriography is the image modality that has the optimal sensitivity and accuracy for highlighting patterns of vascularization within tumors between the sizes of two to five centimeters (Ikeda et al., 1994; Ohki et al., 2013). Alternatively, multiphase perfusion computed tomography takes advantage of contrast dye phasing to determine location of tumors, and hence, is most appropriate for patients that have undergone loco-regional therapy (Bruix et al., 2001). Despite reasonable sensitivity, selectivity, and accuracy of the previously mentioned radiological image modalities, occasionally images lack a well-defined consensus. In such cases, physicians may recommend a percutaneous liver biopsy to clarify poorly resolved masses (Heimbach et al., 2018). With a significant elevation of alpha-fetoprotein and Dickkopf-1 displayed in the serum signature of numerous HCC patients, laboratory exams provide evidence to support a primary diagnosis, and thus, should also be implemented during the course of treatment (Shen et al., 2012; Vibert et

al., 2010). Additionally, pathological scoring procedures are implemented to determine the stage of the disease and inform the choice of therapy. In practice, clinicians use the Barcelona Clinic Liver Cancer staging system to evaluate the size and location of liver tumors, and to determine the extent to which HCC has affected liver function and the patient's overall well-being (Heimbach et al., 2018). Upon completion of clinical, radiological, and laboratory analysis, a confirmed diagnosis requires a discussion surrounding treatment options.

Treatment interventions at early stage disease include curative procedures such as surgical resection or orthotopic liver transplantation (OLT). Importantly, morphological selection parameters governed by the Milan criteria dictate whether a patient is an appropriate candidate for OLT or surgery (Mazzaferro et al., 1996). However, OLT may not be feasible due to donor shortages or intolerance of immunosuppressants, while surgical resection is not appropriate for patients with multiple or large tumors. In specific cases where the patient displays early stage HCC but is not a candidate for OLT or resection, hepatologists may recommend either radio, cryo, or microwave ablation. During radiofrequency ablation, tumor tissue electrodes are inserted locally to destroy tumor tissue and achieve clean margins upon heating to 55°C (Lencioni & Crocetti, 2007). This technique contrasts cryoablation, which relies on freeze-thaw intervals propelled by argon or helium gas, or microwave ablation, which delivers more than 900kHz of electromagnetic frequency (Lencioni et al., 2010). Importantly, as most HCC tumors are discovered at intermediate or late phase, patients are frequently directed to alternative, palliative treatments. Such treatments may include percutaneous ethanol injections, transarterial embolization (TAE), transarterial chemoembolization (TACE), or systemic therapy with small molecule inhibitors. Notably, the current standard-of-care treatment for patients with intermediate disease is TAE/TACE. During this procedure,

interventional radiologists insert a catheter into the patient's groin and flow glass or gelatin microsphere beads, coated with chemotherapeutic agents like doxorubicin, that block tumor blood supply to promote tumor regression (Lencioni et al., 2010). Despite a strong initial response, time-to-progression may occur in as little as five months (Arizumi et al., 2017). Lastly, the most common first-line small molecules approved for advanced stage HCC is the RAF-VEGFR-PDGFR multikinase inhibitor Sorafenib (Sanoff et al., 2016). For patients that progress on Sorafenib treatment, oncologists refer to the administration of Regorafenib, a second-line systemic chemotherapeutic agent approved for HCC management (Bruix et al., 2017). Due to the lack of effective targeted treatment options, especially for patients with advanced stage HCC, the therapeutic landscape must continue to expand to improve overall patient outcome. To provide a unique angle to cancer treatment, subsequent chapters will detail our approach to HCC therapy: targeting copper homeostasis.

Metal Properties and Physiological Roles of Copper

Copper as a Transition Metal

Copper (Cu) is a redox active transition metal that is essential for many aspects in biology and chemistry. Found within the d-block of the periodic table, Cu displays characteristic chemical properties of transition metals including the existence of multiple oxidation states, the ability to form complexes, and the presence of different colored compounds (Flowers et al., 2019). Generally, ligand coordination follows Lewis acid-base principles, where the central metal ion acts as a Lewis acid by accepting electrons donated by atoms acting as the Lewis base. Depending upon whether the reduced cuprous (Cu^{1+}) or oxidized cupric (Cu^{2+}) ion is present, multiple coordinate covalent bonds may be formed. Specifically, cupric ions tend to coordinate between four to six

ligands, whereas cuprous ions have the capacity to bind two to four ligands. Consequently, the diverse ligand coordination to cupric ions usually results in square planar or square pyramidal geometries, which starkly contrasts the linear, trigonal planar, or tetrahedral geometries created by cuprous ion coordination (Balamurugan et al., 2001; Rorabacher, 1999). Due to the covalent nature of these interactions, many biologically relevant Cu-ligand binding affinities are within the femtomolar to sub-femtomolar range (Z. Xiao et al., 2011). Importantly, desirable chemical properties make Cu a robust catalyst in many organic synthesis reactions, including Carbon Azide-Alkyne Cycloadditions, to produce biological or pharmacological agents (Kimber et al., 2019). Moreover, these chemical properties are largely responsible for the evolution of Cu as a quintessential co-factor in biological processes.

As the cytosol of a mammalian cell cultivates a reducing environment with a pH ~7.2, it is not surprising that most intracellular Cu exists in the cuprous state. Although redox cycling between Cu^{1+} and Cu^{2+} is possible, the cell uses a combination of cuproenzymes and chaperones to prevent the generation of free radical species resulting from Fenton chemistry (Wardman & Candeias, 1996). Aberrant regulation of redox cycling fosters uncontrolled protein aggregation, which ultimately drives various pathologies. Well characterized examples of such disease contexts are evidenced by β-Amyloid aggregation in Alzheimer's disease or α-synuclein-derived Lewy bodies found in Parkinson's disease (Chung et al., 2010; Stelmashook et al., 2014). Briefly mentioned above, coordinate ligands will differ depending upon the presence of Cu^{1+} or Cu^{2+} metal centers. Although ligation with donor hydroxyl or carboxyl groups is conceivable, cupric ions tend to form contacts with the nitrogen atoms in the imidazolate ring of histidine (His) side chains. In contrast, cuprous ions have a strong preference for sulfur groups and thus form interactions with the side chains of cysteine (Cys) or methionine (Met)

residues. Interestingly, the thiolate in the Cys side chain is redox active and may form protein crosslinks upon oxidation (Sesham et al., 2013). Considering the interplay between redox status and pH, metal coordination with His or Cys depends on pH as imidazolate and thiolate groups have pK_as of ~6 or ~8.3, respectively (Yousef & Angel, 2020). Conversely, ligation by Met thioester groups, with no accessible protons, is pH independent. Given the biochemical uniqueness of these ligands, Cu-binding pockets have evolved to support protein function by incorporating these ligands accordingly.

Multiple Cu-binding sequences or motifs exist to accommodate a protein's function in either transport, delivery, or catalysis. Notable examples of such motifs are observed in the high-affinity Cu transporter 1 (CTR1), the antioxidant protein 1 (ATOX1), or the cellular respiration cytochrome *c* oxidase (CcO). Importantly, CTR1 transports the majority of intracellular Cu into the cytoplasm of a mammalian cell. To facilitate Cu acquisition, two Met rich motifs (MGMSYM and MMMMPM, where M, G, Y, and P represents methionine, glycine, tyrosine, and proline, respectively) and two His rich motifs (HSHH and HHH, where H and S represent histidine and serine, respectively) are present within the extracellular N-terminus region (J. Jiang et al., 2005). Within the transmembrane domain, a MXXXM motif (where X represents any amino acid) supports movement through the ion channel-like "gate", after which a HCH motif from the intracellular C-terminus tail coordinates Cu entry into the cytoplasm (De Feo et al., 2009; Kahra et al., 2016). Functioning primarily as a delivery protein, ATOX1 ligates Cu through the MXCXXC motif in a mechanism to safely transport Cu to the trans-Golgi network (Arnesano et al., 2002). Lastly, the mitochondrial electron transfer chain (ETC) relies on the multi subunit complex IV, also known as CcO, to generate a proton gradient for downstream ATP synthesis. To initiate electron flow, the catalytic subunits leverage the sequential redox power of two Cu centers, Cu_A and Cu_B, to promote the flow of

electrons toward the ATP synthase. The two Cu ions in the Cu_A center are ligated by two His, two Cys, and a Met residue for ease of surface accessible. Conversely, the coordination site of the Cu_B center comprises of three His residues to keep Cu deeply buried within the active site (Ishigami et al., 2017; Scott, 1995). Collectively, these examples not only illustrate the diversity in Cu binding motifs but introduce a highly regulated transport and delivery system.

Regulation of Copper Trafficking and Homeostasis

Considering the detrimental consequences of the Fenton reaction, mammalian cells have developed an intricate transport system to effectively import, deliver, and export Cu with minimal intracellular recoil (**Fig 1.3**). The extracellular space fosters an oxidative environment that maintains cupric ions; however, most intracellular machinery require cuprous ions for function. Thus, a member of the six-transmembrane epithelial antigen of the prostate (STEAP) family of metalloreductases must reduce cupric ions prior to their cellular import (Ohgami et al., 2006). Following reduction, cuprous ions are transported into the cytoplasm via the ubiquitously expressed, high-affinity Cu specific transporter 1, CTR1 (Kuo et al., 2001; J. Lee et al., 2001). A balance between subcellular localization and vesicular recycling mitigates Cu influxes through CTR1 (Guo et al., 2004; Michael J. Petris et al., 2003). Interestingly, unlike ATP-driven Cu efflux pumps, CTR1 relies on the action of diffusion to move Cu through its ion pore. Despite being the major Cu importer, CTR1 is not the sole facilitator of Cu influx as cells have adapted multiple compensatory mechanisms. Particularly, the divalent metal transporter 1 (DMT1), the transporter primarily responsible for intracellular iron uptake and endosomal iron efflux, may import Cu upon iron deficiency (X. Wang et al., 2016). Although loss of CTR1 manifests in embryonic lethality, genetic depletion of both *CTR1*

and *DMT1* results in a complete suppression of Cu uptake (Kuo et al., 2001; Lin et al., 2015). Additionally, discovered as a homolog of CTR1 through sequence similarity, Cu transporter 2 (CTR2) is postulated to mobilize vesicular Cu by stimulating uptake from endosomes into the cytoplasm (Öhrvik et al., 2013; Van Den Berghe et al., 2007).

Once inside of the cytoplasm, cuprous ions are immediately sequestered by Cu chaperones or antioxidant response proteins to facilitate Cu delivery to various subcellular compartments. Notably, Cytochrome c oxidase copper chaperone (COX17) mediates delivery to the mitochondria, where Cu incorporation is required for proper CcO activity. Prior to insertion into the Cu_A site, the synthesis of CcO 1/2 (SCO1/2) exchanges Cu with COX17 and participates in the metalation of CcO (Banci et al., 2008). CcO functions as a multiunit complex, and thus, requires COX17, SCO1/2, and other COX cochaperones for complex assembly and activation (Carr & Winge, 2003). In parallel, the Cu chaperone for Cu,Zn Superoxide Dismutase (SOD) 1 (CCS) transfers Cu to SOD1 for subsequent superoxide disproportionation activity (Bakavayev et al., 2019). Working alongside SOD1 to combat radical species, metallothioneins (MT) proteins and glutathione (GSH) peptides scavenge free Cu to prevent lipid oxidation of cellular membranes. Furthermore, considering their critical roles in antioxidant response, MT expression and GSH production are induced upon increases in Cu concentration (González et al., 2008; Muller et al., 2007). Lastly, for trafficking to the *trans*-Golgi network (TGN), ATOX1 shuttles Cu to the P-Type ATPase transporters ATP7A and ATP7B (Walker et al., 2004). Through a series of conformational changes initiated by metal binding, ATP7A/B facilitate Cu passage through the TGN lumen and into transport vesicles or secretory cuproenzymes. Although ATP7A is primarily expressed in the brain and intestine while ATP7B is almost exclusive to the liver, both Cu ATPases are localized at the TGN membrane under normal, physiological conditions (Lutsenko et al.,

2007). However, upon sensing Cu excess, ATP7A translocates to the basolateral edge of the cell to promote Cu efflux through vesicular secretion. Conversely, ATP7B responds to elevated Cu levels by translocating to the apical membranes to foster Cu excretion through bile (Hernandez et al., 2008). Beside incorporation into the fundamental proteins associated with its homeostatic regulation, Cu maintains pivotal roles not only as a traditional metal cofactor, but as a novel signaling molecule.

Copper as a Static Cofactor

From a historical perspective, transition metals like Cu, Fe, and Zn, have been functionally categorized as structural or catalytic cofactors. As mentioned previously, the evolutionarily conserved respiratory enzyme, CcO, utilities the redox properties from two distinct Cu sites to proceed with electron transfer (Andreini, Bertini, et al., 2008). To mitigate respiratory damage arising from CcO activity, SOD enzymes require Cu for disproportionation of superoxide (Carroll et al., 2004). Without Cu insertion, impaired catalytic activity and distorted structural conformation will likely ensue. Beyond energy metabolism in mitochondria, Cu remains integrated across various metabolic sectors. As a core enzyme of the catecholamine biosynthesis pathway, Dopamine-β-monooxygenase (DBH) catalyzes the hydroxylation of dopamine to generate norepinephrine. To complete this conversion, two Cu atoms, Cu_M and Cu_H, bridge together the interface of two domains within the catalytic core. Once in close proximity, a molecule of dioxygen binds the reduced Cu_M and enables dopamine hydroxylation while simultaneous transferring electrons to the Cu_H center (Vendelboe et al., 2016). DBH thus highlights a context where Cu acts as both a catalytic and a structural cofactor. Likewise the multicopper ferroxidase ceruloplasmin (CP) exhibits a similar dual functionality as it congregates at the intersection of Cu and Fe homeostasis. Estimated to represent

between 70-90% of Cu-binding serum proteins, CP carries multiple Cu ions that will be used in catalyzing the oxidation of Fe, thus enabling Fe-binding to its respective transport protein transferrin (Z. L. Harris et al., 1998; Pfeiffer, 2011). In a similar regard, hephaestin provides Cu-dependent ferroxidase activity during Fe efflux from enterocytes within the small intestine.

Aside from direct connections to metabolism, cuproenzymes provide intermediates necessary for cell structure and integrity. Namely, lysyl oxidase (LOX), a member of the Cu-requiring amine oxidase family, catalyzes the oxidative deamination of lysine residues to generate aldehyde species that cross-link to form extracellular matrix proteins corresponding to elastin and collagen (X. Zhang et al., 2018). A patch of buried His residues tightly coordinate the catalytic Cu ion to promote contacts with the lysyl tyrosylquinone substrate, while serving to protect this metal from the deleterious effects of surface exposure (Vallet et al., 2019). Parallel assessments may be formed surrounding the rate-limiting pigmentation enzyme, tyrosinase. Utilizing a pair of Cu ions, Cu_A and Cu_B, within its flexible active site, tyrosinase confers both hydroxylation activity during the conversion of L-tyrosine to L-3,4-dihydroxyphenylalanine and subsequent oxidation activity to form L-dopaquinone (Matoba et al., 2006). Downstream reactions spontaneously form melanin, which constitutes the principle metabolite produced by melanocytes (Lerner & Fitzpatrick, 1950). Importantly, mutations to the residues which line Cu-binding sites in LOX or tyrosinase will not only compromise structural stability and Cu-loading, but abrogate catalytic activity (V. S. Lee et al., 2019; Tsai & Lee, 1998). Although these examples outline well-defined roles for cuproproteins, Cu participates in an emerging paradigm where transition metals may act as dynamic cellular signals.

Copper as a Novel Labile Signal

Bioinformatic approaches approximate that one percent of the eukaryotic genome encodes for proteins with Cu-binding capability, suggesting that the current list of known Cu-binding proteins is drastically incomplete (Andreini, Banci, et al., 2008). To further refine this list, recent studies have uncovered novel roles for Cu as a labile signaling molecule. One paramount discovery was revealed when intracellular Cu levels were found to alter conformation, stabilization, and activity of an apoptotic protein, the X-linked inhibitor of apoptosis (XIAP). Specifically, several Cys residues in XIAP become saturated upon Cu accumulation, which in turn, induces a conformational change that both diminishes caspase-3 inhibitory activity and accelerates protein degradation (Mufti et al., 2006). Interestingly, subsequent studies identified the SOD1 chaperone CCS as the likely Cu delivery modality for XIAP, and surprisingly, demonstrated that XIAP modifies CCS through ubiquitination to enhance the Cu delivery activity to SOD1 (G. F. Brady et al., 2010). Furthering the connection between apoptosis and intracellular Cu, recent work by Kim *et al*. established a synergy between the inhibition of specific BCL2 apoptotic proteins and the suppression of bioavailable Cu via TTM in the context of mutant melanoma (Y. J. Kim et al., 2020). Distinct from cell death pathways like apoptosis, Cu has novel functions within cell proliferation and survival pathways.

Riveting studies conducted by Turski *et. al* uncovered that Cu stimulates the kinase activity of the Ras/mitogen-activated protein kinase (MAPK) kinase 1 (MEK1), while chelation by TTM blocks this Cu-dependent phosphorylation (M. L. Turski et al., 2012). Elaborating on these findings, further studies illuminated the malevolent implications of Cu signaling when genetic ablation of CTR1 or disruption of the Cu-MEK1 interaction diminished MAPK signaling and tumorigenic properties in $BRAF^{V600E}$ -driven

lung cancer (D. C. Brady et al., 2014). A recent discovery from our laboratory has identified the essential autophagic UNC-51-like kinases (ULK1/2) as targets of Cu regulation. Here, Cu was found to directly bind to the ULK1/2, and furthermore, a decrease in ULK1/2 kinase activity was observed in the presence of a Cu chelator *in vitro* (Tsang et al., 2020). Moreover, these studies suggest that Cu regulates autophagy through modulation of ULK1/2 in $BRAF^{V600E}$-driven lung adenocarcinoma. In contrast to enzymatic activation, another study demonstrated that Cu-binding directly inhibits the cyclic nucleotide phosphodiesterase activity of phosphodiesterase 3B (PDE3B) in cyclic-AMP dependent lipolysis. By competing for the low affinity Mg^{2+} binding site, Cu^{+} elevation translated to increased cAMP and glycerol production (Krishnamoorthy et al., 2016). Another notable example of Cu-mediated negative regulation may be observed from the potassium ion channel KCa3.1. Researchers found that histidine phosphorylation antagonizes the Cu-mediated suppression of the KCa3.1, resulting in enhanced cytokine production in $CD4^{+}$ T cells (Srivastava et al., 2016). Shifting from ion channels to epigenetics, seminal findings by Attar et al. demonstrate that the histone H3-H4 tetramer, a previously established core element of DNA nucleosomes, confers Cu reductase activity (Attar et al., 2020). Collectively, pivotal discoveries, akin to the examples above, not only mark the foundation towards defining the Cu proteome, but perhaps, support the discovery of novel targets that underlie previously undruggable pathologies.

Pathological States Associated with Dysfunctional Copper Homeostasis

Despite the many instances as an enzymatic or structural cofactor, genetically induced deficiencies in or excess of intracellular Cu directly or indirectly underscore different disease states. Failure to maintain intracellular Cu level at steady state

accentuates the dual essentiality and cytotoxicity features of this metal. Genetic deficiencies in the high-affinity Cu transporter CTR1 result in embryonic lethality (Kuo et al., 2001). Conversely, mutations to the Cu efflux ATPases ATP7A and ATP7B result in Menkes (MD) and Wilson disease (WD), respectively (Peter C. Bull et al., 1993; Nyasae et al., 2007). Although both disorders are consequences of rare genetic inheritances, these conditions have differing manifestations that corresponds to their tissue-specific expression. Specifically, *ATP7A* expression is concentrated to the brain and the intestine, thus, patients with MD present with developmental regression, behavioral abnormalities, kinky hair, and intestinal malabsorption. As *ATP7B* expression occurs almost exclusively in the liver, and mutations or deletions to this transporter reduce Cu biliary excretion from hepatocytes. Therefore, it is not surprising that WD patients present with anemia, jaundice, cirrhosis, and in most cases, Kayser-Fleisher rings. Unlike MD, which has no specific treatments and typically results in premature death, clinicians implement Cu chelation therapy to combat the Cu accumulation observed in WD (Brewer, 2003).

Although MD and WD are direct implications of aberrant Cu homeostasis, a multitude of disorders occur as indirect consequences of Cu misincorporation. Instances of neurological conditions such as Alzheimer and Parkinson's disease are thought to arise from Cu-induced ROS (Stelmashook et al., 2014). Multiple studies reveal that oxidized Cu^{2+} promotes aggregation of β-amyloid, the protein responsible for the neurotoxicity underlining Alzheimer's disease, into degradative-resistant plaques (Dai et al., 2006; Miller et al., 2006; Nguyen et al., 2014; Sarell et al., 2009). In a similar regard, free Cu^{2+} ions exhibit a dual malice in the development of Parkinson's disease. In particular, these ions appear to alter the structural conformation of α-synuclein, a major contributor to the onset of Parkinson's disease, and then propagate these misfolded

proteins to aggregate into toxic Lewy bodies (Paik et al., 1999; Rose et al., 2011; Uversky et al., 2001). Although α-synuclein is largely concentrated at synaptic vesicles and may participate in regulation of dopamine release, its general function is not well understood. However, a study by Davies and colleagues elucidated a novel function of α-synuclein as a Cu-dependent ferrireductase (Davies et al., 2011). In contrast to Alzheimer's and Parkinson's diseases, the lack of Cu metalation present in several SOD mutants emerges as a determinant cause of familial amyotrophic lateral sclerosis (ALS) (Sheng et al., 2013). Indeed, the structural misfolding of SOD in familial ALS truly highlights the significance of Cu misappropriation in neurodegenerative disease initiation.

In recent years, growing incidences of metabolic disorders in the US expose an intricate connection to dysfunctional Cu homeostasis. As rates of obesity and type II diabetes continue to rise, an increased prevalence of non-alcoholic fatty liver disease (NAFLD) and non-alcoholic steatohepatitis (NASH) has emerged (Palmer & Toth, 2019). By clinical definition, NAFLD manifests when lipid accumulates in the liver, whereas NASH develops because of recurrent cycles of NAFLD-induced inflammation and scarring. Preclinical studies denote an elevation of serum cholesterol and triglycerides when rats were exposed to a Cu-deficient diet (Church et al., 2015). These findings are supported by longstanding molecular work where an increase in localization of the sterol regulatory element binding proteins 1 & 2 (SREBP-1/2) occurs upon Cu deficiency (Tang et al., 2000). When intestinal tissue from rats on a copper-deficient diet was genetically profiled using a microarray, Tosco *et al.* documented a transcriptional downregulation of genes within Acyl-CoA pathway and simultaneous upregulation in plasma cholesterol components (Tosco et al., 2010). Consistent with data from molecular and animal studies, clinical investigations revealed a greater risk of hepatic injury in pediatric

populations that present with low circulating Cu and CP levels due to insufficient dietary Cu (Laitinen et al., 1989; Nobili et al., 2013). Interestingly, further lines of evidence suggest that Cu availability influences MAPK signal transduction in MAPK-driven cancer, cytokine signaling in atherosclerosis development, and cellular prion protein-folding in prion diseases (D. C. Brady et al., 2014b; Mitteregger et al., 2009; W. J. Zhang & Frei, 2003). While Cu, Fe, and Zn exhibit significant and individual applications across biology, several functional observations outline an intersection between the homeostasis, trafficking, and metabolism of these metals.

The Relationship between Copper, Iron, and Zinc Homeostasis

Evidently, transition metals have a pronounced and interrelated role in biology. Zn remains redox inactive but stabilizes protein structure, while the redox activity of metals Cu and Fe propels many electron transfer reactions. When further considering their similarities in redox chemistry, it is not surprising that Cu and Fe share transport and delivery mechanisms starting with their entry into the cell. Specifically, the well-established Fe transporter DMT1 exhibits active Cu transport, as several studies have demonstrated that *DMT1* knockdown reduces Cu uptake (Arredondo et al., 2003a; Espinoza et al., 2012) and that *DMT1* overexpression increases Cu uptake during Fe deficiency (L. Jiang et al., 2013; X. Wang et al., 2016). Conversely, multiple studies revealed that Cu excess was sufficient to diminish the mRNA expression of *DMT1* (Gao et al., 2014; Tennant et al., 2002). Beyond intracellular import, further examples of the Cu-Fe linkage may be observed within the circulatory system. Two notable examples that highlight this codependence are the ferroxidases ceruloplasmin (CP) and hephaestin (HEPH). As indicated in their names, both CP and HEPH are enzymes responsible for the Cu-dependent oxidation of Fe^{2+} to Fe^{3+} (Vulpe et al., 1999).

Interestingly, three mononuclear and one trinuclear Cu-binding sites that are buried within CP were identified by X-ray crystallography (Zaitseva et al., 1996). Importantly, lack of adequate dietary Cu not only ceases CP ferroxidase activity in animal models but also diminishes protein abundance, further suggesting that Cu provides an additional structural element (Broderius et al., 2010). In contrast, excessive Cu in the presence of Fe deprivation raises CP protein levels and enhances ferroxidase activity upon Cu loading (Ranganathan et al., 2011). Unlike CP which functions as the major Cu delivery protein in serum, its homologue HEPH lies wedged between the basolateral membrane of enterocytes (Frazer et al., 2001; Vulpe et al., 1999). Moreover, by analyzing existing CP crystal structures, structural modeling analysis of human HEPH by Syed and colleagues uncovered that the characteristic beta fold and Cu-binding sites of CP are conserved in HEPH (Syed et al., 2002). Critically, a colon cancer line subjected to Cu deprivation *in vitro* demonstrated a significant reduction in HEPH activity and synthesis, a result that matched observations from mice fed a Cu-deficient diet (H. Chen et al., 2006). Taken together, these studies further emphasize the pivotal role of Cu in providing stability, structure, and function to quintessential ferroproteins.

In contrast to its supplementary role in maintaining Fe homeostasis, Cu, in tandem with Zn, constitute the basis for antioxidant response proteins. Namely, the free radical scavenging protein SOD1 and the metal detoxification family of metallothioneins (MTs) require both Cu and Zn to either initiate function or upregulate expression. Before driving catalysis of ROS, SOD1 first requires a cooperative endeavor between Cu and Zn to fold properly. In a multi-step reaction, Zn^{2+} ions first serve to coordinate the folding of major Cu ligands, and then transition to the Zn binding pocket upon completion of global protein folding (Leinartaitè et al., 2010). Although the affinity for SOD1 is roughly ~7000-fold higher for Cu than for Zn, the sequential folding permits appropriate ion

metalation that yields a remarkably stable overall structure (Trumbull & Beckman, 2009). Intriguingly, diminished affinity for Zn, as observed in numerous SOD1 mutants, substantiates the clinical connection between dysfunctional SOD1 and development of ALS (Crow et al., 1997). To complement the cell-preserving functions of SOD1, metal scavenging MTs are upregulated to sequester free Cu or Zn ions. These small molecular weight metalloproteins form clusters around transition metals that would otherwise induce ROS via Fenton chemistry (L. Alvarez et al., 2012). Notably, the apparent dissociation constant K_{Cu} for Cu^{+} to MT is ~ $4.1x10^{16}$ while the K_{Zn} for Zn^{2+} is $1.8x10^{11}$ (Banci et al., 2010; Namdarghanbari et al., 2010). Thus, under conditions of Cu overabundance, Zn ions are displaced from Zn-MT proteins and bind to the metal-response element (MRE) transcription factor-1 to induce expression of apo-MT (Günther et al., 2012). Essentially, MTs serve as biological metal buffers to ensure that cellular metal content approaches physiological homeostasis.

Akin to Fe, Zn may compete with Cu for intestinal absorption, and therefore the Cu/Zn ratio should be closely monitored in patients with chronic Cu deficiency (E. D. Harris, 2001). Seminal work has established that the crossroads of dysfunctional Cu and Zn homeostasis potentiates neurological diseases. In addition to direct roles in propagating amyloid-β aggregation, the faulty release of labile pools of Zn or Cu ions alter the plasticity of synaptic clefts, leading to negative modulation of neurotransmitters involved in Alzheimer's disease (Dodani et al., 2014; Sensi et al., 2009). Despite the cell-intrinsic programing that occurs in response to super-physiological metal levels, pharmacological interventions can be useful to further enhance this response.

Copper Chelators in Treatment of Disease

Copper Chelators in Research and the Clinic

Metal chelation is often implemented to effectively modulate the bioavailability of transition metals in cells. This strategy is particularly useful for studying the purpose of metals in a biological system or as a therapeutic modality for curing disease. When investigating the functional significance of Cu in cell biology, the well-established Cu chelator bathocuproine disulfonate (BCS) is used to selectively target cuprous ions (Patel et al., 1997; Rapisarda et al., 2002). This agent may additionally bind cupric ions and generate a geometry that drives their reduction. However, once Cu ions reach the Cu^{1+} state, the chelation properties of BCS prevent further redox cycling (Patel et al., 1997; Seng et al., 2009). Despite the two sulfonate groups that promote its solubility in water, the charged nature of BCS makes it membrane impermeable and should therefore be used to restrict Cu outside of cells (Rasoloson et al., 2004; Z. Xiao et al., 2004). For studies investigating the intracellular role of Cu^{1+}, the hydrophobic chelator neocuproine may be used as a suitable cell-permeable alternative (Bhat et al., 2007; Kumcu et al., 2009).

Moving from bench to bedside, Cu chelators embrace a translational role in medicine. To treat Cu overload resulting from a plethora of diseases, clinicians may select from multiple well-studied Cu chelators. Interestingly, D-penicillamine (D-pen) was the first orally administered Cu chelator that proved successful in alleviating Cu accumulation in WD patients (Peisach & Blumberg, 1969; Yarze et al., 1992). Notably, D-pen contains sulfhydryl, amino, and carboxylate functional groups that permit chelation of both cupric and cuprous ions. Upon chelation, D-pen reduces cupric ions to cuprous ions while simultaneously forming disulfide bonds from oxidized thiol groups (Kato et al., 1999). Despite its selectivity for Cu ions, D-pen may additionally chelate Zn

as both animal and patient studies have denoted a D-pen induced Zn-deficiency after treatment (Cossack & Bouquet, 1986; Fieten et al., 2013). Unfortunately, D-pen has been reported to induce nephrotoxicity in a subset of WD patients (Walshe, 1969). Therefore, the acylic amino chelator trientine has been substituted in cases where adverse effects manifest. In contrast to the multiple functional groups present in D-pen, trientine harnesses the chemistry of amino nitrogen donors to preferentially coordinate Cu^{2+} ions yielding a femtomolar dissociation constant (Lu, 2010). The resulting square-planar geometry promotes a conformation that can effectively inhibit Cu,Zn SOD activity and compete with serum albumin for Cu binding (Brown et al., 2009; Sarkar et al., 1977). With respect to metabolism, trientine both enhances the rate of urinary Cu excretion, in a similar regard to D-pen, and reduces intestinal adsorption to generate Cu deficiency with minimal drug toxicities (Lu, 2010; Pfeiffenberger et al., 2018). Despite the success of trientine regimens for WD, the relevance of tetrathiomolybdate (TTM) has been explored in recent years. A phase III clinical trial demonstrated that TTM was more effective than trientine in WD patients presenting with neurological symptoms (Brewer et al., 2006). TTM is an inorganic chelator that forms polymetallic clusters when Cu moieties are ligated by thiolate ligands (George et al., 2003). Similar to the abovementioned chelators, TTM exerts a high affinity for Cu ($K_d \sim 10^{-19}$) and exists as a TTM-Cu-albumin tripartite complex in serum (Christian Rupp & Weiss, 2019; Suzuki et al., 1995). Remarkedly, TTM demonstrates the capacity to de-copper MT and Cox17 proteins *in vitro* (Smirnova et al., 2018), and can interfere with Cu exchange from Atx1 to its target protein Ccc2a (H. M. Alvarez et al., 2010). As TTM-complexed Cu is no longer bioactive, the tripartite complex is packaged into bile and excreted from the liver into the intestines. Even though TTM is well-tolerated in WD patients, it is important to note that excessive molybdenum is toxic and thus should be dosed accordingly (Vyskočil & Viau, 1999).

Outside of these Cu chelators, the small molecules inhibitors elesclomol and disulfiram, which chelate cupric ions, have attracted attention for their multifunctional indications and will be discussed in further detail in the following section.

Copper Chelation Therapy for Multiple Indications

The Cu chelators D-pen, trientine, and TTM were designated as primary treatments for Wilson disease, an inherited disorder where mutations in the Cu exporter *ATP7B* prompt aberrant Cu accumulation in the liver. Interestingly, mutations to the Cu efflux pump *ATP7A*, another member of the P_{1B}-subfamily of P-Type ATPases, manifest in the X-linked inherited condition Menkes disease (MD) (Telianidis et al., 2013). This disorder induces a Cu deficiency in both the brain and the serum, impairing Cu delivery to cuproenzymes vital to cell structure and metabolism. Unlike Wilson disease, Cu chelating agents, including thiuram, dithiocarbamate, and lipoic acid, used to treat MD act as ionophores and facilitate Cu transport across blood-brain barriers (Horn et al., 2019). Beyond their initial indications for treatment of genetic disease, Cu chelating agents have been repurposed as alternative or supplemental therapies for malignant conditions varying from cardiovascular disease to cancer. In a rat model of vascular injury, TTM was shown to blunt the release of the cytokine IL-1α and the growth factor FGF1 following balloon-induced injury of the carotid artery (Mandinov et al., 2003). These findings complement a preclinical investigation where doxorubicin-induced increases in the cytokines TNF-α, IL-1β, and IL-2, were abrogated in a mouse model of cardiac toxicity after TTM administration (Hou et al., 2005). With respect to vascular inflammation, molecular and pre-clinical studies have demonstrated that TTM administration inhibits both mRNA expression and serum levels of ICAM-1,VCAM-1, and TNF-α, which are key modulators in the development of atherosclerotic lesions (Wei et

al., 2011, 2012, 2014). Moreover, Cu chelation proved successful in mitigating the effects of adjuvant-induced inflammatory arthritis in rats, as TTM attenuated expression of the angiogenesis growth factor VEGF and impeded clinical hallmarks of rheumatoid arthritis (Omoto et al., 2005). In addition to direct mediation of the inflammatory response, the Cu chelator 2,3,2-tetraamine (tet) ablated the lipopolysaccharide-induced production TNF-α, IL-1β, and IL-6 cytokines to suppress human monocyte activity, while tet-mediated Cu deficiency reduced expression and production of IL-2 in human T-lymphocytes (Hopkins & Failla, 1997; Huang & Failla, 2000). Unsurprisingly, the lack of proinflammatory markers upon Cu chelation reduces subsequent signaling to limit fibrotic development, as evidenced by diminished pulmonary fibrosis or liver fibrosis in either bleomycin-induced or bile-duct ligation murine models, respectively (Brewer et al., 2003; Song et al., 2008). Taken together, these findings illustrate the importance of Cu chelation as a modality to restrict both activated and unsolicited immune responses. Considering that several of the abovementioned growth factors and cytokines lie at the axis of angiogenesis and immunity, it is not surprisingly that there is a growing interest in the repurposing of Cu chelators as potent anti-cancer therapeutics.

Although not carcinogenic itself, multiple studies have demonstrated that Cu supplementation at moderate to high doses can increase cellular proliferation in rodent models of mammary, pancreatic, or lung cancer (D. C. Brady et al., 2014; Ishida et al., 2013; Skrajnowska et al., 2013). Despite proliferation number of factors influencing proliferative potential, the formation of blood vessels that supply nutrients to the tumor is a large contributing factor. Accordingly, Cu chelation has been demonstrated to hinder this process, referred to as angiogenesis. A simple study illustrated this concept by dramatically hindering the proliferative and survival capacity at multiple doses of TTM in human umbilical venous or arterial endothelial cells (Carpenter et al., 2007). With

respect to the angiogenic dependency in cancer, trientine suppressed neovascularization, microvessel density, and IL-8 production in murine xenograft models of HCC and fibrosarcoma (Hayashi et al., 2007; Moriguchi et al., 2002; Yoshii et al., 2001). A subsequent study confirmed these findings in xenograft models of colorectal cancer when researchers demonstrated that trientine could block tumor neovascularization in addition to inhibiting tumoral VEGF and IL-8 expression (Yoshiji et al., 2005). Mirroring these results, TTM dosed in both transgenic and xenograft murine models of breast cancer were able to curtail microvessel density. Notably, this study began to uncover the connection between Cu and NFkβ signaling as it pertains to angiogenesis, since nanomolar doses of TTM could suppress NFkβ-dependent transcription and protein abundance (Pan et al., 2002). A mechanistic follow-up investigation using breast carcinoma cells further defined the Cu/NFkβ signaling axis, as TTM treatment depleted proangiogentic mediators and attenuated invasiveness and motility *in vitro* while reducing tumor kinetics and metastasis *in vivo.* Imperatively, both of these findings phenocopied observations made after genetic manipulations were made to the NFkβ pathway (Pan et al., 2003). Preclinical murine models of head and neck squamous cell carcinoma demonstrated that a 30% Cu deficiency induced by TTM was sufficient to significantly reduce microvessel density and tumor volume (Cox et al., 2001). Together, these preclinical findings substantiate the evidence behind the use of Cu chelation in anticancer clinical studies.

Likely due to its favorable toxicity profile, TTM has been selected as either a primary or adjuvant therapy in several human cancer trials. An early phase I clinical trial assessed the effects of TTM dosage in patients with metastatic solid tumors revealed that patients who achieved a clinical Cu deficiency did not progress (Brewer et al., 2000b). Following this study, a phase II clinical trial was conducted with advanced-stage

kidney cancer patients. In addition to TTM being well tolerated, serum measurements revealed a significant reduction in of proangiogenic markers relative to baseline. Moreover, the presence of stable disease in these patients speaks to the cytostatic, instead of cytotoxic, nature of TTM (Redman et al., 2003). Years later, a trial that recruited patients with operative esophageal cancer observed a survival benefit when a two year TTM adjuvant therapy was administered following transhiatal esophagectomy (Schneider et al., 2013). An additional study that enrolled late-stage or triple-negative breast cancer patients found that oral administration of TTM could significantly diminish endothelial progenitor cells (EPC) and prevent relapse in patients that sustained a mild Cu-deficiency (S. Jain et al., 2013). These promising findings prompted another phase II clinical trial in breast cancer patients with the same staging criteria, and intriguingly, 91% of stage II-III patients and 67% of stage IV patients remained EPC biomarker and event-free after two years on TTM adjuvant therapy (Chan et al., 2017).

Despite the clinical success of Cu chelation therapy, the underlying biology of the target cancer must be carefully considered to avoid negative outcomes. For example, even though elimination of myelosuppression and normalized functional liver outputs, a phase II clinical trial in human glioblastoma multiforme patients revealed that no significant survival benefit was evident after penicillamine treatment (Brem et al., 2005). In a phase II trial with hormone refractory prostate cancer patients, TTM administration failed to reduce angiogenic markers and unsurprisingly, resulted in progressive disease status in more than 75% of patients (Henry et al., 2006). In a multi-agent pilot study conducted in metastatic colon cancer patients, a cycling regimen of TTM, irinotecan, 5-flurouracil (5-FU), and leucovorin rendered an unsettling overall response rate of 25% despite being well-tolerated (Gartner et al., 2009). Taken as a whole, these studies illuminate the importance of understanding the underlying biology of the target tumor, as

the tumoral niche influences a tumor's metastatic potential. Learning from these clinical studies, Cu chelation may be best served in micro cancers that have defined genetics, metabolism, vascularization, and bodily location.

Outside of traditional Cu chelators, Cu ionophores have also worked their way into the clinic. In particular, the Cu ionophores disulfiram (DS) and elesclomol have garnered attention as alternatives to conventional chemotherapeutics. Due to its inhibition of aldehyde dehydrogenase, DS emerged in the 1950's with FDA approval as a treatment for chronic alcoholism (Skrott et al., 2017). When this carbamoyl derivative dimerizes and becomes reduced, the resultant sulfur anions can bind to metal ions including Cu (II). This reactivity has been postulated to generate ROS, a feature which partially contributes to the cytotoxicity reported with DS (Tawari et al., 2015). Moreover, several mechanistic studies illustrated an NF-kB-dependent cytotoxicity in multiple cancer types. Colorectal cancer cell lines treated with DS exhibited a block in NF-kB pathway induction and an enhancement in the cytotoxicity of 5-FU when used in combination with DS (W. Wang et al., 2003). Interestingly, melanoma cells with different stages, but not melanocytes, showed both significant reductions in cell viability and elevations in Cu content in response to DS treatment (Cen et al., 2004). *In vitro* experiments using patient-derived myeloma and leukemia cells demonstrated that the presence of DSF or DSF in combination with $CuCl_2$ could activate caspases and induce a potent cell death (Conticello et al., 2012).

Following these promising findings, a pilot trial in men with non-metastatic recurrent prostate cancer was initiated but yielded rather disappointing results. Notably, DS failed to provide a survival benefit and was not well-tolerated in this patient cohort (Schweizer et al., 2013). In light of these results, more recent studies have proposed nanoencapsulation of DS as it allows for more targeted cytotoxicity with less adverse

effects (Tawari et al., 2015). Other studies have provided evidence that inhibiting autophagy enhances DS potency against non-small cell lung cancer (X. Wu et al., 2018) and that DS treatment reduced tumor burden in xenograft models of multiple myeloma (Jin et al., 2018). By mining epidemiological data sets combined with empirical biophysical observations, a landmark study revealed that cancer patients taking DS had a lower risk of cancer-related death and that the functional DS-Cu complex inhibited the essential NPL4 segregase, which is involved in stress-response pathways (Skrott et al., 2017). Despite these compelling findings, whether disulfiram should be used prophylactically to prevent recurrent cancer in first-time diagnosis patients is still a question under investigation.

Conversely, elesclomol is a carbohydrazide-based small molecule designed to selectively target cancer cells by rapidly triggering oxidative stress in mitochondria to induce apoptosis (Kirshner et al., 2008). Biophysical studies have shown that elesclomol binds to Cu (II) in a 1:1 molar ratio and potentiates hydroxyl radicals in an indirect fashion (Hasinoff et al., 2014). In addition to entering cells in complex with Cu (II), the complex is directed immediately to the mitochondria (Nagai et al., 2012). In pursuit of defining a mechanism of action, Blackman *et al.* provided evidence that elescomol affects electron transport chain (ETC) function as growth defects and mitochondria functional outputs manifested in *S. cerevisiae* treated with elescomol or harboring loss of ETC functional components (Blackman et al., 2012). Although a complete mechanism of action has yet to be defined, a recent study discovered that FDX1, a mitochondrial reductase critical to iron-sulfur cluster synthesis, is a novel target of elescomol (Tsvetkov et al., 2019). Building on this mechanism, cell lines and xenograft models of Ewing sarcoma exhibited sensitivity to enhanced to elesclomol when expressing *SOX6*, a transcription factor critical to endochondral ossification (Marchetto et al., 2020). In

human trials, a landmark phase II clinical trial in metastatic melanoma patients uncovered that the combination of elescomol and paclitaxel significantly increased the median disease-free progression and substantially raised the median overall survival (S. O'Day et al., 2009). While the SYMMETRY study, a subsequent phase III clinical trial with similar treatment arms, was terminated early due to an anticipated imbalanced mortality in the paclitaxel group upon survival analysis, it did reveal that LDH levels are an indication of prognosis in late stage melanoma patients lacking previous therapies (S. J. O'Day et al., 2013). More recently, a small dose-escalation study was initiated in patients with acute myeloid leukemia to assess the toxicity of elescomol, and suggested that a dose of 400mg/m^2 or higher was well-tolerated as a monotherapy for AML patients (Hedley et al., 2016). Collectively, targeting Cu transport and delivery in cancer effectively mediates inflammatory regulators, angiogenesis factors, and ROS generation to lessen the tumorigenic properties associated with aggressive behavior and metastatic potential.

Hypoxia and Copper Metabolism

Introduction to Hypoxia

Oxygen (O_2) is a universal requirement for mammals. As the ultimate electron acceptor of the ETC, a sufficient supply of O_2 is necessary to complete aerobic respiration (M. Liu et al., 2020; Semenza, 2007). Without an adequate supply or distribution of O_2, cells must initiate a cascade of transcriptional, metabolic, and signal-transduction related reprogramming in order to adapt to reduced oxygenation (Muz et al., 2015). Although several protein factors mediate the hypoxic response, the hypoxia-inducible factors (HIF) provide a key foundation as they act as the master regulators to drive many associated response pathways. Importantly, the HIF subfamily falls within the

basic helix-loop-helix (bHLH) Per/Arnt/Sim (PAS) family of transcription factors. For transcriptional function, the O_2-responsive subunit, HIF-alpha (α), heterodimerizes with the constitutively expressed HIF-beta (1β) subunit (J.-W. Lee et al., 2004) to bind Hypoxia Response Elements (HRE) of a target gene and initiate transcription (Schönenberger & Kovacs, 2015). The HIF-α subunits have multiple isoforms: HIF-1α, HIF-2α, or HIF-3α, and either isoform can bind to the HIF-1β subunit. While the HIF-3α subunit is relatively understudied, there is an abundance of literature surrounding molecular and regulatory mechanisms of the HIF-1α and HIF-2α subunits. Notably, the HIF-α subunits are degraded in an O_2-responsive fashion by the von Hippel-Lindau (VHL) E3 ubiquitin ligase, which is recruited to HIF-α through a hydroxylation moiety modified by the O_2-, 2-oxogluterate-, and Fe-dependent prolyl hydroxylase (PHD) enzymes (Bruick & McKnight, 2001; Keith et al., 2012). Akin to PHD enzymes, the factor inhibiting HIF (FIH) is another 2-oxogluterate and Fe-dependent dioxygenase that hydroxylates an asparagine residue to prevent recruitment of transcriptional coactivators p300 and CBP (Kaelin, 2008). Thus, under oxygen-replete conditions, HIF-α is targeted for degradation to the 26S proteasome. Conversely, under acute or chronic hypoxic stress, PHD enzymatic activity becomes inhibited enabling the stabilization and subsequent translocation of HIF-α to the nucleus to induce hypoxia-responsive target genes (M. Liu et al., 2020). In addition to hypoxic conditions, HIF-α may be stabilized in response to excess of tricarboxylic acid cycle intermediates fumarate or succinate, which compete for substrate binding with 2-oxogluterate, or as a result of isocitrate dehydrogenase mutations that reduce cytoplasmic 2-oxogluterate levels (Losman & Kaelin, 2013; Thompson, 2009).

Several lines of evidence have identified a number of HIF target genes across multiple biological pathways. Of note, genes associated with glycolysis, angiogenesis,

erythropoiesis, cellular proliferation, migration & invasion, and Fe metabolism are induced upon decreased oxygenation. To drive glucose metabolism, glycolytic enzymes such as HK, ENO1, ALDOA, GAPDH, PKM, and LDHA, as well as solute transporters GLUT1 and MCT1, are upregulated (Eales et al., 2016; Miranda-Gonçalves et al., 2016; Nishimura et al., 2017). Subsequently, hypoxic-mediated exhaustion or poor perfusion of nutrients will lead to upregulation of pro-angiogenic factors, thus promoting the formation of new blood vessels (Semenza, 2012). Although most hypoxic responses are mediated through HIF-1, seminal findings by Kapitsinou et al. demonstrated that erythropoiesis and expression of erythropoietin, a protein key to red blood cell production, is modulated by HIF-2 during hypoxia in renal cells (Kapitsinou et al., 2010). While reduced O_2 increases the likelihood of cell cycle arrest, upregulation of insulin-like growth factor binding proteins (IGFBP) and transforming growth factor-β1 (TGF-β1) stimulate cell growth and proliferation across multiple cell types (Y. Jiang et al., 2007; Minchenko et al., 2015; C. Rupp et al., 2015). To stimulate an oncogenic-like reprogramming, hypoxia enhances the expression of motility factors AMF, WNT2, WNT5A, and c-Met to promote migration, invasion, and metastatic potential of cancer cells (Eckerich et al., 2007; Hara et al., 2006; Niizeki et al., 2002; C. Rupp et al., 2015). As with glycolysis, Fe homeostasis represents another sector of metabolism that is modulated in response to hypoxia. Specifically, reduced tissue oxygenation represses transcription of hepcidin, a small antimicrobial peptide that inhibits Fe transport, while simultaneously inducing transcription of transferrin (Tf), Tf receptor (TfR), heme oxygenase 1 (HO-1), and ceruloplasmin (Cp), each which facilitate either ferric-ion delivery, Tf internalization, heme/Fe recycling, or Fe delivery through the serum (Q. Liu et al., 2012; Motterlini et al., 2000; Mukhopadhyay et al., 2000; Rolfs et al., 1997; Tacchini et al., 1999). Because Cp plays dual roles in Fe and Cu metabolism as a ferroxidase enzyme and serum Cu-

carrier, it has provided a gateway for further investigation of regulatory elements on the hypoxia-Cu homeostasis axis.

Interplay between Hypoxia, HIF Proteins, and Copper Homeostasis

Namely, a landmark paper demonstrated that HIF-1α is Cu regulated as $CuCl_2$ supplementation was sufficient to induce HIF-1α nuclear localization and protein stabilization, resulting in increased HRE-dependent reporter activity and expression of HIF-1 target genes (Martin et al., 2005). Following this finding, an independent research group evaluated the hypothesis that Cu is required for HIF-1 activation in hepatoma cells by performing gene expression and protein interaction assays in the presence of a Cu chelator, tetraethylenepentamine (TEPA), under hypoxic conditions. In addition to confirming Cu-dependent alterations in HRE-dependent reporter activity and hypoxia-responsive genes, TEPA treatment prevented the interaction between HIF-1α and p300, a critical component of the HIF-1 transcriptional activation complex (Feng et al., 2009). Similarly, experiments conducted with $CuSO_4$ concentrations upwards of 200 μM were sufficient to elevate *VEGF*, *HIF-1α*, and G-protein estrogen receptor (*GPER*) mRNA upon hypoxia, while reciprocal experiments with TEPA-mediated chelation abrogated this hypoxia-associated transcription. Moreover, conditioned culture medium from breast cancer cells treated with excessive $CuSO_4$ supplementation elicited an elevation in VEGF protein levels sufficient to stimulate downstream tube vessel formation and cell migration (Rigiracciolo et al., 2015). Furthermore, a clinical investigation involving serum from patients with either HCC, cirrhosis, chronic hepatitis, or non-diseased liver identified an important role for Cu in the activation of HIF-1α as it pertains to hepatocarcinogenesis. Serological assessments uncovered a significant positive correlation between HIF-1α and circulating Cu levels, while observing a negative

correlation between HIF-1α and Zn concentrations. Another correlation was established between elevated HIF-1α and Cu levels and hepatocarcinogenic progression. Imperatively, HIF-1α was present only within the tumors of HCC patients, and completely absent from normal liver tissue or from in patients with liver cirrhosis or chronic hepatitis (Himoto et al., 2016). However, further refinement of the Cu-HIF-1α hypothesis has indicated a cell-type specific and perhaps a gene specific phenomenon. Evidence to support this notion stems from the observation that expression of HIF-1 regulated genes *VEGF*, *GAPDH*, *LDH*, *GLUT1*, and BCL2/adenovirus E1B 19kDa protein-interacting protein 3 (BNIP3) but not insulin-like growth factor 2 (IGF-2), were diminished in the presence of TEPA in human embryonic vein endothelial cells (HUVEC). Using a series of ChIP-PCR and luciferase reporter assays, an in depth investigation in HUVEC revealed that TEPA-mediated Cu suppression was sufficient to block HIF-1α binding to HREs in some but not all hypoxia-responsive genes (X. Liu et al., 2018; Z. Zhang et al., 2014). To complement these discoveries, TTM treatment not only prevented the accumulation of HIF-1α and VEGF protein and the expression of *GLUT1* and *PDK1* mRNA transcripts, but inhibited Complex IV activity such that oxygen consumption rate was reduced in models of human endometrial or ovarian cancer cells (K. K. Kim et al., 2015). In line with previous findings, a recent RNA-seq profiling experiment identified the downregulation of metabolic transcripts *PFKL* and *ENO1* in addition to *GAPDH* in the presence of high concentrations (50 μM) TEPA prior to acute hypoxia exposure (Z. Wu et al., 2019).

Although connections between HIF-1α and Cu have been well-documented, work by several research groups have reported an interplay between HIF-2α and Cu homeostasis. An increase in total protein expression of solute transporters DMT1, GLUT1, and CTR1 was observed under hypoxia in Caco-2 cells. Additional exploration

uncovered a parallel increase in *CTR1* transcripts and Cu uptake, yet, this effect was significantly reversed in the presence of pharmacological suppression or genetic inhibition of murine Hif-2α (Pourvali et al., 2012). Several studies focused in rat duodenum describe a necessary role HIF-2α-mediated regulation of Cu homeostatic genes in the context of anemia. In particular, induction of *Atp7a* expression in the background of Fe deficiency brought into question whether Hif-2α played a role. Sequence analysis of the promoter region identified several HREs that were deemed essential for Hif-2α binding as revealed by ChIP assays (Xie & Collins, 2011). Subsequent studies illuminated this regulation further when the transcription factor Sp1 was identified as a required piece to the Hif-2α transactivation puzzle under hypoxic stress in an anemic background (Xie & Collins, 2013). In contrast to anemia caused by genetic factors, mice with anemia as a consequence of a Cu-deficient diet had elevated expression of Hif-2α and Fe transport genes. When intestinal *Hif-2α* was removed from these mice via tissue specific knock out, an absence of gene induction was observed under the abovementioned nutrient context (Matak et al., 2013). In addition to the genetic regulation established between Cu and HIF-α subunits, the hypoxic-dependent effects of Cu-driven cell biology are an area of current exploration.

Despite the transcriptional studies providing rationale for elevated *Atp7a* expression upon hypoxic conditions, additional work has focused on characterizing these downstream consequences. Acute exposure to hypoxia was sufficient to increase expression of Atp7a and localize it to cytoplasmic vesicles within murine macrophages, which accompanied an increase in ^{64}Cu uptake likely via increased CTR1 expression (C. White et al., 2009a). In a MEF model transformed with oncogenic H-RAS, Zhu et al. knocked out *Atp7a* to uncover that these cells conferred a unique growth sensitivity to

both hypoxia and ROS, which translated to reduced tumorigenesis in xenograft models (Zhu et al., 2017). Lung tissue from mouse models of pulmonary hypertension displayed significant increases in mRNA expression of *Atp7a*, *Ctr1*, and *Lox* and decreases in *Atox1*, *Ccs*, and *Sod1*. Unsurprisingly, these transcriptional escalations corresponded to a rise in CTR1 and LOX protein abundance upon hypoxia and enhanced LOX activity to significantly improve cell motility and migration (Zimnicka et al., 2014). One feature consistent amongst these investigations was the increase in Cu uptake from either tumoral or hypoxic-treated conditions (C. White et al., 2009b; Zhu et al., 2017; Zimnicka et al., 2014). Cu may be present as either the ^{63}Cu or the ^{65}Cu isotope, and simple experiments in HepG2 cells confirm that an enrichment of ^{65}Cu parallels the elevation of total Cu levels after hypoxic treatment (Bondanese et al., 2016). Clinical pertinence was demonstrated when ICP-MS analysis from serum of breast or colorectal cancer patients discovered that the ^{65}Cu/^{63}Cu ratio could predict mortality earlier than traditional clinical biomarkers (Télouk et al., 2015). Cancer patients also demonstrated higher total serum Cu content and higher Cu/Zn ratios than healthy peers. Taken together, there is sufficient evidence to indicate that the relationship between Cu homeostasis and hypoxia extends beyond simple transcriptional modifications.

Thesis Objectives

Despite a substantial body of literature supporting the notion that Cu concentrations in HCC cells deviate from their hepatocyte progenitors, there is a lack of clarity surrounding the underlying molecular features that drive these Cu-specific differences. Additional literature indicates that HCC cells implicate a transcriptional and metabolic program that favors a glycolytic metabolism, a stark contrast to the metabolism of normal hepatocytes, which in turn supports HCC oncogenicity. Moreover,

common embolic procedures used to treat HCC induce a hypoxic microenvironment that further drives a reliance on glucose metabolism. Considering these factors, the primary hypothesis of this thesis project was that Cu acts as an important contributor to HCC tumorigenesis and to HCC glycolytic metabolism. To address this hypothesis, this project aimed to answer the questions that follow. What impact will Cu availability have in regulating HCC tumorigenic properties? To what extent does Cu influence HCC metabolism within a hypoxic environment? In Chapter 2, we uncovered the relevance of Cu to HCC tumorigenic properties by utilizing both genetic and pharmacological approaches to suppress Cu bioavailability. In Chapter 3, we began to elucidate a molecular mechanism by presenting evidence that Cu regulates crucial components of HCC glycolytic reprogramming upon hypoxic stress. Finally, in Chapter 4, we delve further into the mechanism behind the Cu-mediated regulation of glycolysis, and additionally discuss the future directions of the project. Collectively, this thesis project serves to close the gap in knowledge regarding Cu modulation of HCC glycolytic metabolism and its tumorigenic properties while highlighting a novel therapeutic purpose for Cu chelators.

Chapter 1 Figures

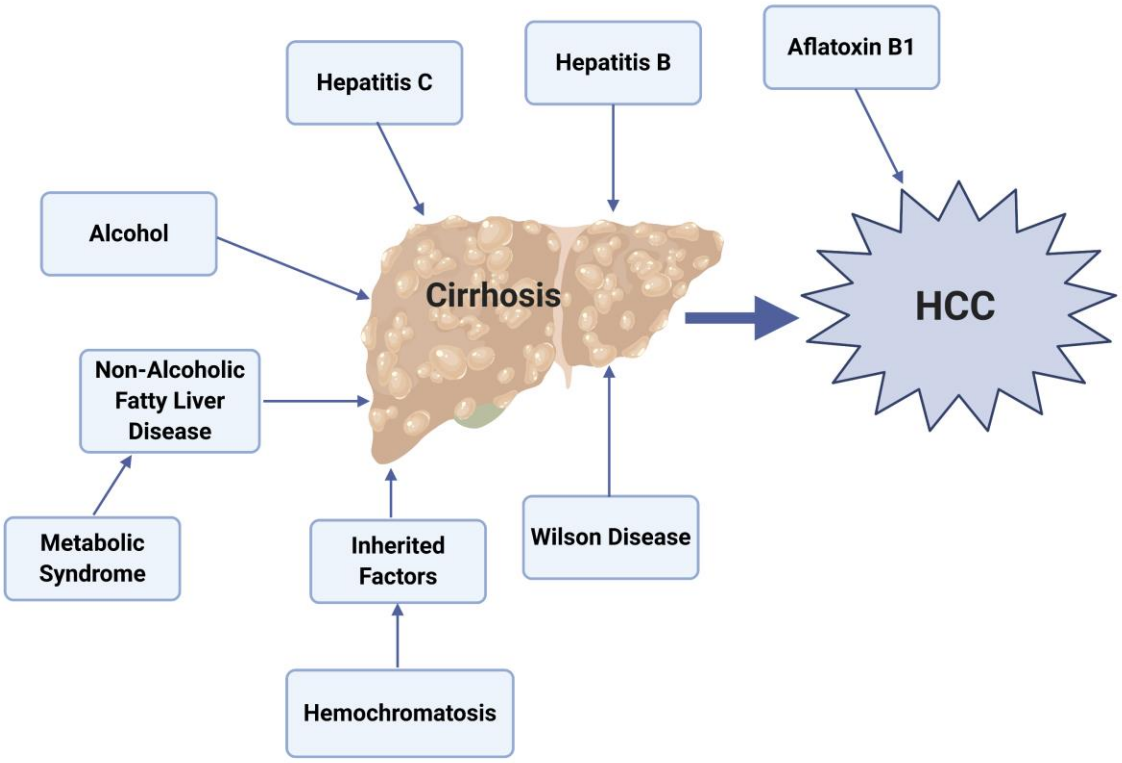

Figure 1.1 Risk Factors for the Development of HCC. Of the above etiologies, chronic hepatitis viral infection and chronic alcoholism are the most frequently observed predisposing factors for HCC development. In developed nations, non-alcoholic fatty liver disease is rapidly becoming a major contributor to the incidence of HCC. Although less prevalent, inherited genetic disorders have been reported to impact liver carcinogenesis. Interestingly, Aflatoxin B1, a mycotoxin produced by the *Aspergillus flavus* fungus found in molded peanuts, is a predisposing factor that increases HCC risk in patients with an existing hepatitis infection. Importantly, the onset of cirrhosis is the factor unifying these vastly different etiologies, and without appropriate clinical surveillance or medicinal interventions, patients remain vulnerable to the development of HCC.

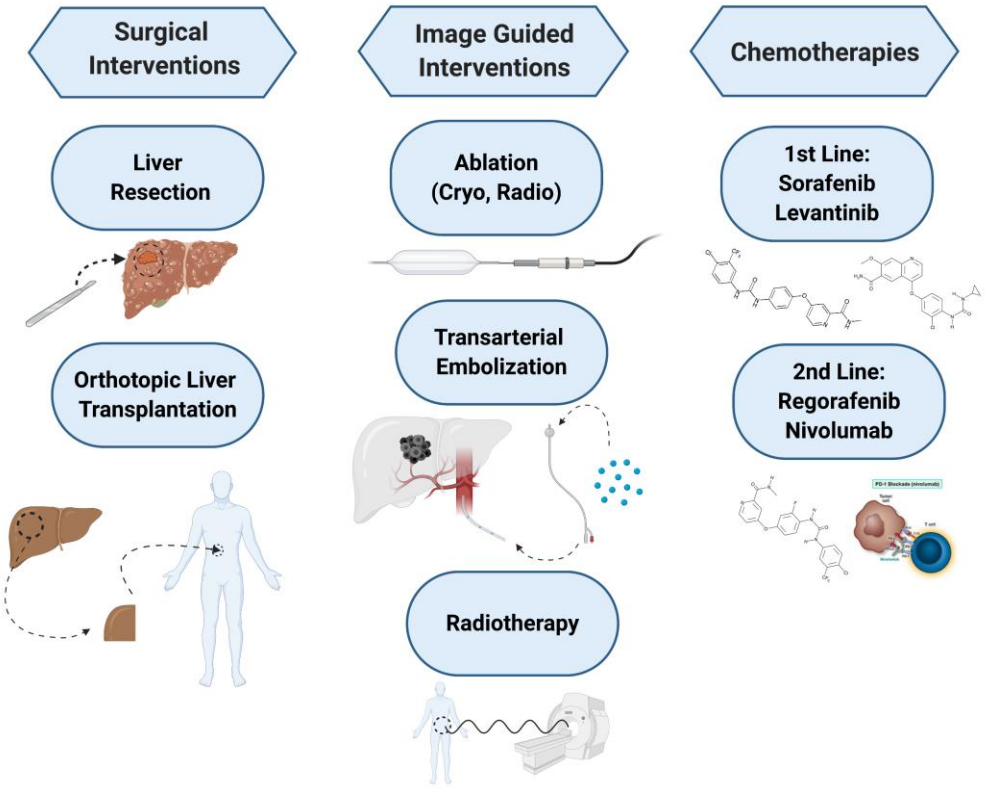

Figure 1.2 Current Therapies for the Treatment of HCC. Although a continuously advancing landscape, the above therapies are commonly implemented to combat HCC. A small percentage of early stage patients may be eligible for liver resection or orthotopic liver transplantation, which are curative therapies that have low rates of recurrence. Conversely, many HCC patients are diagnosed late-stage and must receive palliative care, which generally requires image guidance to accurately define the tumor. Of interest, transarterial embolization (TAE) is a minimally-invasive, image-guided technique that uses microsphere beads to selectively or super selectively block the blood vessels that supply nutrients and oxygen to the tumor. In certain cases, these microsphere beads may be coated in a chemotherapeutic, in addition to an embolizing agent. Unfortunately, the chemotherapies designated for HCC are only minimally effective at prolonging survival. The first line small molecule inhibitors Sorafenib and Levantinib increase survival by approximately three or seven months, respectively. In the event that patients fail to respond to these therapies, Regorafenib, another multikinase small molecule, or Nivolumab, a monoclonal antibody that blocks the programmed death-1 (PD-1) receptor, may be administered.

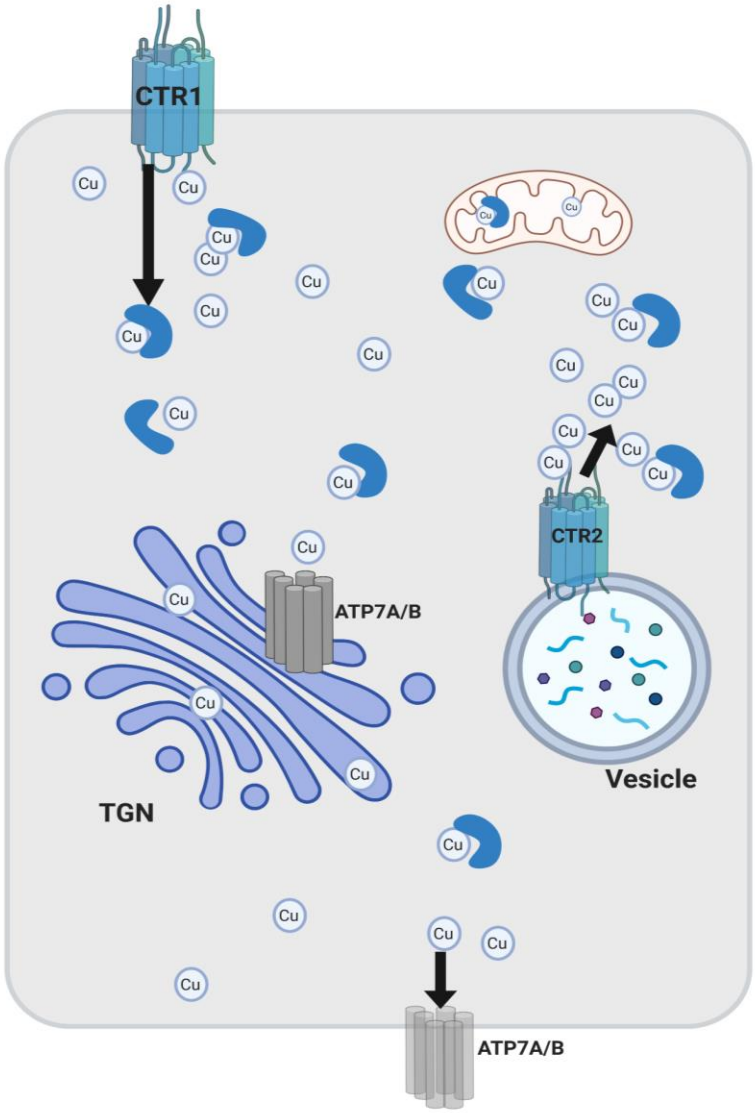

Figure 1.3 Cu Homeostasis in the Cell. Upon reduction, Cu^{1+} enters the cell through the high-affinity Cu importer CTR1. Once inside the cytoplasm, Cu is bound by numerous Cu chaperones (blue concave polygons) and safely delivered to multiple subcellular compartments including the trans-Golgi network (TGN), mitochondria (light pink polygon), and endosomal vesicles within the cytoplasm. CTR2, a homolog of CTR1, functions to mobilize Cu stores from vesicular compartments into the cytoplasm from when intracellular Cu levels are low. ATP7A/B are located at the TGN and function to transport Cu for metalation of newly synthesized cuproproteins. Under conditions of Cu excess, ATP7A/B translocate to the plasma membrane to facilitate Cu transport out of cells.

CHAPTER 2: ALTERED COPPER HOMEOSTASIS UNDERLIES SENSITIVITY OF HEPATOCELLULAR CARCINOMA TO COPPER CHELATION

This Chapter has been reformatted from a submission for publication to *Metallomics:*

Davis, C.I., Gu, X., Kiefer, R.M, Ralle, M., Gade, T.P., and Brady, D.C. Altered copper homeostasis underlies sensitivity of hepatocellular carcinoma to copper chelation. Metallomics. Accepted, October 2020.

Overview

HCC represents an alarming global healthcare problem with an increasing incidence. Current treatment strategies for HCC demonstrate limited efficacy because each is agnostic to molecular and genetic features of the disease. Although significant elevation of the transition metal Cu has been associated with HCC, the contribution of Cu to hepatocarcinogenesis is not well understood. Specifically, numerous studies have reported a correlation between elevated serum or intra-tumoral Cu levels and HCC status. However, these studies fail to provide molecular characteristics or mechanistic details to substantiate these clinical observations. Here, we present an analysis of altered Cu transporter expression in HCC that elucidated a unique Cu-dependent vulnerability necessary for tumorigenesis. These findings uncover a clinically tractable alternative treatment to combat HCC by repurposing Cu chelators.

Introduction

Liver cancer represents the second and the sixth leading cause of cancer-related death in men and women, respectively (Siegel et al., 2019). HCC accounts for 80% of liver cancer cases in the world (Altekruse et al., 2014), and pre-existing conditions associated with cirrhosis, such as hepatitis B viral infection, chronic hepatitis C virus

infection, non-alcoholic fatty liver disease, hereditary hemochromatosis, and Wilson disease contribute to HCC onset (El-Serag, 2011). Genomic alterations within HCC, irrespective of etiologic risk factor, emphasize the heterogeneous nature of the disease and thus, advances in molecular medicine targeting the genetic mutations underlying HCC have been unsuccessful (Schulze et al., 2015). Intriguingly, case studies of patients with Wilson Disease, which harbor germline mutations in the gene encoding the P-type ATPase *ATP7B* (P C Bull et al., 1993; Tanzi et al., 1993), demonstrate that persistently elevated levels of intracellular Cu impair liver function such that HCC results as a complication (Iwadate et al., 2004; Kumagi et al., 2004, 2005; Thattil & Dufour, 2013). Beyond the extensive research from both Wilson disease patients and animals that supports a connection between excessive Cu accumulation and hepatobiliary malignancies (Huster, 2014; Huster et al., 2007; Pfeiffenberger et al., 2015), multiple clinical investigations observed elevated serum (Attia et al., 2019; El Fotouh et al., 2012; Poo et al., 2003; Porcu et al., 2018) and intratumoral (Ebara et al., 2000, 2003; Jie et al., 2007) Cu levels in liver cancer patients. Notably, Cu lies at a unique intersection between chemistry and biology, as Cu-driven redox chemistry is required for a multitude of biological programs. To minimize oxidative damage, Cu homeostasis is a highly regulated process, beginning when Cu enters the cell through the essential copper transporter 1, CTR1 (Kuo et al., 2001; J. Lee et al., 2001). CTR1 is the predominant high-affinity Cu transporter at the plasma membrane, while its low-affinity homolog, CTR2, localizes and facilitates transport from vesicular compartments into the cytoplasm (Bertinato et al., 2008; Van Den Berghe et al., 2007). To complement Cu influx via CTR1, cells are also equipped with Cu efflux machinery. Specifically, the P-type ATPases ATP7A and ATP7B are membrane-bound transport pumps that function to export cytosolic Cu in an ATP-dependent fashion (Nyasae et al., 2007; Pase et al.,

2004). The importance of maintaining a balance between Cu influx and efflux is clear given that deletions in *CTR1* lead to embryonic lethality, while mutations in *ATP7A* and *ATP7B* manifest in Menkes or Wilson disease, respectively. Interestingly, emerging evidence indicates that regulation of Cu homeostasis coincides with other cellular processes, from lipid metabolism (Krishnamoorthy et al., 2016) to cellular proliferation (Michelle L Turski & Thiele, 2009). Our lab has discovered that Cu can enhance oncogenic signaling in the MAPK pathway via a direct interaction with MEK1 and MEK2, resulting in a Cu dependency in mutant $BRAF^{V600E}$ positive melanoma (D. C. Brady et al., 2014b). Similarly, Cu is required for the activity of the autophagic kinases ULK1 and ULK2 and autophagosome formation downstream of ULK1 and ULK2 is sensitive to fluctuations in Cu availability (Tsang et al., 2020). Collectively, these findings create a molecular foundation that directly links Cu homeostasis to deregulated signal transduction events that drive pathological conditions. However, the contribution of Cu to intrinsic and extrinsic cellular mechanisms necessary for liver tumorigenesis and resistance driven by treatment-mediated metabolic reprogramming in HCC patients remains unclear.

In the current study, we sought to bridge this gap by taking a bioinformatic approach utilizing publicly available cancer genome datasets. We evaluated the expression of Cu homeostasis genes, namely those facilitating Cu transport such as *ATP7A*, *ATP7B*, *SLC31A1*, which encodes CTR1, and *SLC31A2*, which encodes CTR2, across HCC and normal tissue samples. From this analysis, we identified significant alterations in the aforementioned Cu transporter genes, and further, found that copy number variations in the Cu transporters correlated with poorer survival and disease-free progression, and was associated with increased Cu levels. Given the importance of Cu modulation in disease management, the manipulation of Cu homeostasis has been

previously exploited as an alternative cancer therapy through the usage of various Cu chelating agents (D. C. Brady et al., 2014b; Brewer et al., 2000a; Chan et al., 2017; Pan et al., 2002a). We explored the relevance of perturbed Cu availability, through genetic ablation of *CTR1* or pharmacologic inhibition via tetrathiomolybdate (TTM), in HCC. Here we demonstrate that targeting Cu homeostasis exposes a unique vulnerability in HCC, as we discovered Cu-dependent contributions to hepatic tumorigenic properties.

Methods

Data Mining

ATP7A, *ATP7B*, *SLC31A1*, or *SLC31A2* mRNA expression in normal or tumor liver tissue samples was obtained from the Gene Expression across Normal and Tumor tissue (GENT2) web-based genome database (http://gent2.appex.kr/gent2/, Korean Research Institute and Biotechnology). A total of 1095 patients and 1089 samples across six hepatocellular adenoma or carcinoma data sets [Memorial Sloan Kettering (MSK), Clin Cancer Res 2018; INSERM, Nat Genet 2015; MSK, PLOS One 2018; AMC, Hepatology 2014; RIKEN, Nat Genet 2012; The Cancer Genome Atlas (TCGA), Firehorse Legacy] were selected for query from cBioportal for *ATP7A*, *ATP7B*, *SLC31A1*, or *SLC31A2* copy number alterations and patient survival data. For overall survival plot, n = 13 patients with altered copy number of Cu transporters and n = 594 for patients with unaltered copy number Cu transporters. For disease-free progression, n = 11 patients with altered copy number of Cu transporters and n = 545 for patients with unaltered copy number Cu transporters.

ICP-MS Sample Preparation of Human HCC Cell Lines and Rat Liver Tissue

Human HCC cell lines were seeded at 2.0 x 10^6 cells in 100mm dishes. After incubation for 48 hours at 21% O_2, cells were washed twice and harvested with 1X Phosphate Buffered Saline. Cell pellets were collected by centrifugation at 2,000 x*g* for 5 minutes, and were flash-frozen in a dry ice-ethanol bath prior to storing at -80°C. HCC tumors and adjacent liver tissues were harvested from the livers of Wistar rats subjected to the Dietylnitrosamine-induced (DEN) diet according to an established protocol (Kiefer et al., 2017). Tissue samples were harvested, weighed, flash-frozen in a dry ice-ethanol bath, and immediately stored at -80°C. All samples were processed by the PADLS New Bolton Center Toxicology Laboratory in the School of Veterinary Medicine at the University of Pennsylvania.

X-Ray Fluorescence Microscopy

For XFM experiments 10 µm sections were transferred to Ultralene®, a XFM compatible window material, mounted on in-house developed lucite sample holders and air-dried. XFM data were collected on beamline 2-ID-E at the Advanced Photon Source (APS), Argonne National Laboratory, Argonne, IL. The incident X-ray energy was tuned to 10 keV using a Si-monochromator and focused with a Fresnel zone plate. X-ray fluorescence was collected using an energy dispersive 4-element detector (Vortex ME-4, SII Nanotechnology, Northridge, CA). Raster scans were collected in fly-scan mode, using 1 µm x 1 µm step size with 200 msec dwell time per point. 2-dimensional elemental maps were created by extracting, background subtracting, and fitting the fluorescence photon counts at each point using the program MAPS(Vogt et al., 2003). The fluorescent counts were transformed into µg/cm^2 using calibrated X-ray standards (AXO products, Dresden, Germany). Quantitative analysis was performed by extracting the fluorescent spectra and fitting and quantifying them against the calibration standards

as mentioned above. Area concentrations were converted into volume concentrations using the tissue thickness of 10 μm under the assumption that the X-ray beam fully penetrated the sample.

Cell Lines & Cell Culture

SNU387, SNU398, and SNU449 HCC cell lines and human plateable hepatocytes, 5-Donor were obtained from the American Type Culture Collection (ATCC) and ThermoFisher Scientific, respectively. Parental cell lines were cultured in Roswell Park Memorial Institute (RPMI 1640, Gibco) Media and supplemented with 10% v/v fetal bovine serum (FBS, GE Lifesciences), 100 U/mL penicillin, and 100 μg/mL streptomycin (Gibco). SNU398 and SNU449 cell lines stably expressing the pLKO.1puro constructs were maintained as above supplemented with 5μg/mL puromycin (Invitrogen). SNU398 and SNU449 were stably infected with lentiviruses derived from the pLKO.1 plasmid (*see* plasmids below) using established protocols. Unless specified, all cell lines were maintained in a humidified Heracell (ThermoFischer Scientific) incubator set to 37°C and 5% CO_2. MycoAlert® mycoplasma test detection kit (Lonza, LT07-418) was used to test for mycoplasma contamination.

Immunoblot Analysis

The indicated HCC cell lines were washed with cold 1x Phosphate-buffered Saline (PBS), and lysed in cold RIPA buffer supplemented with 1x EDTA-free Halt™ protease and phosphatase inhibitor cocktail (ThermoFisher Scientific, #78441). Total protein was quantified using the BCA assay (Pierce, # PI23228), where sample concentrations were interpolated to a BSA standard curve. Equivalent amounts of lysate were resolved by SDS-PAGE using lab established protocols, and protein was detected using the

following antibodies (dilution, catalog#, manufacturer): rabbit anti-CCS (1:2000, 20141, Santa Cruz) or mouse anti-β-actin (1:5000, 3700, Cell Signaling Technologies (CST)), followed by detection with one of the following horseradish-peroxidase-conjugated secondary antibodies: goat anti-mouse IgG (1:4000, 7076, CST) or goat anti-rabbit IgG (1:4000, 7074, CST) using SignalFire ECL (CST, # 6883S) detection reagents.

Plasmids

pLKO.1puro lentiviral shRNA plasmids were obtained from High-Throughput Screening Core at the University of Pennsylvania to express: nontargeted control (sh*SCR*), human *CTR1* target sequence #1 5'-GATGCCTATGACCTTCTACTT-3' (sh*CTR1*#1), or human *CTR1* target sequence #2 5'-CGGTACAGGATACTTCCTCTT-3' (sh*CTR1*#2).

RT-qPCR

To examine the expression of Cu transporter genes, 3.0 x 10^5 cells of the indicated HCC cells were seeded into 60mm dishes. Sixteen hours post-seeding, cells were treated with the indicated concentrations of TTM and/or were moved to hypoxic conditions for 48 hours. To isolate RNA, cells were harvested in TRIzol™ reagent (Invitrogen, #15596018) and RNA was extracted following manufacturer's protocol. Purified RNA was reverse transcribed (RT) into cDNA using the Applied Biosystems™ Taqman™ Reverse Transcription Reagents (Applied Biosystems, # N8080234) and corresponding protocol. Subsequent cDNA was loaded onto a clear 384-well plate (Genesee, #24-305) and quantified on a ViiA 7 Real-Time PCR System with standard protocols using the following Taqman™ probes: Hs00163707_m1 to detect human ATPase copper transporter A (*ATP7A*), Hs01075310_m1 to detect human ATPase copper transporter B (*ATP7B*), Hs00977266_g1 to detect human *SLC31A1* (*CTR1*), Hs00156984_m1 to

detect human copper transporter 2 *SLC31A2* (*CTR2*), and Hs00427620_m1 to detect human TATA-binding proteins (*TBP*). The $\Delta 2^{-Ct}$ or comparative $\Delta\Delta C_t$ method was used as described previously(Schmittgen & Livak, 2008) to analyze mRNA after transcript levels were normalized to *TBP*. For validation of *CTR1* knock-down, cells transduced with shRNA targeting *CTR1* were harvested and processed as above upon selection with puromycin, and then assayed for relative *CTR1* expression following the procedure above.

Reagents

The Cu chelator TTM (#323446) and the crystal violet (# C0775-100G) used for colony staining were purchased from Sigma-Aldrich.

Clonogenic Assay

SNU398 and SNU449 cell lines stably expressing indicated constructs were seeded at 3.0 x 10^3 cells per well in six-well plates. After incubation for seven days, cells were washed once with 1X Phosphate Buffered Saline (PBS) and stained with 1mL of a crystal violet staining solution (0.5% w/v crystal violet (CV), 20% v/v methanol, distilled water) for 15 minutes. After 15 minutes, all wells were washed three times with distilled water to minimize background staining. CV stained colonies were imaged using a ChemiDoc Touch Imagining System (Bio-Rad). To quantify colony abundance, stained cell colonies were dissolved in a 10% acetic acid solution for 30 minutes at room temperature, and extracted CV was measured at an absorbance of 590nm in a plate reader (Synergy, BioTek). For TTM treatments, cells were treated 24 hours after seeding with either a vehicle or a final indicated concentration of TTM for seven days and then processed as mentioned above.

Measurement of Cell Proliferation with Trypan Blue

SNU398 and SNU449 cell lines stably expressing the indicated constructs were seeded at 1.5 x 10^4 cells per well in a six-well plate on Day 0. Proliferation curves using cell lines stably expressing indicated constructs in the presence or absence of TTM were performed at identical times. On Day 1, DMSO or TTM treatment was added to a final concentration of 25 μM. Cell counts were performed every other day by washing cells with 1x PBS, detaching cells with 0.05% Trypsin (Gibco, #25300054). Cells were then resuspended in an equal volume of complete DMEM, and centrifuged at 1000*xg* for 5 mins. Following aspiration of media, cell pellets were then resuspended in identical volumes of complete DMEM. Cell counting was performed using an automated cell counter (Invitrogen Cell Countess II) by taking an aliquot of cell culture and diluting 1:1 with 0.4% Trypan Blue Solution (Life Technologies/Invitrogen, #15250061) before plating on and reading with a hemocytometer.

Anchorage-Independent Growth on Ultra-Low Attachment Plates

SNU398 and SNU449 cell lines stably expressing the indicated constructs were seeded at 2.0 x 10^3 cells per well in a 96-well clear flat bottom ultra-low attachment plates (Corning, #3474) on Day 0. For the TTM-treated groups, indicated concentrations of TTM were added 16 hours post-seeding. On Day 5, cells were imaged using an EVOS XL Core Imaging System brightfield microscope with a x10 dry objective. The mean number of spheroids (cells) per field was quantified by a researcher blinded to the genetic manipulations or TTM treatment groups using Fiji software (https://imagej.net/Fiji). Data was normalized to the respective control (sh*SCR*) or vehicle-treated (DMSO) control group.

Measurement of ATP Using CellTiter-Glo ® Viability Assay

SNU398 and SNU449 cell lines stably expressing indicated constructs were seeded in triplicate at 5.0 x 10^2 cells per well in 96-well white walled flat bottom plates (Fisher Scientific, #655098) or 96-well clear flat bottom ultra-low attachment plates for IC_{50} determinations in anchorage-dependent (2D) or anchorage-independent (3D) conditions, respectively. Sixteen hours post-seeding, indicated concentrations of TTM were added to appropriate wells and cells were incubated for 72 hours. Cell viability was assessed using the CellTiter-Glo® Luminescent (Promega, #G7572) or 3D (Promega, #9682) Cell Viability Assay for 2D or 3D conditions, respectively, following the manufacturer's protocol. Normalized %ATP values were calculated by normalizing the raw luminescent values of wells containing the vehicle (DMSO) to wells containing each dose of TTM. To determine the IC_{50} values, the data was transformed using the nonlinear fit of Log(TTM) versus normalized response (%ATP Normalized to DMSO) with a variable slope function in GraphPad Prism8 software.

Statistical Analysis

Data are reported as mean $\pm$s.e.m. Each sample size (*n*) represents biologically independent experiments or fields of view. For biologically independent experiments, data was collected from three independent experiments unless otherwise specified within the figure legend. For fields of view, data presented are from 9 fields of view taken from three biologically independent experiments. Statistical significance was determined using an unpaired one- or two-tailed Student's t-test, a Mantel-Cox test, a one-way or two-way ANOVA followed by Dunnett's or Tukey's multiple comparisons test, where

significance was defined as $P \leq 0.05$. All statistical analysis was performed in GraphPad Prism 8 software.

Results

Expression of Cu Transporters is Dysregulated in Hepatocellular Carcinoma

Clinical measurements of transition metals demonstrated that HCC tumors exhibit elevated Cu levels when compared to normal liver tissue (Ebara et al., 2003) and higher serum Cu levels correlate with the presence of cirrhosis or HCC (Porcu et al., 2018). In agreement, Wilson disease patients accumulate Cu in the liver and exhibit cirrhosis and thus, have a higher propensity to develop HCC. To further investigate these clinically relevant observations that connect Cu to HCC development (Iwadate et al., 2004; Kumagi et al., 2004, 2005; Thattil & Dufour, 2013),(Ebara et al., 2003),(Porcu et al., 2018), we examined the expression of Cu influx and efflux transporters across human liver cancer and normal liver tissue utilizing the Gene Expression database of Normal and Tumor tissues 2 (GENT2). We found that mRNA expression of both Cu transporters *SLC31A1* and *SLC31A2*, along with the Cu exporter *ATP7B* was significantly lower, while the mRNA expression of the Cu exporter *ATP7A* was significantly higher in liver cancer (**Fig. 2.1a,b**). Intrigued by this finding, we investigated the relationship between patient survival and copy number alterations of Cu transporter loci in six HCC patient data sets in cBioPortal. Although a small cohort, HCC patients with copy number alterations of Cu influx or efflux transporters had a significantly worse outcome with respect to overall survival and likelihood of recurrence (**Fig. 2.1c,d**). Taken together, these data suggest that Cu transport into or out of the cell is dysfunctional in a subset of HCC patients. Consistent with clinical findings, we observed elevated Cu levels in HCC tumors compared to adjacent liver tissue collected from a DEN-induced

rat model of HCC using inductively coupled plasma mass spectrometry (ICP-MS) (**Fig. 2.2a**). Closer examination of the Cu concentration in the rat liver tumor tissue with X-Ray Fluorescence Microscopy (XFM), revealed heterogeneous Cu concentration. In an example shown in **Figure 2.2b** from HCC rat tumor tissue, Cu was localized to highly concentrated focal areas of approximately 10 to 15μm diameter that exceeded 5mg/g (~80mM), while the average concentration across the scan was 40μg/g (~60μM). To establish a model that is more amenable to genetic and pharmacologic perturbations, we measured total intracellular Cu levels using ICP-MS from a panel of human HCC cell lines (**Fig. 2.2c**). In agreement with the rodent model data, HCC cell lines exhibited significant elevation in Cu levels when compared to a primary hepatocyte line, HMCPP. Recognizing that Cu transporters mediate cellular Cu influx and efflux, we investigated whether there was evidence of differential Cu transporter expression as measured by quantitative PCR (qPCR) (**Fig. 2.2d**). Interestingly, mRNA expression of *ATP7B*, *SLC31A1*, and *SLC31A2* was significantly lower in HCC cells, which parallels the observations made from patient genomic data sets (**Fig 2.1a,b**). Further, elevated Cu levels were confirmed by lower protein expression of CCS, which is degraded in a Cu-dependent fashion (Graham F. Brady et al., 2010), in all of the HCC cell lines when compared to normal hepatocytes (**Fig. 2.2e**), suggesting that HCC cells accumulate excess Cu levels that may contribute to oncogenic properties.

Genetic Depletion of *CTR1* Diminished HCC Tumorigenic Properties

To interrogate whether these increased Cu levels are essential for HCC tumorigenic properties, we generated stable genetic knockdown of *CTR1* with two independent short-hairpin RNAs (shRNA) targeting the *SLC31A1* gene in both SNU398

and SNU 449 cells, as measured by qPCR (**Fig. 2.2a,b**). Disruption of *CTR1* significantly reduced the proliferation of SNU398 and SNU449 cells (**Fig. 2.3c,d**). In addition to cellular proliferation, colony formation of SNU398 and SNU449 cells when plated at low density, a property that distinguishes tumorigenic cells from healthy cells, was dependent on *CTR1* expression (**Fig. 2.3e,f**). Furthermore, patients with HCC may develop metastases which requires detachment from the extracellular matrix and invasion into nearby organs (Zimmermann, 2016). Thus, to complement our findings of reduced HCC proliferation and colony formation in the context of *CTR1* deficiency, ultra-low attachment (ULA) polystyrene plates were used to evaluate the effects of *CTR1* depletion on anchorage-independent growth in SNU398 and SNU449 cells. Knockdown of *CTR1* significantly diminished the anchorage-independent growth of SNU398 and SNU449 cells (**Fig. 2.4a,b**). Taken together, these findings demonstrate that HCC cell lines depend on Cu transport via CTR1 for proliferation, colony formation, and anchorage-independent growth, suggesting that altered Cu availability contributes to hepatocarcinogenesis.

TTM Treatment Attenuated HCC Proliferation and Anchorage-Independent Growth

The repurposing of TTM, a Cu-specific chelator used in the treatment of Wilson disease, has been explored as a cancer therapy in several contexts (D. C. Brady et al., 2017; Brewer et al., 2000a; Chan et al., 2017; Cox et al., 2001). Mechanistically, preclinical studies and phase I/II clinical trials suggest that Cu-dependent components of the tumor microenvironment (Chan et al., 2017), oncogenic kinase signaling pathways (D. C. Brady et al., 2014a, 2017; Tsang et al., 2020), and metabolic pathways (Ishida et al., 2013) mediate sensitivity to TTM (Chan et al., 2017; Pan et al., 2002a). Considering that HCC tumors are well-vascularized (Fodor et al., 2019) and demonstrate amplified

receptor tyrosine kinase signaling (Schulze et al., 2015), as well as a dependency on glycolytic metabolism (Amann et al., 2009; H. Wu et al., 2019), we hypothesized that disruption of Cu accessibility through pharmacological interventions would diminish HCC tumorigenic properties. To begin evaluating this hypothesis, SNU398 and SNU449 cells were treated with increasing concentrations of TTM and then cell viability was measured using a high-throughput luminescent-based assay that detects ATP. TTM treatment decreased ATP, and thus viability of SNU398 and SNU449 cells, in a dose-dependent manner **(Fig. 2.5a-c**). To determine whether TTM would remain as efficacious in 3D cultures, the IC_{50} of TTM-treated SNU398 and SNU449 cells seeded in ULA plates was determined (**Fig. 2.5d-f**). Interestingly, there was nearly a two-fold and three and a half-fold increase in the IC_{50} concentration of TTM from 2D to 3D cultures in SNU398 cells and SNU449 cells, respectively (**Fig. 2.5c,f**). This finding is in agreement with other observations that HCC cells grown in 3D have enhanced drug-resistance and aggressiveness as compared to their 2D counterparts (Jung et al., 2017). In accordance, when treated with TTM at a concentration at or above the IC_{50}, SNU398 and SNU449 cells still exhibited reduced proliferation as measured by trypan blue exclusion staining (**Fig. 2.6a,b**). Moreover, when cultured with increasing concentrations of TTM in anchorage-independent conditions, spheroid formation was significantly reduced in SNU449 cells and trended downwards in SNU398 cells (**Fig. 2.6c,d**). Collectively, these results are early indications that Cu chelation through TTM may be effective in reducing the properties that comprise HCC tumorigenesis.

Discussion

In the present study, we highlighted Cu homeostasis as a targetable vulnerability within HCC and provided early evidence to suggest Cu chelation as a supplemental

treatment option for patients with this disease. The mining of publicly available, cancer genomic data sets uncovered several features that may explain the consistent clinical findings of elevated Cu levels across HCC patients. We demonstrated that dysregulation of Cu homeostasis, through altered expression of Cu transporter genes, correlated with unfavorable outcomes in HCC patients. In support of this data, Cu transporter expression in a panel of human liver cell lines reflected these observations. While the *SLC31A1* (*CTR1*) levels were decreased in both human liver tumor tissues and cell lines, which suggests HCC tumors could be Cu deficient, Cu levels were significantly elevated in rat liver tumors and several human HCC cell lines that aligned with reduced CCS protein abundance. Thus, we have demonstrated utilizing both molecular and genetic approaches that Cu levels are indeed elevated in the context of liver cancer and this marked increase is associated with reduced mRNA expression of *SLC31A1*, *SLC31A2*, and *ATP7B,* suggesting that increased Cu content of HCC tumors may be driven by the loss of *ATP7B* instead of the downregulation of *SLC31A1* (*CTR1*) and *SLC31A2* (*CTR2*). Alternatively, cancer cell lines increase nutrient scavenging in the form of micropinocytosis (Aubert et al., 2020), which was recently proven to be a mechanism for cancer cells to acquire Cu and could be responsible for the increased Cu levels in HCC cell lines and tumor tissue. However, future studies must be conducted to further investigate this concept. To the best of our knowledge, this study is the first to identify a relationship between the expression of Cu transporter genes and prognosis in HCC patients. These results support previous studies that described Cu levels as significantly higher in both patient serum (Attia et al., 2019; El Fotouh et al., 2012; Poo et al., 2003; Porcu et al., 2018) and resected tumors (Ebara et al., 2000, 2003; Jie et al., 2007). Considering the trend of poorer disease-free survival for HCC patients with altered Cu transporter copy number (**Fig. 2.1d**), and a previous report where small

tumors (<35 mm) yielded high Cu levels that correlated positively with differentiation status of the tumor (Ebara et al., 2003), it is likely that Cu homeostasis contributes more to hepatocarcinogenesis than to HCC progression. Even though our findings reveal dysfunctional Cu transport and provide essential insights toward the development of alternative therapeutics in the treatment of HCC, further molecular studies are needed define the role of cuproproteins in the pathogenesis of HCC.

In addition, we demonstrated that *CTR1* is necessary for cellular proliferation, clonogenic survival, and anchorage-independent growth of HCC cell lines. These results complement experiments performed by Porcu *et al.,* where transient knockdown of *CTR1* reduced cell viability, cell cycle progression, and cell migration in human immortalized hepatic progenitor or hepatoma cells, while treatment with $CuSO_4$ slightly enhanced these properties (Porcu et al., 2018). Although the authors suggested that MYC is responsive to Cu levels, whether other transcriptional regulators mediate these Cu-dependent responses remains to be determined. However, elementary proof may lie in the correspondence between MYC target genes and microarray data that revealed an upregulation in genes associated with cell growth, cell migration, angiogenesis, and small GTPase mediated signal transduction upon exposure to high concentrations of $CuSO_4$ in HepG2 cells (Min et al., 2009). Taken together, protein factors that regulate the above processes, such as the frequently mutated TERT, β-Catenin, or p16, may influence Cu-dependent responses and represent important targets for future studies. In parallel, we demonstrated that treatment with the Cu specific chelator TTM inhibits HCC tumorigenic properties. Although animal studies in HCC have not yet been performed using TTM, an early study of HCC tumor xenografts showed that Cu chelation with trientine, another Cu chelator, can induce apoptosis and reduce tumor volume (Yoshii et

al., 2001). Despite this preclinical study that explored Cu chelation as a treatment option for HCC (Yoshii et al., 2001), the efficacy of Cu chelation in combination with the standard-of-care therapies, TAE and TACE, has yet to be investigated. Thus, future studies involving the use of ischemic culture conditions, which are characterized growth at 1% O_2 in the presence of low FBS, glucose, and glutamine concentrations, should be conducted to decipher the Cu-dependent sensitivities upon minimal oxygenation versus nutrient deprivation.

Chapter 2 Figures

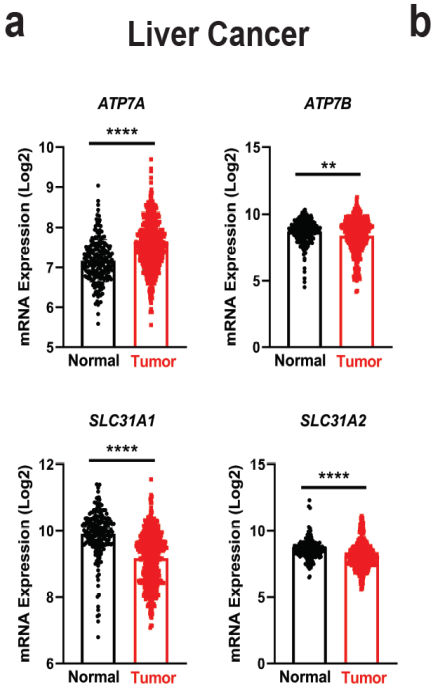

b

Gene Name	Mean Normal Tissue mRNA Expression (Log2)	Mean Tumor Tissue mRNA Expression (Log2)	P-value	Log2 Fold-Change
ATP7A	7.169	7.543	<0.0001	0.3748
ATP7B	8.892	8.397	0.0018	-0.2958
SLC31A1	9.908	9.171	<0.0001	-0.7369
SLC31A2	8.609	8.104	<0.0001	-0.5055

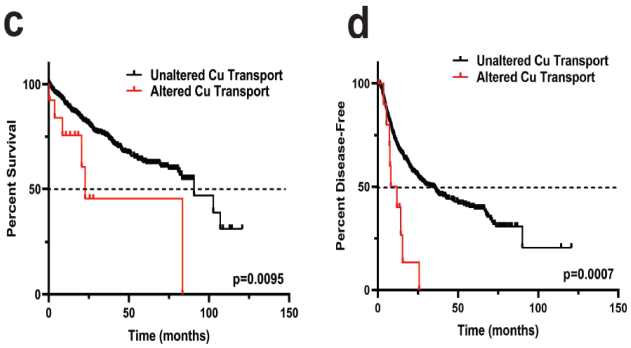

Figure 2.1 Aberrant Cu homeostasis is observed in liver cancer and specifically in HCC. (a) Scatter dot plot with bar at mean +s.e.m. of mRNA expression of ATP7A, ATP7B, SLC31A1 (CTR1), and SLC31A2 (CTR2) from normal and tumor liver tissue samples from the online, open-access database GENT2. Statistical analysis was performed using an unpaired, two-tailed Student's t-test. *P < 0.0332,**P < 0.0021, ***P < 0.0002, ****P < 0.0001. (b) Summary table of mRNA expression data shown in (a). (c and d) Kaplan-Meier analysis of overall survival (c) and disease-free progression (d) with median (dashed black lines) from HCC patients with either altered (solid red lines) or unaltered (solid black lines) copy number of Cu transporter genes mentioned in (a) and (b). For overall survival plot, n = 25 patients with altered and n = 582 for patients with unaltered copy number of Cu transporter genes. For disease-free progression, n = 20 patients with altered expression and n = 536 for patients with unaltered copy number of Cu transporter genes. Results were compared using a Mantel-Cox test. *P < 0.0332,**P < 0.0021.

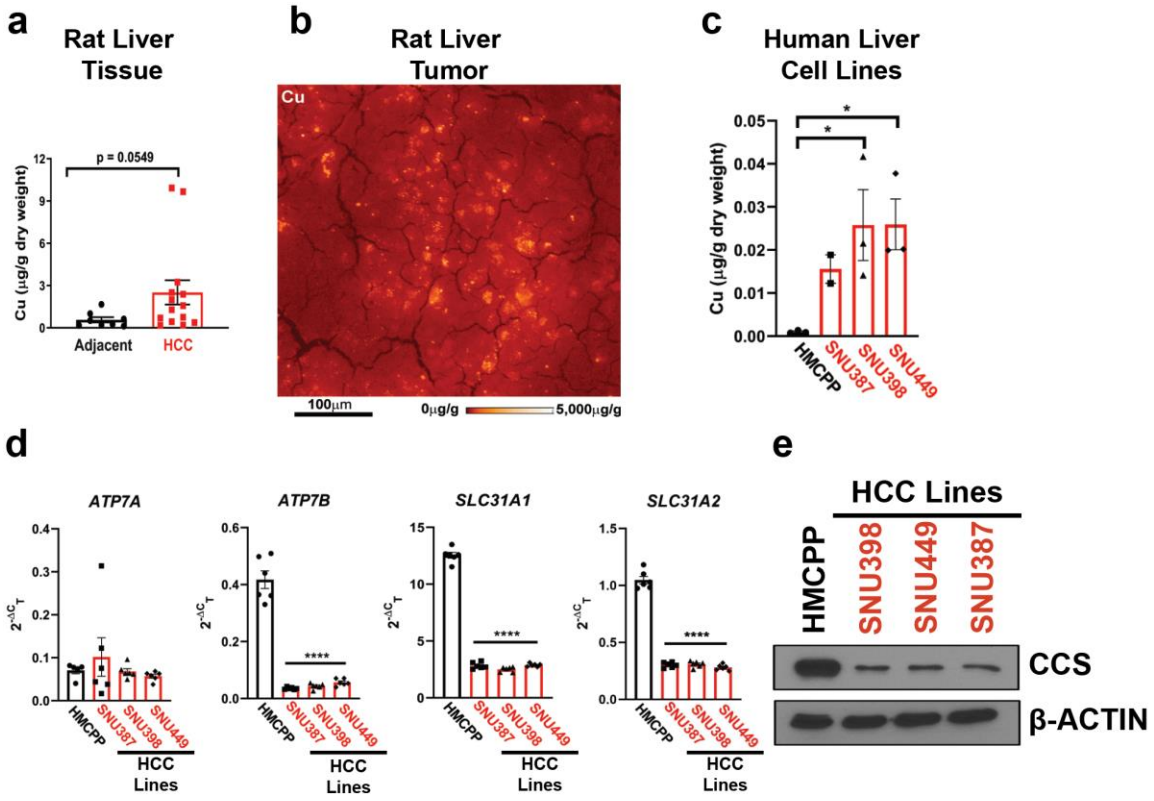

Figure 2.2 Aberrant Cu homeostasis is observed in rat HCC tumors and HCC cell lines. (a) Scatter dot plot of inductively coupled plasma mass spectrometry (ICP-MS) detection with bar at mean Cu (µg/g dry weight) from HCC tumors or adjacent liver tissue from rats per sample dry weight ± s.e.m. n = 8 adjacent liver tissue or n = 14 HCC tumors. Results were compared using an unpaired, one-tailed t-test . (b) XFM elemental distribution for Cu of a representative tumor section. The sections was scanned with 1 µm spot size in x and y. Elemental concentrations are shown using false coloring (red temperature, logarithmic scale). (c) Scatter dot plot of ICP-MS detection with bar at mean Cu (µg/g dry weight) from human liver cell lines per sample dry weight ± s.e.m. n = 3 biologically independent samples. Results were compared using a one-way ANOVA followed by a Tukey's multiple-comparisons test where $*P < 0.0332$. (d) Scatter dot plot with bar at mean ±s.e.m. of $\Delta 2^{-Ct}$ normalized quantitative PCR (qPCR) expression of *ATP7A*, *ATP7B*, *SLC31A1*, and *SLC31A2* mRNA from normal liver cells (HMCPP) or HCC cell lines (SNU387, SNU398, SNU449) (e) Immunoblot detection of CCS or β-Actin from normal liver cells (primary hepatocytes) or HCC cell lines (SNU398, SNU449, or SNU387). *n* = 1 biologically independent experiment.

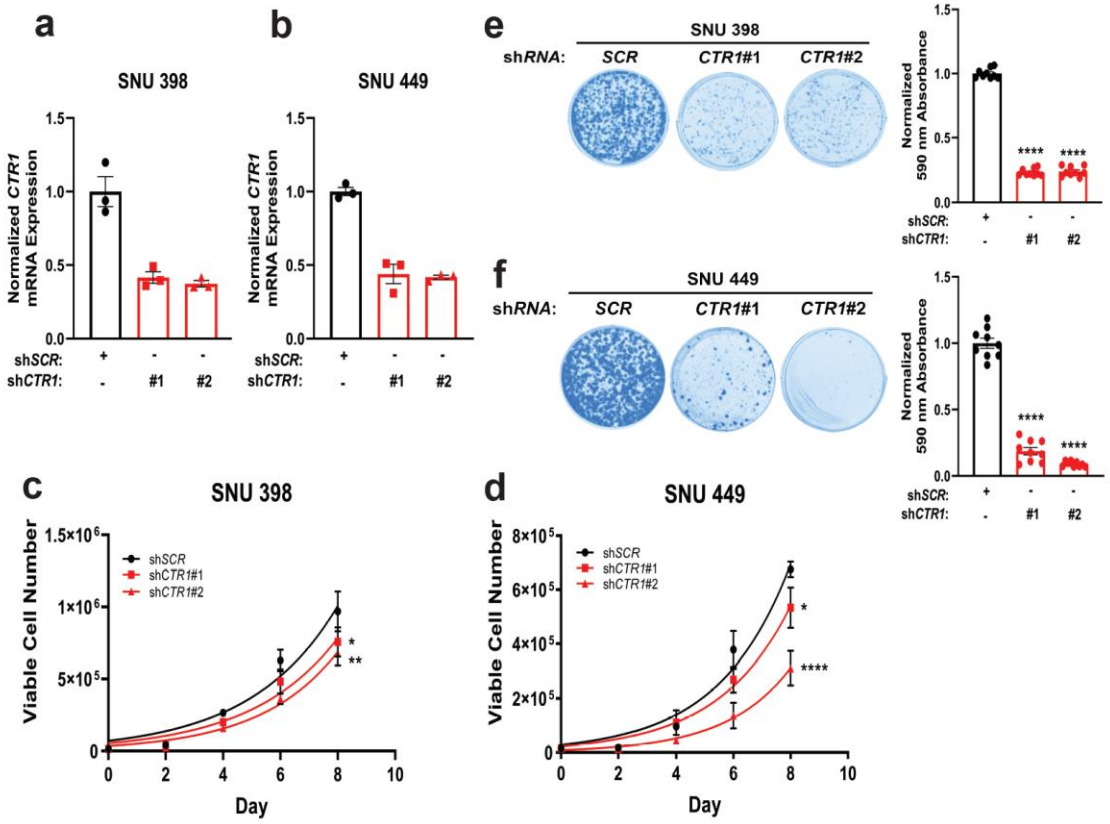

Figure 2.3 Loss of the major Cu transporter *CTR1* reduces tumorigenic properties of HCC. (a and b) Scatter dot plot with bar at mean ±s.e.m. of normalized quantitative PCR (qPCR) expression of *CTR1* mRNA from SNU398 (a) and SNU449 (b) HCC cell lines stably expressing *shRNA* against *CTR1* or a non-targeting scramble sequence (*SCR*). *n* = 1 biologically independent experiment performed in technical triplicate. (c and d) Non-linear fit to the exponential growth equation of cellular proliferation from SNU398 (c) and SNU449 (d) HCC cell lines expressing *shRNA* against *CTR1* or *SCR*. *n* = 3 independent biological experiments, with each experiment plated in technical triplicate. Statistical analysis was performed using a two-way ANOVA followed by Dunnett's multiple comparison test. (e and f) Representative images (left) of crystal violet stained colonies from SNU398 (e) and SNU449 (f) HCC cells expressing *shRNA* against *CTR1* or *SCR*, and scatter dot plot (bottom) of mean absorbance of extracted crystal violet at 590 nm ±s.e.m. of crystal violet staining from three independent experiments plated in technical triplicate. The results were compared using a one-way ANOVA followed by Dunnett's multiple comparison test. **P* < 0.0332, ***P* < 0.0021, ****P* < 0.0002, *****P* < 0.0001.

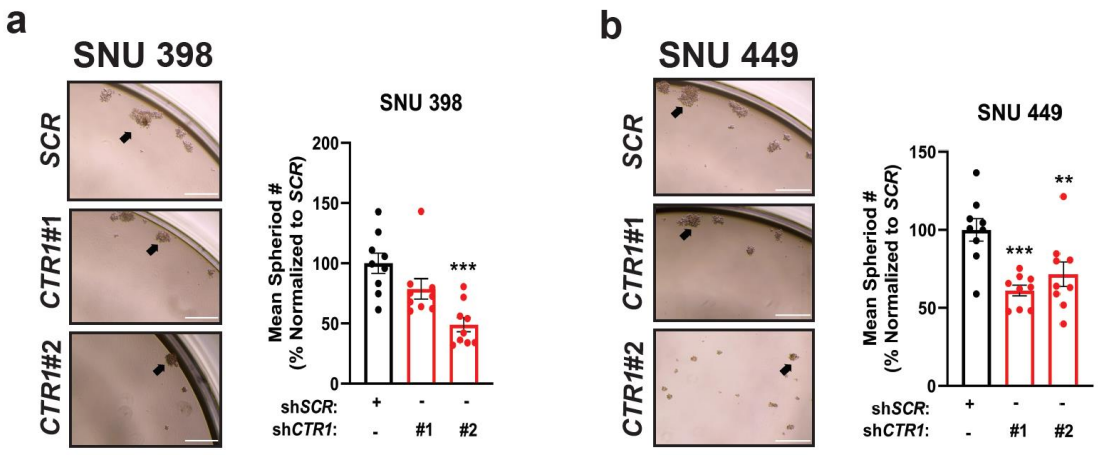

Figure 2.4 Loss of *CTR1* reduces anchorage-independent growth in HCC. (a and b) Representative images of anchorage-independent growth in ultra-low attachment plates in SNU398 (a, left) or SNU449 (b, left) cell lines stably expressing *shRNA* against *CTR1* or *SCR*, with the normalized mean number of spheroids per field of view represented as a scatter dot plot for SNU398 (a, right) and SNU449 (b, right) from n = 9 fields of view per condition from three independent biological experiments. Data was analyzed using a one-way ANOVA followed by Dunnett's multiple comparison test *P < 0.0332, **P < 0.0021, ***P < 0.0002, ****P < 0.0001. 10x magnification, scale bar = 400 µm.

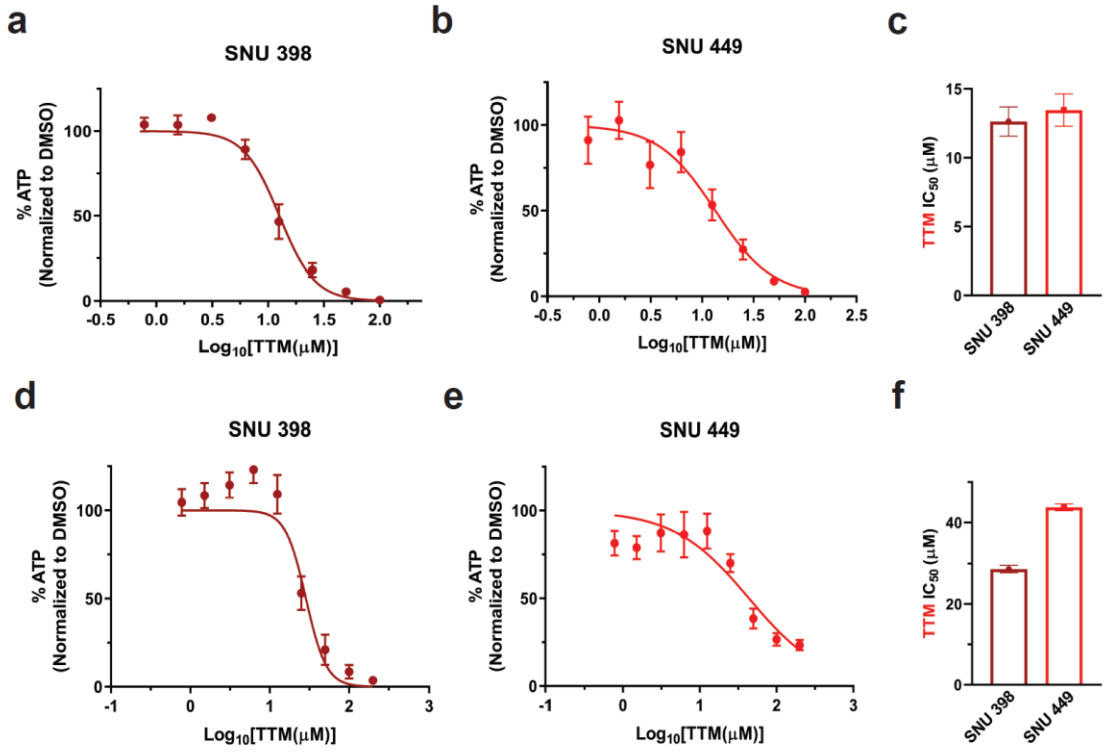

Figure 2.5 TTM, a Cu specific chelator, hinders anchorage-dependent and anchorage-independent growth. (a and b) Relative CellTiter-Glo® cell viability ± s.e.m. of SNU398 (a) or SNU449 (b) HCC cells treated with the indicated concentrations of TTM upon plating in anchorage-dependent (2D) conditions. *n* = 2 independent biological experiments, with each experiment plated in technical triplicate. (c) Bar graph of TTM IC_{50} values from (a) and (b) ± s.e.m. (d and e) Relative CellTiter-Glo 3D® cell viability ± s.e.m. of SNU398 (d) or SNU449 (e) HCC cells treated with the indicated concentrations of TTM upon seeding into ultra-low attachment (3D) plates. *n* = 3 independent biological experiments, with each experiment plated in technical triplicate. (f) Bar graph of TTM IC_{50} values from (d) and (e) ± s.e.m.

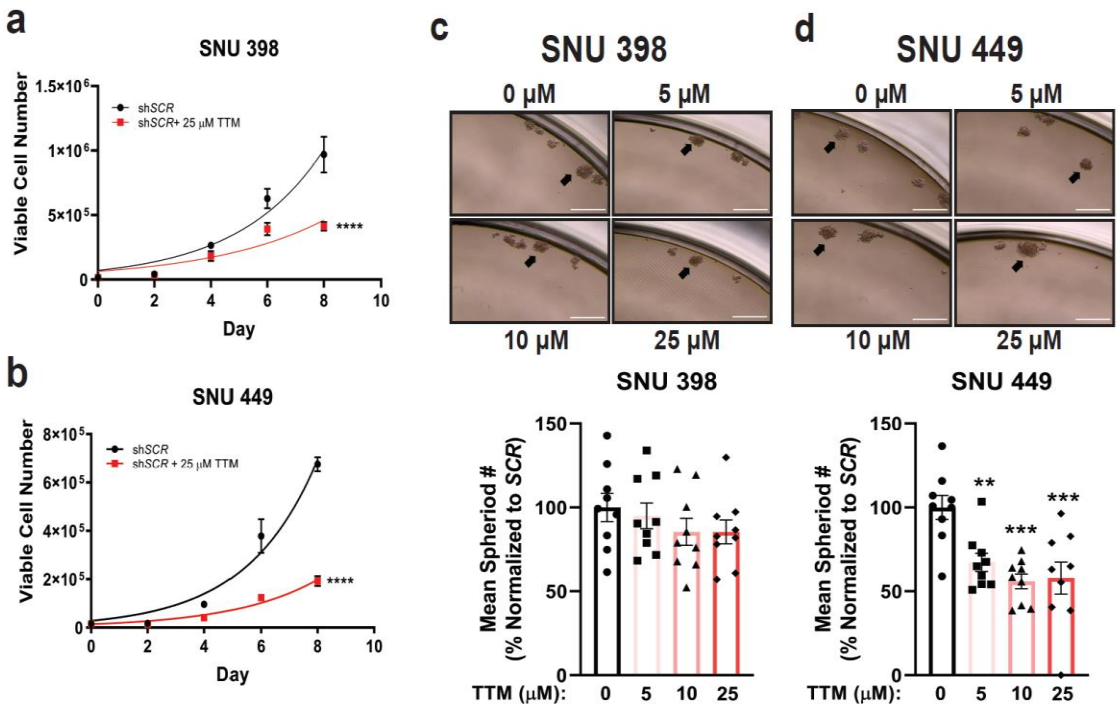

Figure 2.6 TTM reduces cellular proliferation and spheroid formation in HCC cells. (a and b) Non-linear fit to the exponential growth equation of cellular proliferation from SNU398 (a) and SNU449 (b) cell lines, seeded side-by-side with cells in Fig. 2.3c and 2.3d, except treated with 25 μM TTM. *n* = 3 independent biological experiments, with each experiment plated in technical triplicate. Statistical analysis was performed using a two-way ANOVA followed by Dunnett's multiple comparison test. ****$P < 0.0001$. (c and d) Representative images of anchorage-independent growth in ultra-low attachment plates in SNU398 (c, top) or SNU449 (d, top) cell lines treated with the indicated concentration of TTM, with the normalized mean number of spheroids per field of view represented as a scatter dot plot for SNU398 (c, bottom) and SNU449 (d, bottom) from *n* = 9 fields of view per condition from three independent biological experiments. Data was analyzed using a one-way ANOVA followed by Dunnett's multiple comparison test *$P < 0.0332$, **$P < 0.0021$, ***$P < 0.0002$, ****$P < 0.0001$. 10x magnification, scale bar = 400 μm.

CHAPTER 3: HYPOXIA IN COMBINATION WITH THE GENETIC SUPPRESSION OR PHARMACOLOGICAL INHIBITION OF CU IMPORT RESTIRCTS HCC METABOLISM

This Chapter has been reformatted from a submission for publication to *Metallomics:*

Davis, C.I., Gu, X., Kiefer, R.M, Ralle, M., Gade, T.P., and Brady, D.C. Altered copper homeostasis underlies sensitivity of hepatocellular carcinoma to copper chelation. Metallomics. Accepted, October 2020.

Overview

Among the available palliative treatments, TAE or TACE prevail as the favored embolic techniques that interventional radiologists implement when patients present with advanced stage HCC. During this procedure, microsphere beads may be coded in a chemotherapeutic agent to contribute to cancer cell toxicity. Alternatively, patients may be recommended for oral administration of a systemic chemotherapeutic, depending upon several pre-disposing factors. TTM is an FDA-approved Cu chelation agent for the use in mitigating Cu overload in Wilson disease patients, and has shown success as an anti-cancer agent in preclinical and clinical trials of head and neck, breast, and skin cancers. Thus, it is plausible that the combination of TTM with TAE or TACE may be an alternative to prevent refractory disease in HCC. To molecularly dissect this concept using conditions that recapitulate the poorly perfused, embolic-induced microenvironment, the following chapter provides evidence of a novel vulnerability at the intersection of Cu metabolism and glucose metabolism in HCC.

Introduction

Like most cancers, surgical therapies (resection and liver transplantation) and locoregional procedures (radiofrequency ablation) are an effective first line of treatment for localized HCC, with five-year survival rates of up to 60 to 70% (Bruix & Sherman, 2011). Unfortunately, the majority of HCC cases are diagnosed at late stage with only 20% of patients meeting criteria for curative intervention, and the treatment options for intermediate and advanced disease are limited (Terzi et al., 2014). Specifically for intermediate or advanced stage HCC, locoregional therapies including, transarterial embolization (TAE) and transarterial chemoembolization (TACE) (Bruix & Sherman, 2011), which take advantage of obstructing tumor blood supply with or without local chemotherapy, or systemic therapy with sorafenib (Llovet et al., 2008; Sanoff et al., 2016), a small molecule multikinase inhibitor, provide limited survival benefits. If first line therapies fail, second line chemotherapies such as Regorafenib or Nivolumab may be used, though these therapies do not reduce the likelihood of recurrence. Although obstruction of tumor blood flow limits the delivery of oxygen and nutrients to promote cancer cell death, surviving cells contribute to recurrent HCC following TAE or TACE (Gade et al., 2017; Paul et al., 2011; Perkons et al., 2019; Terzi et al., 2014), The local hypoxic environment induced by TAE and TACE stabilizes the oxygen sensitive master transcription factor, hypoxia inducible factor 1 (HIF-1), which upregulates numerous genes in pro-survival pathways, including angiogenesis, migration, invasion, Fe metabolism and glucose metabolism, essential for cancer cell adaptation (Xu et al., 2014). Critically, HCC exemplifies a unidirectional switch to a glycolytic metabolism as compared to normal hepatocytes (Hay, 2016). Thus, there is a great need to discover unique cellular and molecular features of HCC that can be exploited as novel approaches to treat advanced disease and limit resistance. In this work, we demonstrate that the genetic suppression or pharmacologic depletion of bioavailable Cu is sufficient

to lessen hypoxia-induced glycolytic metabolism and impede resultant HCC tumorigenic properties.

Methods

ICP-MS Sample Preparation of Human HCC Cell Lines

Human HCC cell lines were seeded at 2.0 x 10^6 cells in 100mm dishes. After incubation for 48 hours in either 21% O_2 or 1% O_2, cells were washed twice and harvested with 1X Phosphate Buffered Saline. Cell pellets were collected by centrifugation at 2,000 x*g* for 5 minutes, and were flash-frozen in a dry ice-ethanol bath prior to storing at -80°C. All samples were processed by the PADLS New Bolton Center Toxicology Laboratory in the School of Veterinary Medicine at the University of Pennsylvania.

Cell Culture

SNU398, and SNU449 HCC cell lines r were obtained from the American Type Culture Collection (ATCC). Parental cell lines were cultured in Roswell Park Memorial Institute (RPMI 1640, Gibco) Media and supplemented with 10% v/v fetal bovine serum (FBS, GE Lifesciences), 100 U/mL penicillin, and 100 μg/mL streptomycin (Gibco). SNU398 and SNU449 cell lines stably expressing the pLKO.1puro constructs were maintained as above supplemented with 5μg/mL puromycin (Invitrogen). SNU398 and SNU449 were stably infected with lentiviruses derived from the pLKO.1 plasmid (*see* plasmids below) using established protocols. Unless specified, all cell lines were maintained in a humidified Heracell (ThermoFischer Scientific) incubator set to 37°C and 5% CO_2. For hypoxic cell culture, cells were maintained at 37°C and 1% O_2 in Whitley H35 Hypoxystation (Don Whitley Scientific). MycoAlert® mycoplasma test detection kit (Lonza, LT07-418) was used to test for mycoplasma contamination.

Plasmids

pLKO.1puro lentiviral shRNA plasmids were obtained from High-Throughput Screening Core at the University of Pennsylvania to express: nontargeted control (sh*SCR*), human *CTR1* target sequence #1 5'-GATGCCTATGACCTTCTACTT-3' (sh*CTR1*#1), or human *CTR1* target sequence #2 5'-CGGTACAGGATACTTCCTCTT-3' (sh*CTR1*#2).

RT-qPCR

To examine the expression of Cu transporter and glycolytic genes upon hypoxia, 3.0 x 10^5 cells of the indicated HCC cells were seeded into 60mm dishes. Sixteen hours post-seeding, cells were treated with the indicated concentrations of TTM and/or were moved to hypoxic conditions for 48 hours. To isolate RNA, cells were harvested in TRIzol™ reagent (Invitrogen, #15596018) and RNA was extracted following manufacturer's protocol. Purified RNA was reverse transcribed (RT) into cDNA using the Applied Biosystems™ Taqman™ Reverse Transcription Reagents (Applied Biosystems, # N8080234) and corresponding protocol. Subsequent cDNA was loaded onto a clear 384-well plate (Genesee, #24-305) and quantified on a ViiA 7 Real-Time PCR System with standard protocols using the following Taqman™ probes: Hs00163707_m1 to detect human ATPase copper transporter A (*ATP7A*), Hs01075310_m1 to detect human ATPase copper transporter B (*ATP7B*), Hs00977266_g1 to detect human *SLC31A1* (*CTR1*), Hs00156984_m1 to detect human copper transporter 2 *SLC31A2* (*CTR2*), Hs00761782_s1 to detect human pyruvate kinase muscle isoform (*PKM*), Hs01378790_g1 to detect human lactate dehydrogenase A (*LDHA*), Hs00892681_m1 to detect human glucose transporter 1 (*GLUT1*), and Hs00427620_m1 to detect human TATA-binding proteins (*TBP*). The comparative $\Delta\Delta C_t$ method was used to analyze mRNA after transcript levels were normalized to *TBP*.

Reagents

The Cu chelator TTM (#323446) and the crystal violet (# C0775-100G) used for colony staining were purchased from Sigma-Aldrich.

Clonogenic Assay

SNU398 and SNU449 cell lines stably expressing indicated constructs were seeded at 3.0 x 10^3 cells per well in six-well plates. For TTM treatments, cells were treated 24 hours after seeding with either a vehicle or a final indicated concentration of TTM for seven days. For hypoxia (1% O_2) exposures, cells were seeded in normoxic (21% O_2) conditions for 24 hours, and then moved to the hypoxic condition where pre-equilibrated hypoxic media was applied for the remainder of the seven-day incubation time. After incubation for seven days, cells were washed once with 1X Phosphate Buffered Saline (PBS) and stained with 1mL of a crystal violet staining solution (0.5% w/v crystal violet (CV), 20% v/v methanol, distilled water) for 15 minutes. After 15 minutes, all wells were washed three times with distilled water to minimize background staining. CV stained colonies were imaged using a ChemiDoc Touch Imagining System (Bio-Rad). To quantify colony abundance, stained cell colonies were dissolved in a 10% acetic acid solution for 30 minutes at room temperature, and extracted CV was measured at an absorbance of 590nm in a plate reader (Synergy, BioTek).

Measurement of Glucose Consumption and Lactate Production

To determine relative glucose consumption and lactate production, 3.0 x 10^5 cells of the indicated HCC cells were seeded into 60mm dishes (GenClon, #25-260). Approximately 16 hours post-seeding, cells were treated with indicated concentrations of TTM for 48 hours. For hypoxic conditions, cells were moved to the hypoxic condition where pre-

equilibrated hypoxic media was applied for the 48-hour incubation time. Both spent media, collected upon completion of the incubation time, and fresh media, collected at the start of the experiment, were harvested from cell cultures, and following a brief centrifugation (500 x *g* for five minutes), supernatant was transferred to a fresh Eppendorf tube, flash frozen on an ethanol-dry ice bath, and stored at -80°C until further processing. Glucose consumption and lactate production were measured using a YSI2950 immobilized enzyme analyzer from YSI Life Sciences. Prior to sample analysis, the linearity of the analyzer was calibrated using standards from the manufacturer. Metabolite consumption or production was calculated following the cell number area under the curve normalization as previously described. (M. Jain et al., 2012) Briefly, metabolite consumption is defined as $v = V(x_{\text{fresh medium}} - x_{\text{spent medium}})/A$, where v is glucose consumption or lactate production, V is the culture volume used, x is the metabolite concentration, and A is the cell number area under the curve. A is obtained by integrating the final cell count and doubling time across the duration (time) of the experiment. Initial and final cell counts used to determine A were obtained using an automated cell counter.

Results

Genetic Loss of *CTR1* under Hypoxic Conditions Hinders HCC Metabolism

Intriguingly, HCC cells adapt to accommodate the larger energy demands required for rapid growth and proliferation. HCC cells reprogram their glucose metabolism (Hay, 2016) to fulfill these requirements at baseline and upon stress induced by the hypoxic environment driven by the metabolic zonation of the liver (Kang et al., 2018) and treatment-induced ischemia through TAE/TACE (Gade et al., 2017; Kung-

Chun Chiu et al., 2019; Perkons et al., 2019; C. C. L. Wong et al., 2014). In the latter, oxygen-depleted conditions stabilize HIF-1, which induces the transcription of genes in multiple hypoxia response pathways. In particular, HIF-1 elevates the mRNA expression of genes that encode critical glycolytic proteins, such as glucose importer 1 (GLUT1), pyruvate kinase muscle isoform (PKM), and lactate dehydrogenase A (LDHA). It has been well-established that cells under hypoxia survive by relying on glycolytic metabolism to produce ATP. However, questions remain regarding the effects of Cu depletion in a hypoxic environment, which more closely recapitulates the glycolytic state of HCC cells under standard-of-care TAE and TACE treatment. Given the requirement for elevated intracellular Cu levels in HCC cells (Ebara et al., 2003), we investigated whether Cu depletion would alter the metabolic flexibility of HCC cells under hypoxic conditions. To address this question, SNU398 or SNU449 cells harboring stable genetic knockdown of *CTR1* were exposed to hypoxic (1% O_2) or normoxic (21% O_2) conditions and evaluated for expression of key glycolytic genes (**Fig 3.1a,b**). As predicted, exposure to hypoxia for 48 hours significantly induced expression of the glycolytic genes *PKM*, *GLUT1*, and *LDHA*. However, mRNA knockdown of *CTR1* significantly blocked the hypoxia-mediated increase in *GLUT1* transcripts, while also reducing *PKM* or *LDHA* transcripts in SNU398 or SNU449 cells, respectively. These findings that reduced *CTR1* expression decreases the hypoxia-dependent transcription of several glycolytic genes suggest that this response is partly Cu-dependent. In parallel to monitoring glycolytic gene expression upon hypoxic exposure, we investigated whether hypoxia would alter Cu transporter expression in a similar fashion to that previously observed in human pulmonary arterial smooth muscle cells (Zimnicka et al., 2014), murine macrophages (C. White et al., 2009), or rodent intestinal epithelial cells (Xie & Collins, 2011). Similar to previous work, hypoxia exposure significantly elevated transcription of *ATP7A,* but only

illustrated modest changes in *SLC31A1*, *SLC31A2*, and *ATP7B* across both cell lines (**Fig. 3.2a,b**). Notably, this response was further enhanced in the presence of reduced *CTR1* upon hypoxic exposure. Following the trends in the transcriptional data, glucose consumption and lactate production increased upon exposure to hypoxia but significantly decreased upon stable knockdown of *CTR1* in SNU398 and SNU449 cells (**Fig. 3.3c,d**). To examine the functional consequences of a Cu-dependent alteration in metabolic rewiring, we assessed whether SNU398 or SNU449 cells deficient in *CTR1* could survive in a hypoxic environment (**Fig. 3.4a,b**). While *CTR1* knockdown alone was sufficient to significantly reduce clonogenic survival, this effect was further accentuated under hypoxic conditions after seven days. Taken as a whole, a sustained reduction in *CTR1* is sufficient to alter the glycolytic metabolism required to propel the tumorigenic properties of HCC cells undergoing hypoxic stress.

Hypoxia in Combination with TTM Treatment Curtailed HCC Metabolism

To determine whether Cu chelation would alter metabolic flexibility in HCC, SNU 398 and SNU449 cells treated with TTM were exposed to hypoxic or normoxic conditions and expression of key glycolytic genes was evaluated (**Fig. 3.5a,b**). As expected, exposure to hypoxia induced the robust and significant transcription of *PKM*, *GLUT1*, and *LDHA* genes (**Fig. 3.5a,b**). However, treatment with TTM revealed a significant Cu-dependent reduction in *PKM*, *GLUT1*, and *LDHA* when compared to hypoxia treatment alone in SNU398 cells, while trending similarly in SNU449 cells (**Fig. 3.5a,b**). These results agree with a previous study from Feng and colleagues (Feng et al., 2009) that demonstrated that the Cu and Zn chelator tetraethylenepentamine (TEPA) could suppress HIF-1 transcriptional activity and the subsequent expression of hypoxia-responsive genes. Akin to the transcriptional findings from *CTR1* knock down lines, TTM

treatment induced a variable expression pattern in Cu transporter genes across the two HCC cell lines, but significantly increased *ATP7A* mRNA transcripts upon hypoxia exposure alone (**Fig. 3.6a,b**). Next, to assess whether differential oxygen tensions foster differential Cu uptake, we measured intracellular Cu levels using ICP-MS analysis from SNU398 and SNU449 cells after exposure to hypoxia (1% O_2) for 48 hours. Accordingly, intracellular Cu levels were significantly elevated upon hypoxic conditions in SNU398 cells and trended upwards in SNU449 cells (**Fig. 3.6c,d**). These data support the idea that hypoxia induces differential Cu utilization within HCC cells.

Importantly, both glucose consumption and lactate production aligned with the transcriptional findings, as these measurements significantly diminished upon the TTM-hypoxia combination compared to hypoxia exposure alone (**Fig. 3.7a,b**). Hence, these observations indicate that pharmacologic reductions in Cu availability hinder the reprogramming of glucose metabolism in HCC. Finally, to evaluate whether targeting intracellular Cu levels within a hypoxic environment will change HCC tumorigenic properties, we assessed the ability for TTM-treated SNU398 and SNU449 cells to survive under hypoxia upon seeding at low density. TTM treatment alone significantly blunted clonogenic growth in a dose-dependent manner and when combined with hypoxic conditions (**Fig. 3.8a,b**). Taken together, these results support the notion that limiting Cu availability within a uniform hypoxic microenvironment works to restrict both glucose metabolism and survival ability of HCC cells.

Discussion

Importantly, we demonstrated that hypoxia in combination with *CTR1* deficiency attenuated HCC glycolytic metabolism and tumorigenic properties. Importantly, the liver

is one of few organs that maintains an oxygen gradient, however, liver cancers seem to nurture a remarkedly hypoxic environment (Brooks et al., 2004; Leary et al., 2002). Hypoxia is a known driver of oncogenesis and regulates processes including epithelial-to-mesenchymal transition (Higgins et al., 2007), angiogenesis (Du et al., 2008), and invasion (Krishnamachary et al., 2003). Considered in conjunction, manipulating Cu availability may therefore represent a useful approach for modulating one or more of these hypoxic-dependent responses which shape tumorigenesis in HCC.

Here we provide evidence that TTM reduces the hypoxia-induced expression of glycolytic genes, which in turn, reduces both glucose utilization and lactate excretion. Based on previous work, several molecular phenomena may further support the contribution of our findings. Firstly, HCC cells exhibit “metabolic flexibility”, where glucose metabolism is reprogrammed in response to increased demand for biological building blocks required of rapidly proliferating cells or stress associated with the nutrient deprivation induced by TAE or TACE (Perkons et al., 2019). Key elements of liver rewiring include upregulation of *GLUT1*, *LDHA*, and *PKM*, which drive flux through glycolysis and towards lactate production (Hay, 2016). Additionally, the consistent upregulation of *ATP7A* upon hypoxia suggests that liver rewiring may even extend to the reprogramming of trace metal metabolism. Moreover, metabolic flexibility can influence the angiogenic properties of tumors under hypoxia.(Sonveaux et al., 2012) In linking angiogenesis to metabolism, Végran and colleagues provided evidence to assert that lactate is sufficient to promote tumor angiogenesis through the lactate/NF-kB/IL-8 axis (Végran et al., 2011). In accordance with these studies, our data suggest that TTM may reduce tumorigenic properties in the context of hypoxia by significantly blocking glucose consumption and lactate production, which constrains vascularization.

Secondly, findings from Martin *et al.* and Feng *et al.* demonstrate that Cu contributes to the regulation of HIF-1α. Specifically, excessive Cu in the presence of hypoxia resulted in a Cu-dependent enhancement of both HRE-reporter activity and mRNA expression of hypoxia-responsive genes, while Cu chelation with TEPA suppressed these outputs by blocking HIF-1α-mediated interactions (Feng et al., 2009; Martin et al., 2005). Thus, another explanation may be that Cu merely functions to inhibit the upstream negative regulators of HIF-1α, perhaps by competing with iron for binding to prolyl-4-hydroxylases (PHD) enzymes. Finally, while the concentration of TTM required to reduce the tumorigenic properties of HCC cell lines was in the micromolar range, Cu chelation could improve outcomes with locoregional therapies like TACE in which chemotherapy and embolic are applied directly to the tumor vasculature. In conclusion, this work provides genetic evidence of disrupted Cu homeostasis in the context of HCC. Moreover, we have provided a foundation for further exploration of TTM treatment in HCC. Specifically, future studies will focus on the combination of TTM with standard-of-care locoregional therapy, as this pairing may prove a suitable strategy to combat the recurrence observed in a majority of HCC patients.

Chapter 3 Figures

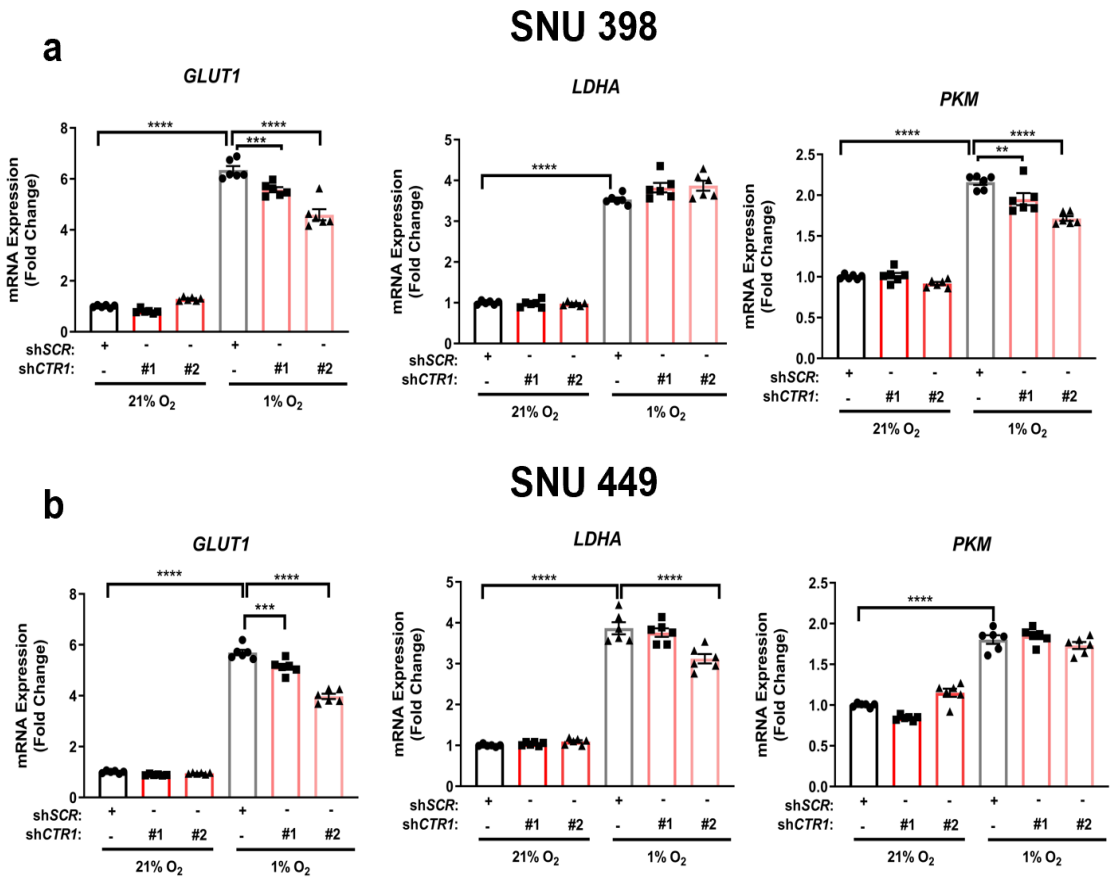

Figure 3.1 Genetic loss of *CTR1* under hypoxic conditions reduces glycolytic gene expression. (a and b) Scatter dot plot with bar at mean ±s.e.m. of normalized quantitative PCR (qPCR) mRNA expression of glycolytic genes from SNU398 (a) and SNU449 (b) cells stably expressing *shRNA* against *CTR1* or a non-targeting scramble sequence (*SCR*) with exposure to hypoxic (1% O_2) for conditions for 48 hours. *n* = 3 biologically independent experiments performed in technical duplicate. Statistical analysis was performed using a one-way ANOVA followed by Tukey's multiple comparison test. **P* < 0.0332, ***P* < 0.0021, ****P* < 0.0002, *****P* < 0.0001.

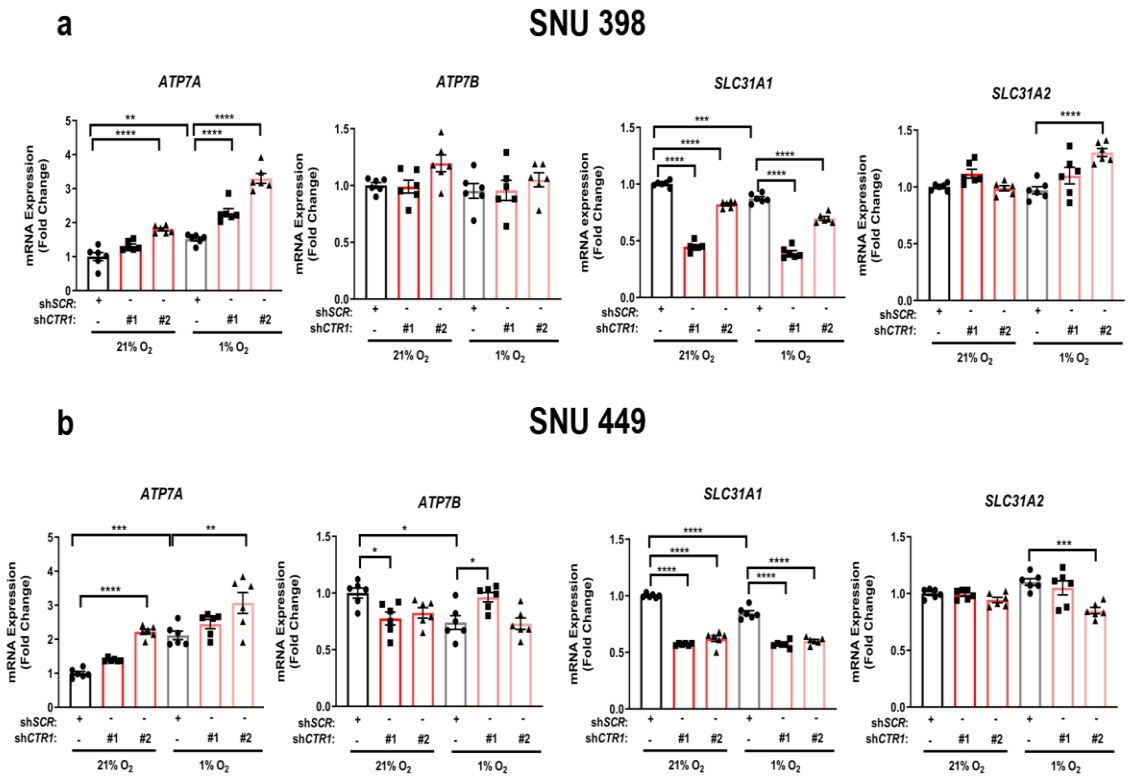

Figure 3.2 Genetic loss of *CTR1* under hypoxic enhances *ATP7A* expression. (a and b) Scatter dot plot with bar at mean ±s.e.m. of normalized quantitative PCR (qPCR) mRNA expression of Cu transporter genes from SNU398 (a) and SNU449 (b) cells stably expressing *shRNA* against *CTR1* or a non-targeting scramble sequence (*SCR*) with exposure to hypoxic (1% O_2) for conditions for 48 hours. *n* = 3 biologically independent experiments performed in technical duplicate. Statistical analysis was performed using a one-way ANOVA followed by Tukey's multiple comparison test. **P* < 0.0332, ***P* < 0.0021, ****P* < 0.0002, *****P* < 0.0001.

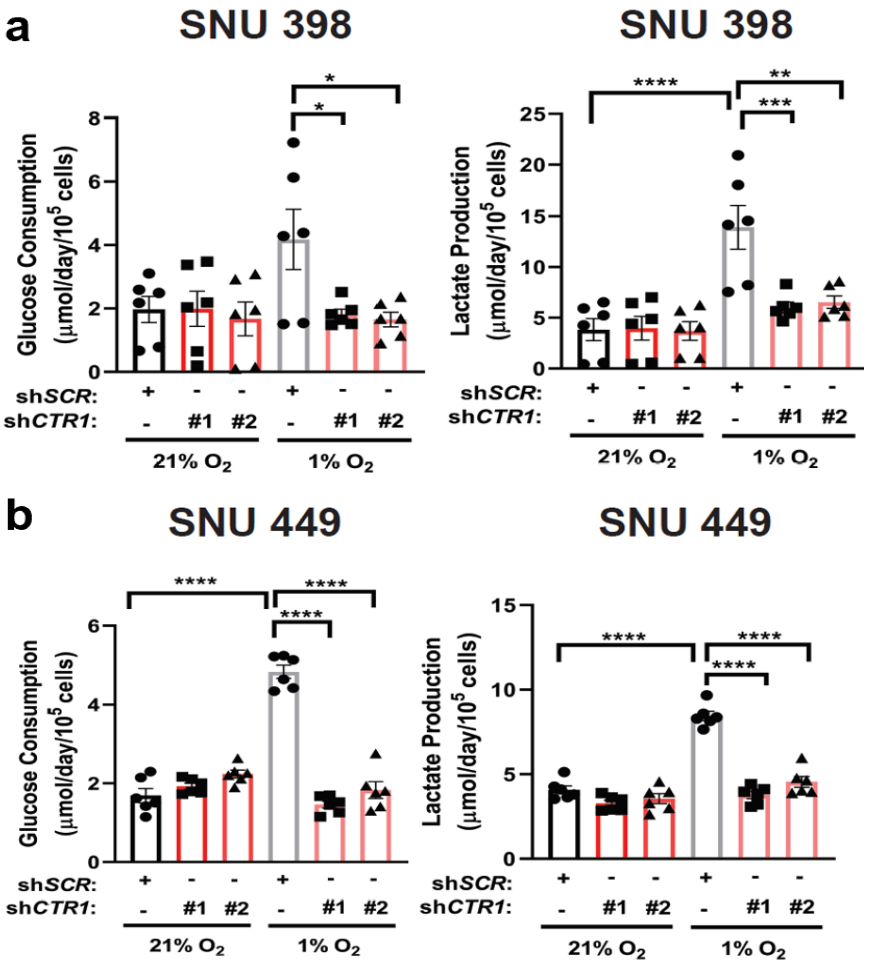

Figure 3.3 Genetic loss of *CTR1* under hypoxic conditions blunts glucose uptake and lactate production. (a and b) Scatter dot plot with bar at mean ±s.e.m. of glucose consumption (left) or lactate production (right) rates from SNU398 (c) and SNU449 (d) cells stably expressing *shRNA* against *CTR1* or a non-targeting scramble sequence (*SCR*) with exposure to hypoxic conditions for 48 hours. *n* = 3 biologically independent experiments performed in technical duplicate. Statistical analysis was performed using a one-way ANOVA followed by Tukey's multiple comparison test. **P* < 0.0332, ***P* < 0.0021, ****P* < 0.0002, *****P* < 0.0001.

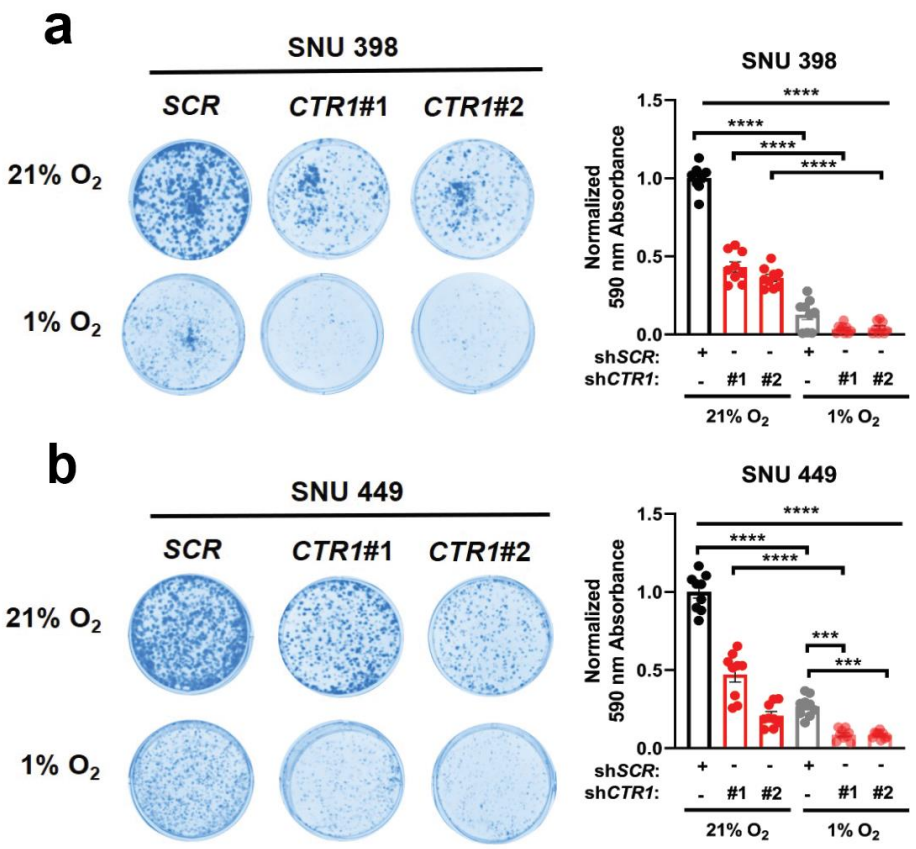

Figure 3.4 Genetic depletion of *CTR1* diminished clonogenic survival upon hypoxia exposure. (a and b) Representative images (left) of crystal violet stained colonies from SNU398 (a) and SNU449 (b) cells stably expressing *shRNA* against *CTR1* or a non-targeting scramble sequence (*SCR*) in normoxic (21% O_2) or (1% O_2) hypoxic conditions for seven days and scatter dot plot (right) of mean absorbance of extracted crystal violet at 590 nm ±s.e.m. of crystal violet staining from three independent experiments plated in technical triplicate. Statistical analysis was performed using a one-way ANOVA followed by Tukey's multiple comparison test. **P* < 0.0332, ***P* < 0.0021, ****P* < 0.0002, *****P* < 0.0001.

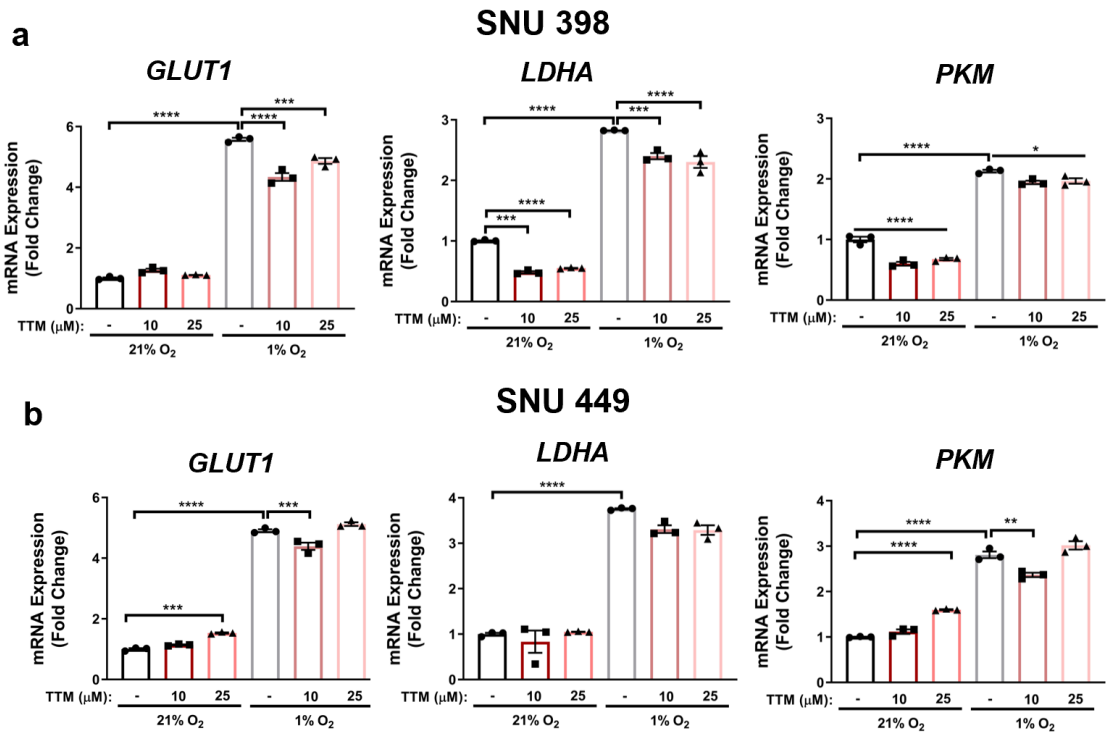

Figure 3.5 Hypoxic conditions in combination with TTM alter glycolytic gene expression. (a and b) Scatter dot plot with bar at mean ±s.e.m. of normalized quantitative PCR (qPCR) mRNA expression of glycolytic genes from SNU398 (a) and SNU449 (b) cells upon treatment with 10 μM or 25 μM TTM or exposure to hypoxic (1% O_2) conditions for 48 hours. Representative *n* of three biologically independent experiments performed in technical triplicate. Statistical analysis was performed using a one-way ANOVA followed by Tukey's multiple comparison test. *P < 0.0332, **P < 0.0021, ***P < 0.0002, ****P < 0.0001.

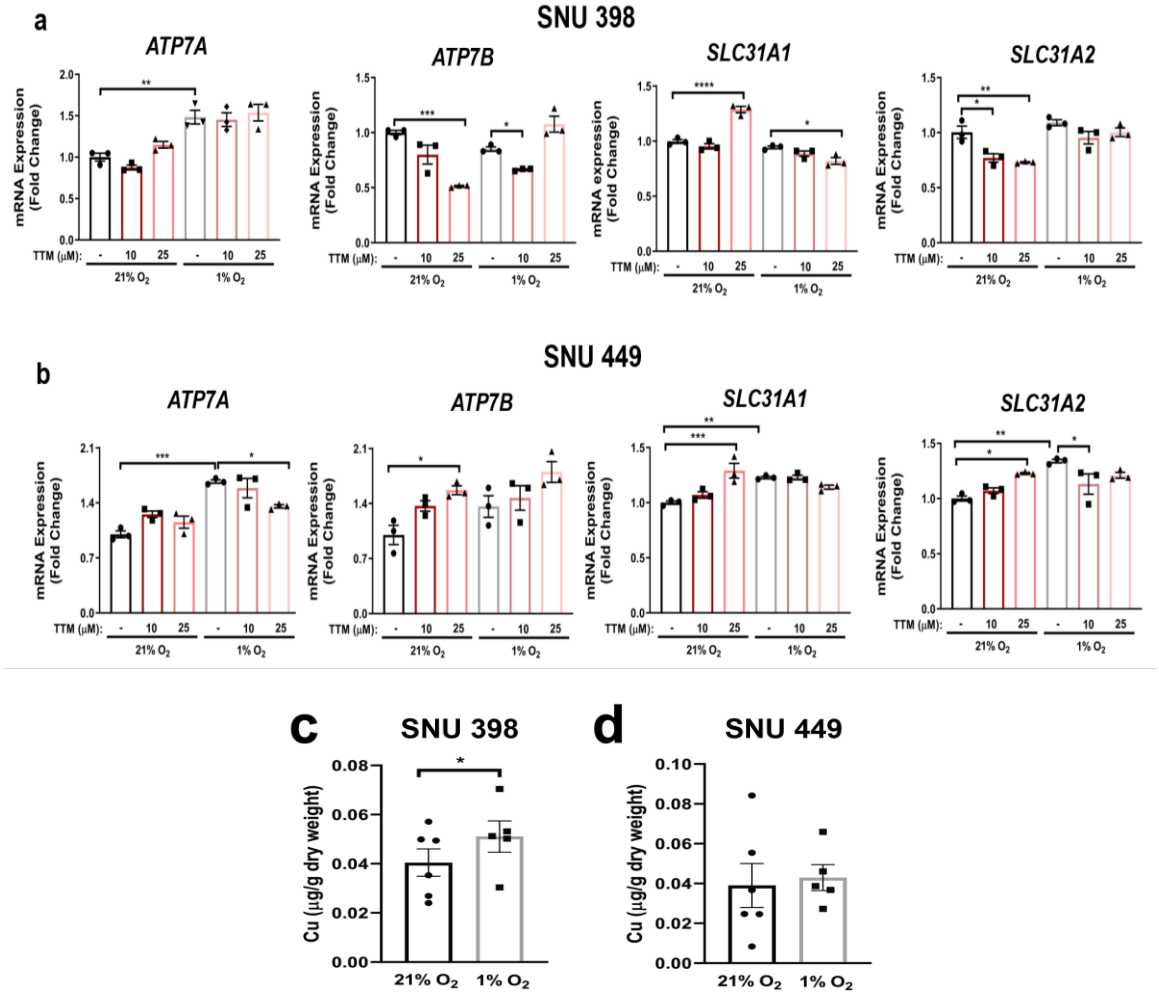

Figure 3.6 Hypoxic conditions in combination with TTM induce *ATP7A* gene expression and Cu uptake. (a and b) Scatter dot plot with bar at mean ±s.e.m. of normalized quantitative PCR (qPCR) mRNA expression of Cu transporter genes from SNU398 (a) and SNU449 (b) cells upon treatment with 10 μM or 25 μM TTM or exposure to hypoxic (1% O_2) conditions for 48 hours. Representative *n* of three biologically independent experiments performed in technical triplicate. Statistical analysis was performed using a one-way ANOVA followed by Tukey's multiple comparison test. **P* < 0.0332, ***P* < 0.0021, ****P* < 0.0002, *****P* < 0.0001. (c and d) Scatter dot plot of ICP-MS detection with bar at mean Cu (μg/g dry weight) from SNU398 (c) and SNU449 (d) HCC cell lines exposed to normoxic or hypoxic conditions. *n* = 6 biologically independent experiments performed and statistical analysis was performed with a paired, two-tailed student t-test *P = 0.0257.

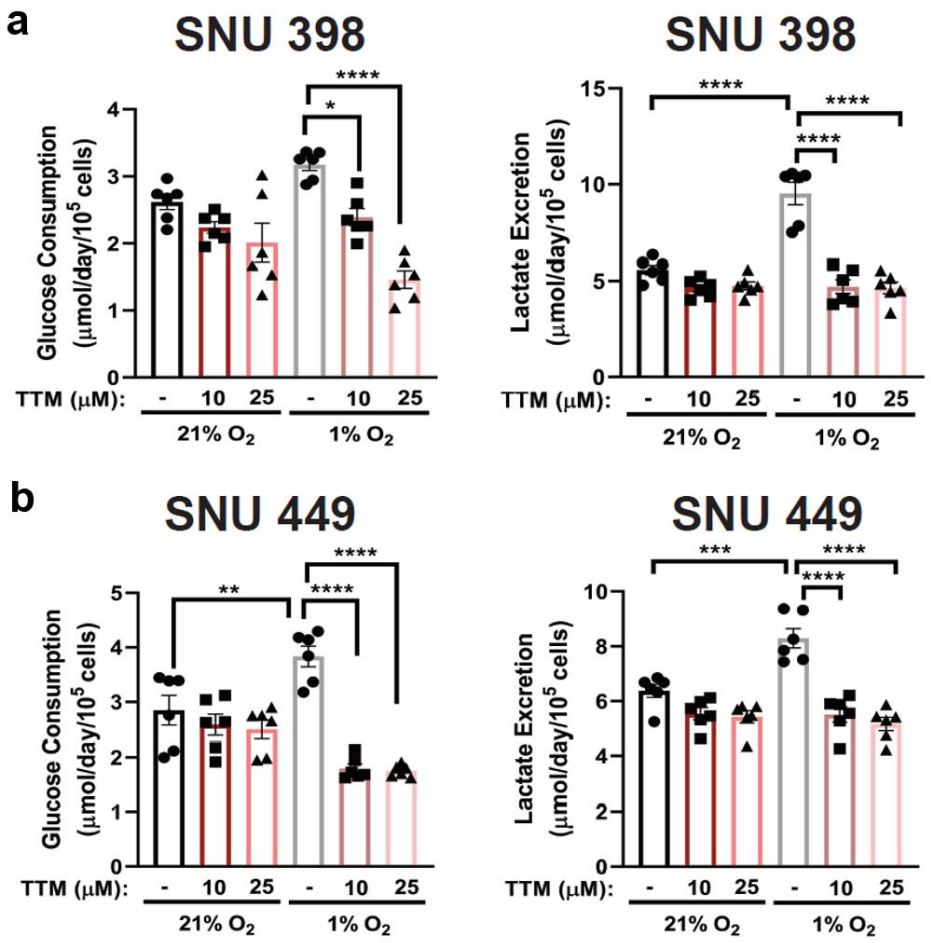

Figure 3.7 Hypoxia in combination with TTM restricts HCC glycolytic metabolism. (a and b) Scatter dot plot with bar at mean ±s.e.m. of glucose consumption (left) or lactate excretion (right) rates from SNU398 (a) and SNU449 (b) cells upon treatment with 10 μM or 25 μM TTM or exposure to hypoxic conditions for 48 hours. *n* = 3 biologically independent experiments performed in technical duplicate. Statistical analysis was performed using a one-way ANOVA followed by Tukey's multiple comparison test. **P* < 0.0332, ***P* < 0.0021, ****P* < 0.0002, *****P* < 0.0001.

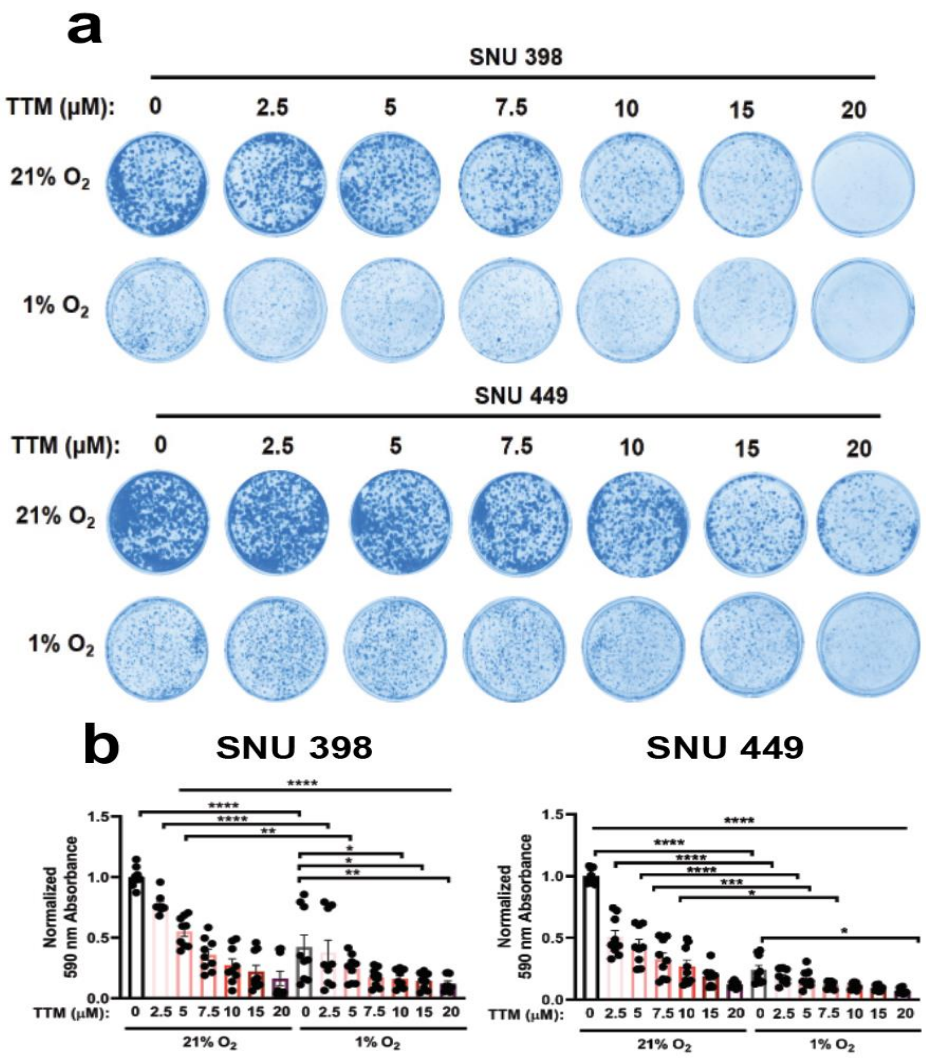

Figure 3.8 TTM attenuated clonogenic survival upon hypoxia exposure. (a) Representative images of crystal violet stained colonies from SNU398 (top) and SNU449 (bottom) HCC cells treated with vehicle (DMSO) or increasing concentrations of TTM in normoxic (21% O_2) or hypoxic conditions for seven days of three independent experiments plated in technical triplicate. (b) Scatter dot plot of mean absorbance of extracted crystal violet at 590 nm ±s.e.m. of crystal violet staining experiments in (a). Statistical analysis was performed using a one-way ANOVA followed by Tukey's multiple comparison test. *P < 0.0332, **P < 0.0021, ***P < 0.0002, ****P < 0.0001.

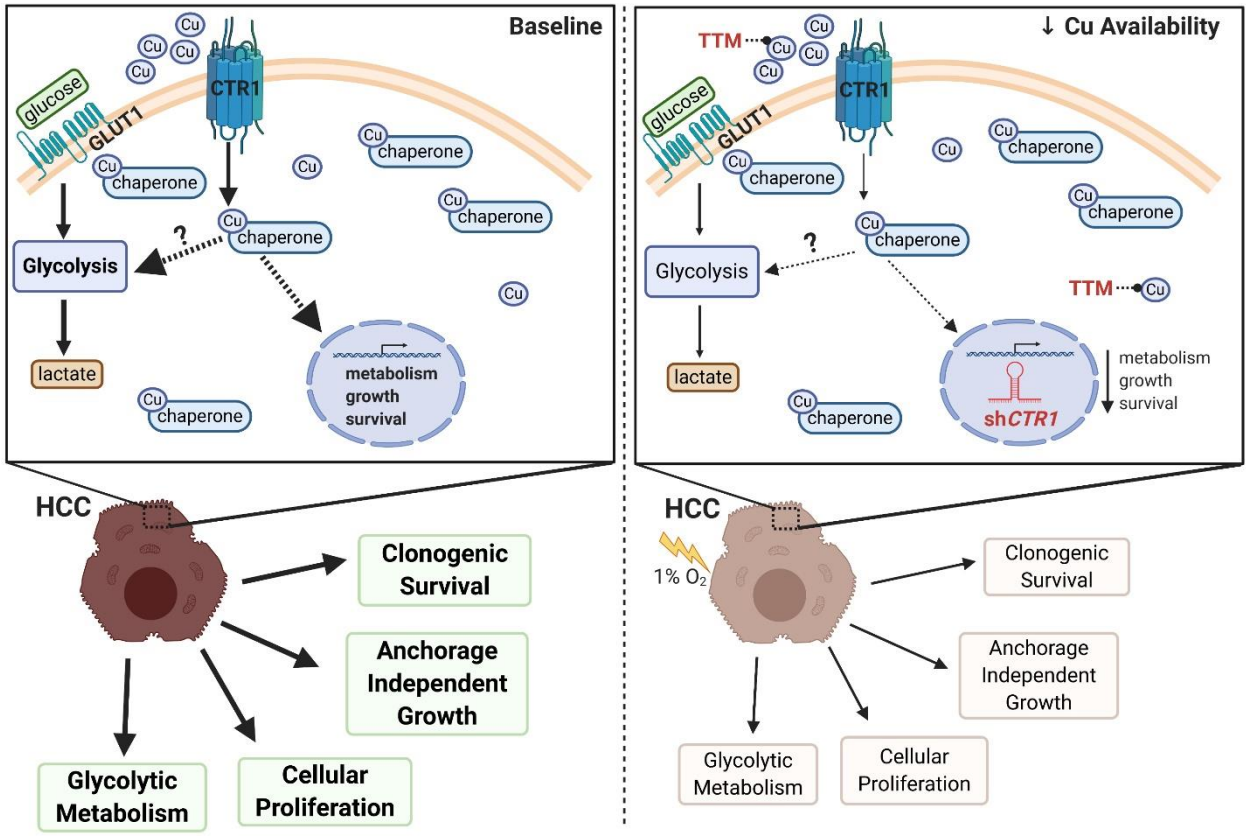

Figure 3.9 Altered copper homeostasis underlies sensitivity of HCC to copper chelation. In glycolytic-addicted HCC cells, bioavailable Cu fuels oncogenic pathways that drive tumorigenesis. Intriguingly, genetic manipulation or pharmacologic inhibition of intracellular Cu diminishes hypoxia-induced glycolytic metabolism and attenuates HCC tumorigenic properties.

CHAPTER 4: FUTURE DIRECTIONS FOR INVESTIGATING THE LINK BETWEEN CU HOMEOSTASIS AND CELLULAR METABOLISM IN HCC

Overview

After discovering that HCC cells increase tumoral Cu uptake, and that depleting Cu availability results in reduced glycolytic output in HCC cells, several questions remain unanswered. In light of the upregulation of *ATP7A* and downregulation of *ATP7B*, *CTR1*, and *CTR2* transcripts in HCC cells, what is the mechanism for Cu accumulation by these cells? Considering the modest Cu-dependent reductions in glycolytic gene expression, hypoxia-induced glycolytic metabolite utilization was greatly reduced in HCC cells. Although these transcriptional changes may contribute to the downstream effects, it is more probable that a Cu-dependent regulation exists within glycolysis at the biochemical level. These data beg the question: what glycolytic protein or upstream factor regulating a glycolytic protein have the potential to be modified by Cu? Despite preliminary experiments that uncovered a unique vulnerability under hypoxic conditions, nutrient deprivation in combination with a hypoxic environment would further recapitulate the microenvironment of HCC tumor cells exposed to TAE/TACE treatment. Thus, potential experiments distinguishing the essentiality of Cu under low oxygenation versus nutrient deprivation will be discussed. Most excitingly, the question of whether TTM will add a survival benefit to patients receiving TAE/TACE still remains to be answered. Therefore, we will describe a study design for a preclinical undertaking on the use of Cu chelation in combination with TAE treatment.

Defining the Mechanism for Cu Uptake by HCC Tumors

Importantly, we provided evidence from a DEN-induced rat model of HCC illustrated that HCC tumors exhibit elevated levels of total intracellular Cu when compared to adjacent liver parenchyma. This evidence was further corroborated by Cu levels measured from primary hepatocytes and HCC cell lines. Our findings validate those previously described in the literature, however, this Cu phenomenon is not only limited to HCC since significant elevations in Cu levels have been observed in both serum and tissue of breast, ovarian, stomach, and colorectal cancer patients (Gupte & Mumper, 2009). These observations draw attention to an intriguing question: is elevated Cu the cause of carcinogenesis or are malignant cells adapting such that high intracellular Cu is simply the consequence? Thus, we propose several narrower lines of investigation that, if answered, may solve this over-arching "cause-versus-consequence" question.

In trying to explain our findings, we monitored the mRNA expression of Cu exporters *ATP7A* and *ATP7B* as well as the Cu importers *CTR1* (*SLC31A1*) and *CTR2* (*SLC31A2*) (**Fig. 2.2d**). Because HCC cells downregulated *CTR1*, *CTR2*, and *ATP7B* in comparison to normal hepatocytes, the question of increased Cu uptake becomes more complex since transcriptional evidence would suggest that the factors mediating Cu export and Cu import are both reduced. Therefore, more experiments exploring the regulation of Cu transporters must be performed to determine a complete mechanism. One may begin with a simple experiment where Cu transporter protein expression is compared between HCC cell lines and normal hepatocytes. Based on these results, protein stability of differentially expressed Cu transporters may be examined by applying cycloheximide, an inhibitor of translation, to hepatocytes and HCC cells at various time points (Buchanan et al., 2016). In addition to determining if protein abundance is sufficient to support Cu uptake, experiments should be conducted to observe the

subcellular localization or trafficking of Cu transporters. For example, the Cu-ATPase ATP7A, which shows expression across all tissues, translocates from the trans-Golgi network to the plasma membrane when Cu concentrations are elevated (M. J. Petris et al., 1996). The ATP-requiring Cu transporter pump ATP7B demonstrates differential localization in response to Cu levels as it is present in the trans-Golgi network at physiological concentrations but fuses to endolysosomal compartments or vesicles that localize to apical membranes to remove excess Cu (Hasan et al., 2012). CTR2 localizes to vesicular compartment membranes to import Cu into the cytosol as a response to Cu shortage (Rees et al., 2004). To determine whether Cu transporter subcellular localization differs between normal hepatocytes and HCC cells, ATP7A or ATP7B may be visualized through immunofluorescence microscopy in tandem with protein markers for the plasma membrane, TGN, and endosomes. To validate these visualizations, an orthogonal technique such as subcellular fractionation followed by immunoblot should also be conducted. To determine whether there is a redistribution of Cu in HCC cells compared to hepatocytes precursors, recent advances in direct elemental analysis via ICP-MS from soluble, insoluble, and membrane-bound subcellular compartments would provide this insight (Genoud et al., 2017). To measure the rate of Cu uptake, HCC cells may be supplemented with radiolabeled ^{64}Cu, chased at several time points, and processed for analysis by ICP-MS. Moreover, the Cu^{+}-specific fluorescent sensor CF4 would also be helpful in visualizing labile pools of Cu across cellular compartments (T. Xiao et al., 2018). Taken together, these proposed experiments should provide details surrounding the regulation of Cu uptake in carcinogenic versus healthy liver cells.

Interestingly, a similar pattern of expression was discovered in HCC patients, however, an upregulation of *ATP7A* accompanied these changes. However, the biological consequence of this increase is not clear. ATP7B is the major isoform

expressed in adult hepatocytes, however, ATP7A expression occurs in liver tissues during embryogenesis and trace levels are detected in adult liver (Lenartowicz et al., 2010). Considering this in conjunction, perhaps HCC cells are either adapting a more embryogenic-like transcriptional program or the HCC tumor cells sampled resemble a cancer stem cell or hepatocyte progenitor phenotype. If differences in Cu levels cannot be attributed to differential expression, abundance, or localization of Cu transporters, then this would suggest an alternative Cu import mechanism. Recent findings from mutant KRAS colorectal cancer (CRC) revealed that these cells modulate Cu import via macropinocytosis (Aubert et al., 2020). HCC cells scavenge nutrients by internalizing exosomes released by neighboring cells through multiple modes of endocytosis including macropinocytosis (R. Chen et al., 2019). Thus, to test if HCC cells facilitate intracellular Cu delivery through this non-canonical form of Cu import, it should first be confirmed that HCC cells enhance macropinocytic uptake (relative to hepatocytes) by measuring the uptake of tetramethylrodamine (TMR)-conjugated dextran in the presence or absence of the macropinocytic inhibitor 5-(N-ethyl-N-isopropyl) amiloride (EIPA). If HCC cells respond with increased rates of TMR uptake, measurements of Cu availability should be conducted. Namely, the Cu-dependent degradation of CCS should be measured via immunoblot, and the mean fluorescence of the ratiometric FRET Cu sensor FCP-1 should be imaged and quantitated with confocal fluorescence microscopy. In addition to macropinocytosis intersecting with Cu metabolism, shared Cu-Fe transport proteins may also influence Cu uptake. A recent study implicated STEAP4 as a promoter of colon tumorigenesis through a mechanism where enhanced Cu uptake activates NF-kB signaling to inhibit apoptosis and drive metastasis in the presence IL-17 (Liao et al., 2020). Through a series of molecular techniques and omics-based approaches, the major Fe transporter DMT1 was highly expressed in and pivotal to the tumorigenesis of

CRC (Xue et al., 2016). Moreover, evidence from esophageal adenocarcinoma patient samples demonstrated overexpressed DMT1 transporter mRNA, and showed significant immunoreactivity for TfR1 and DMT1 in Barrett's metaplasia but not normal esophageal tissue (Boult et al., 2008). From the GENT2 cancer genomic data set, we observed an increase in *STEAP2* expression, and a decrease in *STEAP3* and *STEAP4* expression (**Fig 4.1a**), while also observing a significant increase in *DMT1* expression in liver cancer (**Fig 4.1b**). Of particular note, DMT1 functions as a physiologically relevant Cu+ importer in addition to its function as an Fe importer (Arredondo et al., 2003). Hence, future studies surrounding the role of Fe/Cu shared delivery systems may be helpful to define their contributions to aberrant Cu concentrations observed in HCC.

Methods

Data Mining

STEAP1, *STEAP2*, *STEAP3*, *STEAP4*, and *DMT1* mRNA expression in normal or tumor liver tissue samples was obtained from the Gene Expression across Normal and Tumor tissue (GENT2) web-based genome database (http://gent2.appex.kr/gent2/, Korean Research Institute and Biotechnology). A total of n = 215 normal and n = 517 tumor liver tissue samples were used for analysis.

Determining the Glycolytic Enzyme(s) Responsible for the Metabolic Sensitivity Observed When Cu Availability is Reduced

Introduction

A key finding from this thesis project was that the hypoxia-induced glycolytic utilization in HCC cells was diminished in the presence of a Cu chelator or through a genetic block in Cu import. Although previously thought to function as a structural or

catalytic cofactor, recent work has described a role for Cu as a signaling molecule important for modulation of neuronal circuit spontaneous activity (Dodani et al., 2014), enhancement of oncogenic MAPK signaling (D. C. Brady et al., 2014; M. L. Turski et al., 2012), and inhibition of a cyclic-AMP (cAMP) dependent lipolysis enzyme (Krishnamoorthy et al., 2016). In light of these findings and those presented in Chapters 2 & 3 of this thesis, we sought to further investigate the Cu-mediated regulation of glycolysis by determining if a novel interaction exists between Cu and glycolytic enzymes, or their upstream mediators, in both non-transformed and cancerous liver cells. To begin to dissect this question, we performed an *insilico* screen using the publicly available Basic Local Alignment Search Tool (BLAST) from the National Center for Biotechnology Information (NCBI) to identify kinase sites that matched the predicted MEK1/2 Cu-binding sites. Additionally, we conducted an extensive literature review to determine whether information linking kinases and Cu had been published previously. This search acknowledged that several metabolic kinases were Cu-binding, and of particular interest, that the kinase pyruvate kinase muscle isoform (PKM) was at the forefront. More specifically, a study characterized the Cu and Zn metalloproteomes from human hepatoma lines using an Immobilized Metal Affinity Chromatography (IMAC) screen approach (She et al., 2003). Whole cell extract was applied to either Cu or Zn loaded columns, and followed by an on-column tryptic digest after which the eluent was subjected to tandem MS to identify peptide sequences. Upon peptide mapping, PKM1/2 was one of a several metabolic enzymes that was identified (She et al., 2003). This group identified a putative N-terminal HXXHXXH motif within PKM1/2, and then speculated that this motif had potential Cu-binding capabilities. Preliminary data from our lab and others demonstrates that Cu may also interact with PKM1/2 at cysteine residues, some of which lie near key structural components of PKM1/2. Taking these

findings into account, we asked: what exactly is PKM1/2 and how does if function in biology?

PKM1/2 are splice isoforms resulting from a mutual exclusive alternative splicing event of the *PKM* gene. Both isoforms catalyze the transphosphoryation between phosphoenolpyruvate (PEP) to adenosine diphosphate (ADP) to yield pyruvate and ATP. Pyruvate in the cytosol can be converted into lactate via lactate dehydrogenase (LDH), or can be transported into the mitochondria where it can be converted into acetyl-CoA via the pyruvate dehydrogenase complex (PDH) or oxaloacetate via pyruvate carboxylase (PC). Understanding that the pyruvate generated from this final step in glycolysis serves as the center of carbon metabolism, it is critical to regulate the pyruvate kinase (PK) step. Of note, the PKM2 enzyme has been implicated in metabolic reprogramming of HCC. Specifically, the PKM2 isoform is inherently less active than the PKM1 isoform, which is constitutively expressed as a tetramer (Vander Heiden et al., 2010). On the contrary, PKM2 may exist as a monomer, dimer, or tetramer depending upon the metabolic needs of the cell. Association between the dimeric and tetrameric states is highly regulated by several site-specific post-translational modifications including acetylation (Lv et al., 2011) and phosphorylation (Hitosugi et al., 2009), which function to inhibit its enzyme activity in these contexts. Further regulation by upstream glycolytic intermediates or byproducts such as fructose-1,6-bisphosphate (FBP) (Dombrauckas et al., 2005) or serine (Chaneton et al., 2012) allosterically activate PKM2 to form the fully active tetramer. These multiple layers of regulation have proved crucial to understanding the role of PKM2 in the context of cancer metabolism, as this enzyme was previously regarded as a metabolic “housekeeping” protein.

However, a landmark paper in *Nature* demonstrated an exclusive expression of PKM2 and simultaneous absence of PKM1 in cancerous or transformed cell lines (Christofk et al., 2008). Moreover, the authors demonstrated that tumor burden and tumor volume increased significantly in mice genetically engineered to exclusively express PKM2 when compared to mice exclusively expressing PKM1. In addition to the cancers characterized by Christofk et al., preferential expression of PKM2 is commonly observed in HCC as PKM2 overexpression is associated with poor prognosis (Z. Chen et al., 2015; Hu et al., 2015) and early recurrence in HCC patients (Tai et al., 2016; C. C.-L. Wong et al., 2014). Although one preclinical study explored Cu chelation as a treatment option for HCC (Yoshii et al., 2001), the role of Cu chelation in combination with the standard-of-care therapy, TACE, has yet to be elucidated. Understanding that: a) TACE therapy drives a hypoxic-induced metabolic reprograming, b) PKM2 is a key factor underlying HCC tumorigenesis, and c) Cu has been previously implicated in the tumorigenesis of other cancers, targeting PKM2 through its interaction with Cu may elucidate a context-specific, novel vulnerability that may be effective in limiting the recurrence of HCC in patients after TACE treatment.

HCC Cells Depend on PKM2 for Tumorigenic Properties as PKM2 Expression is Associated with Unfavorable Outcomes in Liver Cancer Patients

Imperatively, the contribution of physiological Cu levels to glycolytic metabolism in HCC patients and the molecular mechanism that may underlie this proposed link remains unclear. Before investigating the Cu-mediated role of PKM2 regulation in glycolysis, we first sought to validate the relevance of PKM2 to HCC development and tumorigenesis. Exploring the publicly available cancer genome database GENT2, we evaluated the mRNA expression of *PKLR*, the PK isozyme predominantly expressed in

normal liver tissue and red blood cells, and *PKM*, the PK isoform preferentially expressed by cancers including HCC (Mendez-Lucas et al., 2017; C. C.-L. Wong et al., 2014). We observed that expression of *PKM* was significantly higher in liver cancer, while *PKLR* expression was significantly reduced (**Fig 4.2a**). Following these results, we interrogated the relationship between liver cancer patient survival and level of RNA expression of *PKM* using the TCGA Pan Cancer Atlas data set obtained from the protein web-based platform The Human Protein Atlas (**Fig 4.2b**). Patients were categorized as having high or low *PKM* expression if *PKM* expression exceeded or fell below the 9.62 FPKM (median expression, number fragments per kilobase of exon per million reads), respectively. Strikingly, liver cancer patients that expressed high levels of *PKM* had a significantly worse survival outcome when compared to patients with low *PKM* expression as demonstrated by a median survival of ~30 months compared to ~60 months in the low *PKM* expression group. To complement these transcriptional findings, we further explored PKM protein expression in normal and tumor liver tissues deposited in The Human Protein Atlas. Importantly, immunohistochemical analysis confirmed elevated expression of PKM from liver cancer tissue but did not detect expression in normal hepatocytes (**Fig 4.2c**). Taken together, the combined results of these genomic and proteomic open-access cancer databases align with previous reports of an unfavorable association between PKM2 expression and HCC tumorigenesis and metastasis (Hu et al., 2015; W. R. Liu et al., 2015; C. C.-L. Wong et al., 2014). To start uncovering a molecular mechanism that would connect Cu content to PKM2 regulation in HCC, we validated PKM2 protein expression by immunoblot from either primary hepatocytes (HMCPP) or established HCC cell lines (SNU398, SNU449, SNU387). Remarkably, we observed a complete absence of PKM2 expression in the hepatocytes, and moreover, did not detect PKLR expression in the HCC lines (**Fig 4.2d**). Additionally,

the enhanced human Telomerase Reverse Transcriptase (TERT) expression reported from a large proportion of HCCs that harbor mutations in the TERT promoter region was recapitulated (S. E. Lee et al., 2016). To investigate whether these HCC cell lines depend on PKM2 to promote tumorigenesis, stable genetic knockdown of *PKM2* were generated by screening SNU398 cells that were stably transduced with a panel of independent short-hairpin RNAs (shRNA*)* against *PKM* (**Fig 4.2e**). After selecting the sh*PKMs* that most efficiently depleted PKM2, it was interrogated whether disruption of *PKM2* would alter the proliferative ability of HCC cells. In line with previous findings, genetic depletion of *PKM2* significantly reduced the proliferation of SNU398 (**Fig 4.2f**). Aside from cellular proliferation, clonogenic survival of SNU398 cells was dependent on *PKM2* expression (**Fig 4.2g**). Collectively, these results demonstrate that HCC cells rely on PKM2 for to sustain tumorigenic properties including proliferative capability and clonogenic survival.

PKM2 Interacts with a Cu-Charged Resin

After highlighting the critically of PKM2 to HCC viability, the next question to answer was whether PKM2 could bind to the transition metal Cu. To confirm the mass spectrometry analysis from the metal-ion screen conducted by She et *al*., immobilized metal affinity chromatography was performed by applying whole cell extract (WCE) from mouse embryonic fibroblasts (MEFs) to either Cu^{2+}, Fe^{3+}, or Zn^{2+} charged resins (**Fig 4.3a**). Immunoblot analysis detected enrichment of both MEK1, a known Cu binding protein, and PKM2 in the eluent from a Cu-charged resin, but not from those of Fe or Zn charged resins. Evidently, PKM2 forms multiple, well-characterized protein-protein interactions with several transcription factors and oncogenes (Liang et al., 2017; Luo et al., 2011; Yu et al., 2013; Zhao et al., 2018), thus, to determine if PKM2 forms a direct

interaction with Cu, recombinant human PKM2 (rPKM2) applied to iminodiacetic acid beads preloaded with Cu^{2+} (**Fig 4.3b**). Affinity purification of rPKM2 from the Cu column specifically suggests that a direct interaction exists between Cu and PKM2. Similar to the results obtained from MEF WCE, rPKM2 was not enriched after incubation with other divalently-charged resins, suggesting that PKM2 binds Cu selectively. Taken together, these affinity purifications revealed a surprising yet unique interaction between a previously established static metal cofactor and a glycolytic enzyme favorably expressed in cancer.

Location of Predicted Cu-Binding Residues Provide Insight for Novel Regulation

Previous work identified that PKM1/2 interacts with Cu through the histidine motif that is present in both the PKM1 and PKM2 isoforms (She et al., 2003). Importantly, ligation of Cu by the same number of histidine residues has been observed in the crystallographic structures of essential Cu-binding enzymes Cu,Zn-SOD1 and CCO (Tainer et al., 1982; Tsukihara et al., 1995). Interestingly, an unbiased reactivity-based protein profiling screen showed that several cysteine residues of PKM (**Fig 4.4a,b**) are differentially occupied in a Cu-dependent manner (Chang Lab, unpublished data). Coordination of Cu through CC motifs is a phenomenon previously observed in the copper chaperone COX17, which relies on these cysteine residues for proper Cu transfer to other cochaperones (Banci et al., 2008). Although evidence demonstrates that PKM2 interacts with Cu potentially through motifs that are conserved in cuproproteins, the residues that are required for binding have yet to be characterized. Furthermore, the oligomeric state of PKM2 has been shown to influence its catalytic activity (Chaneton et al., 2012; Dombrauckas et al., 2005; Hitosugi et al., 2009; Lv et al., 2011), and subsequently altering regulation of glycolytic metabolism. After inspection of

a crystallographic structure of PKM2 (**Fig 4.4c,** PDB: 4B2D), several of the proposed Cu binding residues (**Fig 4.4a**) lay near important structural features of PKM2. For example, Cys 423 and Cys 424 are two residues that are included in the alternative exon specific to PKM2. This region forms the dimer-dimer inter subunit contact region, and subtle differences in these amino acids account for the differences in allosteric effector binding observed between PKM1 and PKM2. Additionally, Cys 152 is found within the flexible B domain that closes upon the active site during transphosphorylation. Although the allosteric regulation of PKM2 is well-characterized, whether Cu allosterically regulates PKM2 from a distant site or directly in the active site is unknown.

Thus, to interrogate the functional relevance of Cu-binding to PKM2, recombinant human PKM2 constructs harboring site-specific mutations at the histidine or cysteine residues (**Fig 4.4a**) proposed to interact with Cu via site-directed mutagenesis must be generated. After initial purification, metal pull-down assays followed by immunoblot analysis to assess the Cu-binding ability of each PKM2 mutant should be performed. We would expect that mutations to amino acids that are interacting with Cu will show a complete loss or a reduced ability to bind to a Cu-charged resin. To corroborate this mutagenesis strategy, direct incorporation of Cu in both wild-type and mutant PKM2 constructs using ICP-MS will be obtained. If these data collectively suggest that there may be multiple Cu binding pockets present, dialysis of wild-type PKM2 against a range of copper chloride ($CuCl_2$) concentrations will be executed to determine the Cu:PKM2 binding stoichiometry. To establish the impact of Cu-binding on PKM2 enzymatic activity, the Kinase-Glo® assay kit may be repurposed to measure the pyruvate kinase activity of each mutant by determining the value for maximal velocity (V_{max}) and the Michaelis constant (K_m) in the presence or absence of Cu as compared to wild-type. Additionally, we would expect to observe a reduction of pyruvate kinase activity for the PKM2 mutants

that lack the relevant Cu-binding residues. Taken together, these proposed experiments will elucidate where Cu binds to PKM2 and provide specifics regarding the contribution of this interaction to PKM2 catalytic function.

Cu Availability Reduces PKM2 Tyrosine Phosphorylation

Several well-established protein partners and metabolites bind to PKM2 and serve to allosterically activate or inhibit PKM2 function. Additionally, a number of post-translation modifications (PTM) act directly to also enhance or reduce PKM2 activity, where usually the latter is favored in cancer cell metabolism (Prakasam et al., 2018). Thus, we questioned whether Cu would contribute to the PTM-mediated regulation of PKM2. To answer this question, the PhosphoSitePlus database was used to observe putative PTM sites on PKM2. Upon inspection of known PTMs (**Fig 4.5a**), phosphorylation was most frequently detected with over 50 phosphorylation sites reported on PKM2. Interestingly, the phosphorylation at tyrosine 105 (Tyr105) was the most well characterized (**Fig 4.5a**, indicated by a red star). Specifically, this FGFR1-mediated phosphorylation inhibits PKM2 function by forcing a closed conformation that is less flexible and amendable to FBP binding, thus reducing pyruvate kinase activity (Hitosugi et al., 2009; Kalaiarasan et al., 2014). Considering this point of regulation, we assessed the effect of reduced intracellular Cu on PKM2 phosphorylation at Tyr105 via immunoblot analysis from MEFs that were genetically null for *Ctr1* or MEFS where the human WT CTR1 transporter was re-expressed (**Fig 4.5b**). Additionally, the effect of Cu chelation was assessed in these rescue MEFs using a Cu^{1+}-specific Cu chelator, BCS, as well as TTM. Interestingly, phosphorylation at Tyr105 was reduced in conditions with reduced levels of bioavailable Cu. A possible hypothesis explaining this finding could be that a population of PKM2 exists already as a dimer in cells with diminished Cu

bioavailability, thus, already rendering PKM2 inactive. Preliminary cross-linking experiments in the same cellular system demonstrate that MEFs with physiological Cu accessibility have PKM2 that exists mainly as a tetramer (data not shown). However, in MEFs with either pharmacologically or genetically suppressed intracellular Cu levels, a dimeric PKM2 species appears, further supporting the notion that Cu withdrawal may push PKM2 into an inactive state. In light of these results, it is necessary to confirm that upstream regulators of PKM2 phosphorylation, such as FGFR1, are not Cu-dependent. Collectively, these data suggest a novel Cu-dependent role in the regulation of PKM2. To corroborate these studies as well as further the mechanistic rationale for these observations, future *in vitro* biochemical, like those described in the previous section, as well as biophysical studies must be performed to elucidate the role of Cu in PKM2 tetramer:dimer:monomer equilibrium and the PKM2 enzymatic function that results.

Methods

Data Mining

PKM and *PKLR* mRNA expression in normal or tumor liver tissue samples was obtained from the Gene Expression across Normal and Tumor tissue (GENT2) web-based genome database (http://gent2.appex.kr/gent2/, Korean Research Institute and Biotechnology). A total of n = 215 normal and n = 517 tumor liver tissue samples were used for analysis. A total of 347 samples from the Pan-Cancer Atlas dataset from The Cancer Genome Atlas (TCGA) was selected for analysis from The Human Protein Atlas (THPA) for *PKM* mRNA expression and patient survival data. For survival plot, n = 177 patients with high expression and n = 170 patients with low expression of *PKM*, where expression below cut-off value of 9.62 FPKM (median expression) categorized patients as low expression and values above 9.62 were categorized with high expression.

Representative immunohistochemical staining for PKM from normal liver and liver cancer tissue were observed from the open-access, web-based database (https://www.proteinatlas.org/ENSG00000067225-PKM/pathology/liver+cancer). Post-translational modifications of PKM2 were viewed and adapted from querying PKM2 in the PhosphoSite Plus database (CST, https://www.phosphosite.org/homeAction.action).

Cell lines & cell culture

Cell culture SNU387, SNU398, and SNU449 HCC cell lines and human plateable hepatocytes, 5-Donor were obtained from the American Type Culture Collection (ATCC) and ThermoFisher Scientific, respectively. Parental cell lines were cultured in Roswell Park Memorial Institute (RPMI 1640, Gibco) Media and supplemented with 10% v/v fetal bovine serum (FBS, GE Lifesciences), 100 U/mL penicillin, and 100 ug/mL streptomycin (Gibco). SNU398 and SNU449 cell lines stably expressing the pLKO.1puro constructs were maintained as above supplemented with 5ug/mL puromycin (Invitrogen). SNU398 and SNU449 were stably infected with lentiviruses derived from the pLKO.1 plasmid (see plasmids below) using established protocols. Mouse embryonic fibroblasts (MEF) lines used were derived as described previously (D. C. Brady et al., 2014). MEF lines were cultured in Dulbecco's Modified Eagle Medium (DMEM high glucose, Gibco), 100 U/mL penicillin, and 100 ug/mL streptomycin (Gibco). MEF lines reconstituted with the human CTR1 transporter were cultured as above with the addition of 5ug/mL Blasticidin (Gibco). Unless specified, all cell lines were maintained in a humidified Heracell (ThermoFischer Scientific) incubator set to 37°C and 5% CO2. MycoAlert® mycoplasma test detection kit (Lonza, LT07-418) was used to test for mycoplasma contamination.

Immunoblot analysis

Immunoblot analysis was performed following a previously described protocol with slight modifications (Davis et al., 2020). Protein from whole cell lysate was detected using the following antibodies (dilution, catalog#, manufacturer): mouse anti-β-actin (1:5000, 3700, Cell Signaling Technologies (CST)), mouse anti-MEK1 (1:2000, 2352, CST) rabbit anti-PKLR (1:1000, NBP1-32314, Novus Biologicals), rabbit anti-PKM1 (1:1000, 7067, CST), rabbit anti-PKM2 (1:3000, 4053, CST), rabbit-anti-Phospho(Tyr105)-PKM2 (1:1000, 3827, CST), rabbit anti-Telomerase reverse transcriptase (TERT) (1:1000, ab32030, Abcam), followed by detection with one of the following horseradish-peroxidase-conjugated secondary antibodies: goat anti-mouse IgG (1:4000, 7076, CST) or goat anti-rabbit IgG (1:4000, 7074, CST) using SignalFire ECL (CST, # 6883S) detection reagents.

Plasmids

pLKO.1puro lentiviral shRNA plasmids were obtained from High-Throughput Screening Core at the University of Pennsylvania to express: nontargeted control (sh*SCR*) or sequences targeted against human PKM obtained from The RNAi Consortium (TRC) shRNA library (sh*PKM*#1,sh*PKM*#2, sh*PKM*#3, sh*PKM*#4, sh*PKM*#5). The pWZLblasti-CTR1^{WT} and pWZLblasti vector generated as previously described (D. C. Brady et al., 2014). pETDUET-6xHIS-TEV-PKM2 was created by subcloning human PKM2 cDNA into the pETDUET-6xHIS-TEV empty vector.

Measurement of cell proliferation with trypan blue

Cell proliferation was measured as previously described (Davis et al., 2020). SNU398 cells stably expressing the indicated constructs were seeded at 1.5 x 10^4 cells per well in a six-well plate on Day 0. Cell counts were performed every other day by washing cells

with 1x PBS, detaching cells with 0.05% Trypsin (Gibco, #25300054). Cells were then resuspended in an equal volume of complete RPMI, and centrifuged at 1000xg for 5 mins. Following aspiration of media, cell pellets were then resuspended in identical volumes of complete RPMI. Cell counting was performed using an automated cell counter (Invitrogen Cell Countess II) by taking an aliquot of cell culture and diluting 1:1 with 0.4% Trypan Blue Solution (Life Technologies/Invitrogen, #15250061) before plating on and reading with a hemocytometer.

Clonogenic assay

Clonogenic survival was measured as previously described (Davis et al., 2020). SNU398 cells stably expressing indicated constructs were seeded at 3.0 x 10^3 cells per well in six-well plates. After incubation for seven days, cells were washed once with 1X Phosphate Buffered Saline (PBS) and stained with 1mL of a crystal violet staining solution (0.5% w/v crystal violet (CV), 20% v/v methanol, distilled water) for 15 minutes. After 15 minutes, all wells were washed three times with distilled water to minimize background staining. CV stained colonies were imaged using a ChemiDoc Touch Imagining System (Bio-Rad). To quantify colony abundance, stained cell colonies were dissolved in a 10% acetic acid solution for 30 minutes at room temperature, and extracted CV was measured at an absorbance of 590nm in a plate reader (Synergy, BioTek).

PKM2 Purification

Human recombinant PKM2 (rPKM2) was purified from a previously established protocol (Tsang et al., 2020), see Protein purification section.

Metal affinity chromatography experiments

Metal pulldown assays were performed as previously described (M. L. Turski et al., 2012). Briefly, 20 µg of MEF whole cell extract was incubated in radioimmunopreciptation assay (RIPA) buffer containing 10 µl of Profinity IMAC resin (Bio-Rad) charged with Cu, Zn, or Fe or without metal for 30 minutes at 4°C. For pulldown assays requiring rPKM2, 500 ng of rPKM2 was incubated in HEPES buffer (see Protein purification section) as described above. Samples were washed 4x in 500 µl HEPES buffer prior to elution and then prepared for SDS-PAGE analysis followed by immunoblot detection as performed above.

PKM2 Crystal Structure

The tetrameric human PKM2 crystal structure was downloaded, examined, and modified from the publicly available structural biology database Protein Data Bank (PDB) from a previously deposited structure, PDB: 4B2D, (Chaneton et al., 2012).

Statistical analysis

Data are reported as mean $\pm$s.e.m. Each sample size (*n*) represents biologically independent experiments. Data was collected from three independent experiments unless otherwise specified within the figure legend. Statistical significance was determined using an unpaired two-tailed Student's t-test, a Mantel-Cox test, a one-way ANOVA followed by Dunnett's or Tukey's multiple comparisons test, where significance was defined as $P \leq 0.05$. All statistical analysis was performed in GraphPad Prism 8 software.

Distinguishing the Role for Cu under Oxygen Deplete versus Nutrient & Oxygen Deplete (Ischemic) Conditions

Our findings from Chapter 3 revealed a Cu-dependent impairment of the metabolic flexibility of HCC cells under hypoxic stress upon reduced Cu accessibility. These nominal findings contribute to elucidating the mechanism behind the TAE-induced metabolic reprogramming that occurs from surviving residual cells. However, it is important to note that during TAE or TACE, the microsphere beads administered obstruct blood flow to the tumor, causing a serve restriction in both oxygen and nutrient availability. Although our previous results under reduced oxygen tension illuminate a Cu-sensitivity, whether a Cu-sensitivity exists after the combination of nutrient and oxygen deprivation, referred to as ischemia, remains to be elucidated. Thus, we performed several experiments to begin to investigate whether ischemic conditions conferred a unique Cu-dependency. When HCC cells, SNU398 were exposed to ischemia [hypoxia (1% O_2) and nutrient deprivation (1% FBS, 1mM glucose, 1mM glutamine)] for 48 hours, mRNA expression of *GLUT1*, *HK2*, and *LDHA* significantly increased in comparison to normoxic (1% O_2) conditions. However, upon addition of 25 µM TTM, a Cu-dependent attenuation in ischemia-induced transcription of *GLUT1* and *LDHA* manifested (data not shown). Additionally, we evaluated whether ischemic conditions would elicit changes in Cu homeostasis gene expression by measuring mRNA transcripts of *ATP7A*, *ATOX1*, *CCS*, *CTR1*, and *CTR2* via RT-qPCR. Akin to observations made under hypoxic conditions, an ischemic-induced elevation was observed only in *ATP7A* transcripts, however, this response was blunted with supplementation of 25 µM TTM. Together, these findings suggest that reduced Cu accessibility restricts the transcript-level metabolic rewiring of HCC cells after exposure to TAE-mimic conditions. These results are promising leads, however, there are still many questions left to answer. Specifically, what effects will Cu depletion have on metabolite utilization, namely glucose consumption or lactate excretion, within an ischemic environment in HCC cells?

Moreover, does Cu chelation via TTM mediate a differential metabolic sensitivity in HCC cells under ischemic conditions as compared to hypoxic conditions alone? Further studies must be performed to provide molecular insight towards distinguishing the sensitivity mediated by hypoxic stress versus that evoked by nutrient deprivation. To meticulously determine the differences between these conditions, it will be necessary to conduct experiments where HCC cells are treated in normoxic, hypoxic, or ischemic conditions in the presence or absence of TTM. HCC cells then may be harvested and examined for expression of Cu homeostatic and glycolytic genes, while cultured media may be collected and analyzed to determine rates of glucose consumption and lactate excretion. To complement these experiments, a genetic approach where HCC cells are transduced with several independent sh*RNA*s against *CTR1* may be effective to orthogonal confirm a potential Cu-dependency within ischemic conditions.

However, in light of the promising findings in Chapter 3, future studies should also be conducted to determine whether Cu chelation in combination with TACE provides a survival advantage in an established *in vivo* rat model of HCC (**Fig 4.6**). Here, we provide a provisional plan for a preclinical study to investigate whether Cu chelation will be advantageous during TACE. Following methods previously established by the Gade laboratory (Gade et al., 2015), chemical induction of autochthonous HCC will be achieved over a 12-week period through oral administration of 0.01% Diethylnitrosamine (DEN), a carcinogen commonly used to induce HCC (Ha et al., 2001). HCC tumors will be visualized with magnetic resonance (MR) imaging before and after TACE treatment. Rats with tumors >0.5 cm in diameter will be selected for treatment with TACE. Four cohorts of 10 rats each will be established: **a)** no treatment group **b)** selective TACE **c)** selective TACE and a low dose of TTM (5 mg/kg body weight) **d)** selective TACE and a high dose of TTM (25 mg/kg body weight). TTM dosing will be based on that required to

chelate hepatic Cu from rat models of WD (Ogra & Suzuki, 1998). Leveraging the expertise of the Gade laboratory, TACE will be performed as previously described with slight modification (Gade et al., 2015). A daily subcutaneous injection of meloxicam, an inhibitor of proteins involved in HCC cell migration and invasion, will be dosed at 2 ug/kg body weight for **group b,c,d** for 3 days following embolization (Li et al., 2016). Additionally, a single orthotopic injection of TTM at 5 mg/kg or 25 mg/kg will be applied to **group c** or **group d**, respectively, once a day for one week following TACE treatment. Tumor regression will be assessed by MR imaging and by tumor volume (cm^3). Percent overall survival will be determined from Kaplan-Meier plots for each group. It is predicted that rats in either **group c** or **group d** would have the best outcome, which would be demonstrated by greater percent survival compared to rats from treatment **group b**. Tumors and adjacent surrounding liver parenchyma will be excised and subjected to immunohistological analysis to assess the degree of tumor hypoxia via HIF1-α levels and tumor necrosis via Hematoxylin and Eosin (H&E) staining. The staining from **group c & d** would likely reveal increased percent necrosis if Cu chelation provides a therapeutic advantage, which would also be reflected in a corresponding decrease in tumor volume. Since HIF-1α should be induced upon TACE treatment, elevated levels of HIF-1α from **groups b,c,d** compared to control **group a** are anticipated**.** To determine the efficiency of Cu chelation, immunoblot for the copper chaperone for SOD1 (CCS) (Bertinato et al., 2003) or measurement of serum ceruloplasmin (Cp) oxidase activity, which is used to assess reduced levels of circulating Cu (Broderius et al., 2010), should be performed. Following effective Cu chelation, I would expect to observe elevated levels of CCS from HCC tumor tissue and reduced levels of Cp oxidase from the serum of rats in **groups c** and **d**. These biological read-outs may be corroborated with the

direct assessment of intracellular Cu and molybdenum, an indicator of TTM content, levels through ICP-MS measurements. Taken together, these experiments will illuminate whether the combination of TACE with TTM will provide a survival advantage by limiting the drug resistance evoked from residual HCC cells.

Chapter 4 Figures

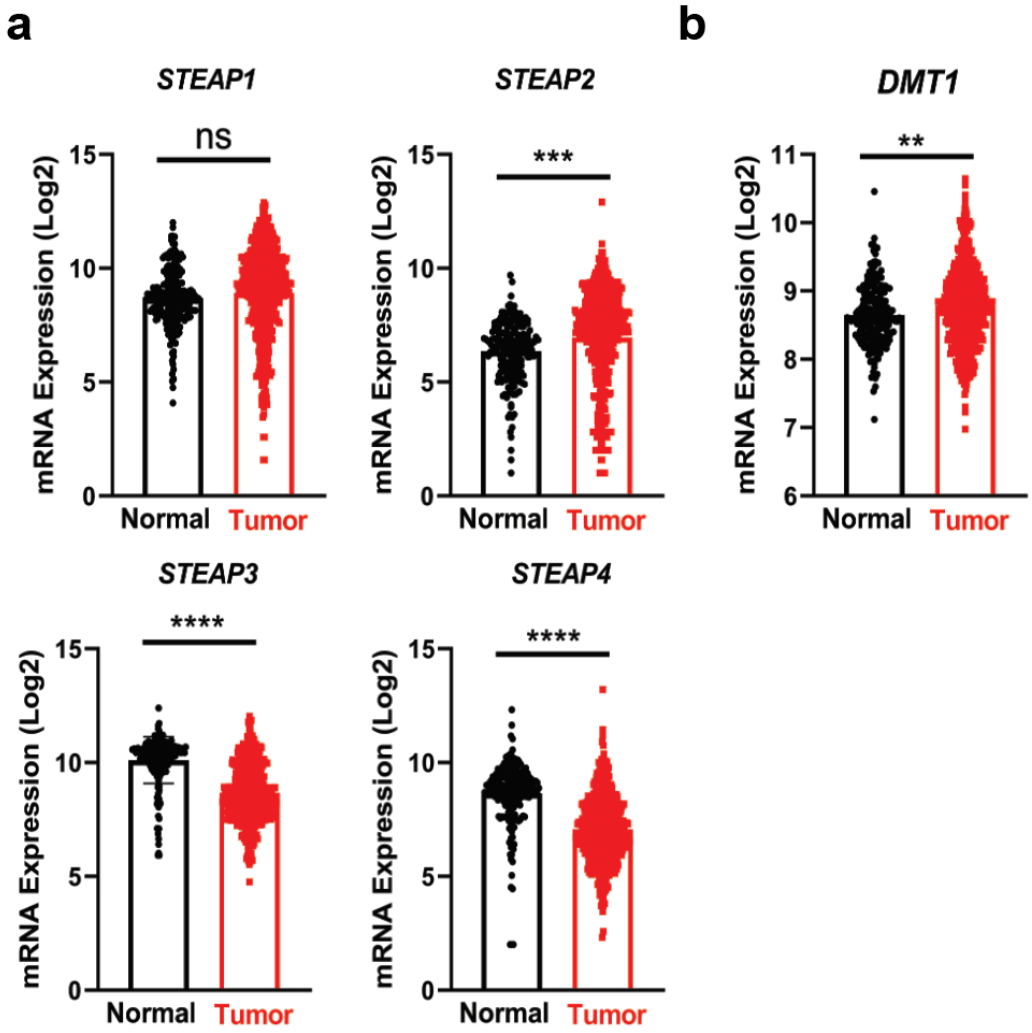

Figure 4.1 Varied expression of genes shared in Cu and Fe homeostasis in liver cancer. (a and b) Scatter dot plot with bar at mean +s.e.m. of mRNA expression of STEAP1, STEAP2, STEAP3, STEAP4, and DMT1 (b) from normal (n = 215) and tumor (n = 517) liver tissue samples from the online, open-access database GENT2. Statistical analysis was performed using an unpaired, two-tailed Student's t-test. *P < 0.0332,**P < 0.0021, ***P < 0.0002, ****P < 0.0001.

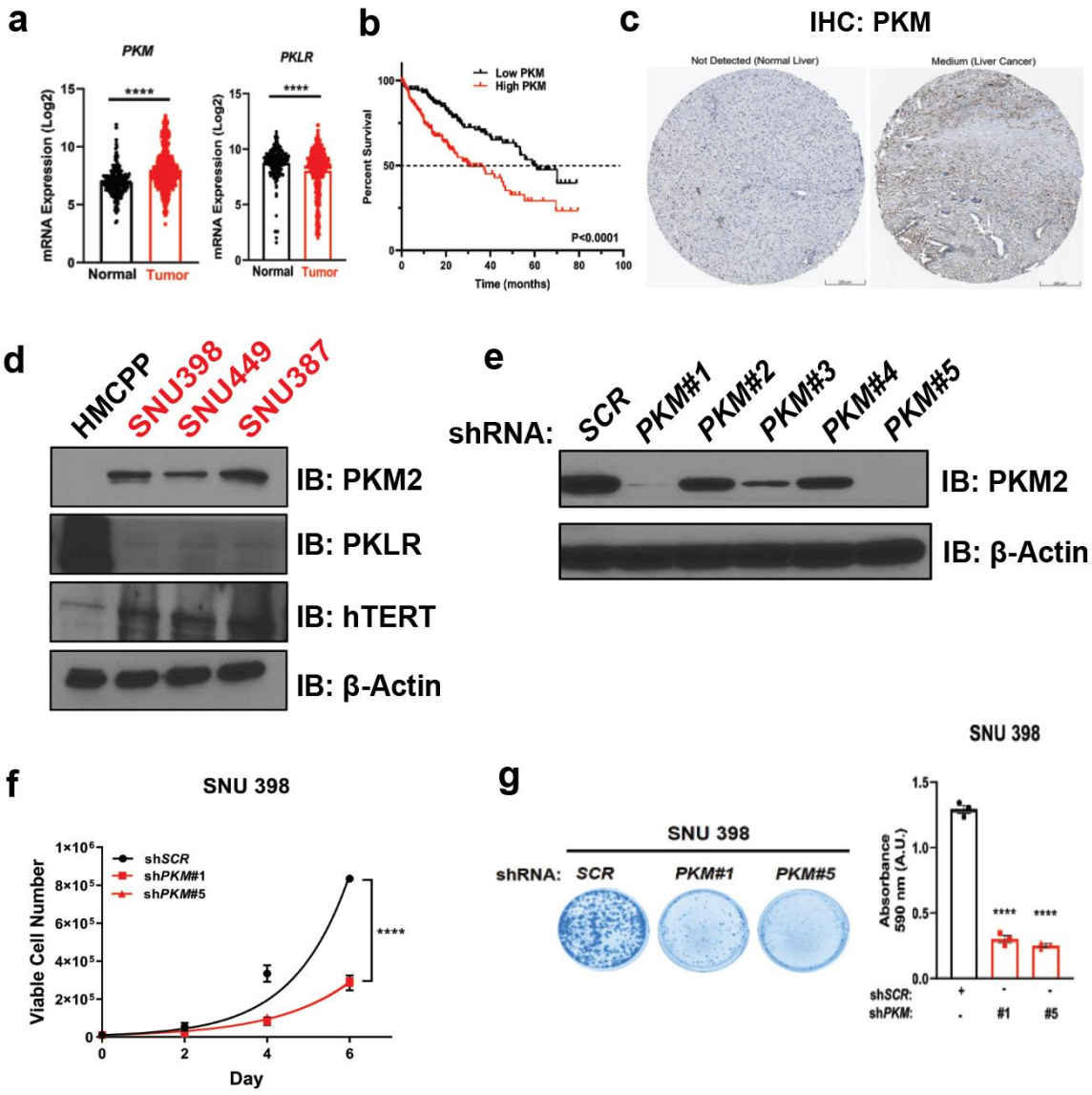

Figure 4.2 HCC cells depend on PKM2 for tumorigenic properties as PKM2 expression is associated with unfavorable outcomes in liver cancer patients (a) Scatter dot plot with bar at mean +s.e.m. of mRNA expression of *PKM* and *PKLR* from normal (*n* = 215) and tumor (*n* = 517) liver tissue samples from the online, open-access database GENT2. Statistical analysis was performed using an unpaired, two-tailed Student's t-test. ****P < 0.0001. (b) Kaplan-Meier analysis of overall survival with median (dashed black lines) from HCC patients with either high (solid red lines) or low (solid black lines) mRNA expression of PKM. For overall survival plot, *n* = 177 patients with high PKM expression and *n* = 170 for patients with low PKM expression. Results were compared using a Mantel-Cox test. P <0.0001. (c) Representative immunohistochemistry staining of PKM in normal liver (left) and liver cancer (right) tissues. IHC was extracted and adapted from the online, open-access database The Human Protein Atlas. (d) Immunoblot detection of PKM2, PKLR, hTERT, or β-Actin from normal liver cells (HMCPP) or HCC cell lines (SNU387, SNU398, SNU449) previously

screened in (Davis et al., 2020). (e) Immunoblot detection of PKM2 and β-Actin from SNU398 cell lines stably expressing *shRNA* against *PKM2* (indicated as *PKM*#1-5) or a non-targeting scramble sequence (*SCR*). (f) Non-linear fit to the exponential growth equation of cellular proliferation from SNU398 cells expressing *shRNA* against *PKM2* or *SCR*. *n* = 3 independent biological experiments, with each experiment plated in technical triplicate. Statistical analysis was performed using a two-way ANOVA followed by Dunnett's multiple comparison test, ****P < 0.0001. (g) Representative images (left) of crystal violet stained colonies from SNU398 cells expressing *shRNA* against *PKM2* or *SCR*, and scatter dot plot (right) of mean absorbance of extracted crystal violet at 590 nm +s.e.m. of crystal violet staining from three independent experiments plated in technical triplicate. The results were compared using a one-way ANOVA followed by Tukey's multiple comparison test. *P < 0.0332, **P < 0.0021, ***P < 0.0002, ****P < 0.0001.

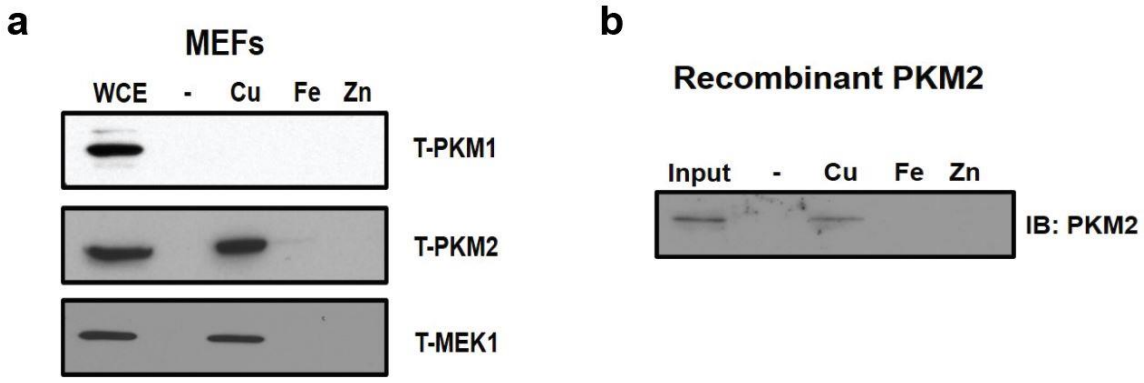

Figure 4.3 PKM2 interacts with a Cu-charged resin. (a and b) Immunoblot analysis of affinity-purified total PKM1 (T-PKM1), total PKM2 (T-PKM2), and total MEK1 (T-MEK1) obtained from mouse embryonic fibroblasts (MEFs) whole cell extract (WCE) (a) and from purified recombinant PKM2 (b) from resins loaded with indicated metals. Selected immunoblots are representative of at least 3 independent experiments.

a

Residues Identified	Domain	Structural or Functional Importance
His 78	A1	Site for ATP coordination
His 81	A1	Site for ATP coordination
His 84	A1	Site for ATP coordination
Cys 423	C	In alternative exon
Cys 424	C	In alternative exon

b

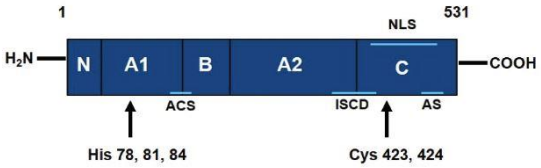

c

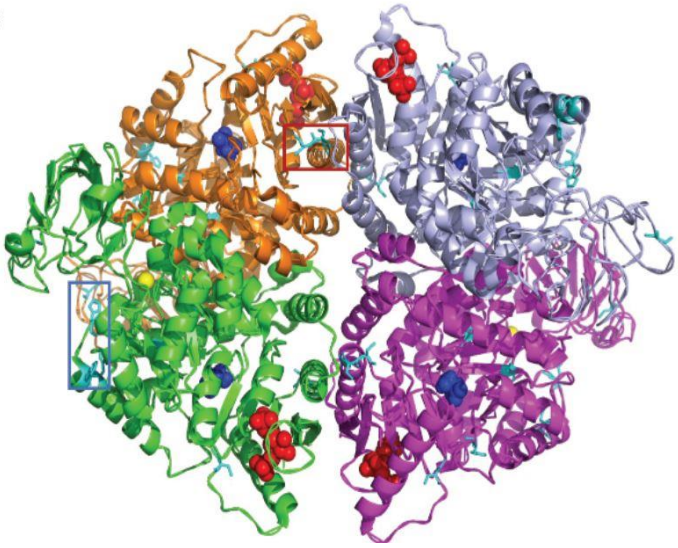

Figure 4.4 The location of several predicted Cu-binding residues may provide insight for novel regulation of PKM2. (a) List of candidate residues predicted to be involved in the PKM2-Cu interaction. (b) Domain map of PKM2 that includes the active site (ACS), the isomerization domain (ISCD), the allosteric site (AS), and the nuclear localization sequence (NLS). Bolded arrows represent the location where potential Cu-binding histidine (H) or cysteine (C) residues are located. (c) Adapted crystal structure [PDB: 4B2D, (Chaneton et al., 2012)] of tetrameric PKM2 bound to the allosteric regulator Fructose-1,6-Bisphosphate (FBP) and serine (S). Red box insert depicts the two C residues, encoded within the alternative exon, that lie on the dimer-dimer interface. Blue box insert represents the three H residues which reside within the co-factor (Mg^{2+}) binding site. Distinct colors (orange, green, magenta, periwinkle) depict each monomeric unit within the tetramer. Within each monomer, the red spheres in the C-lobe represent the FBP, blue spheres in A-lobe represent a serine residue, the teal sticks represent H or C residues of interest, and yellow spheres represent the Mg^{2+}.

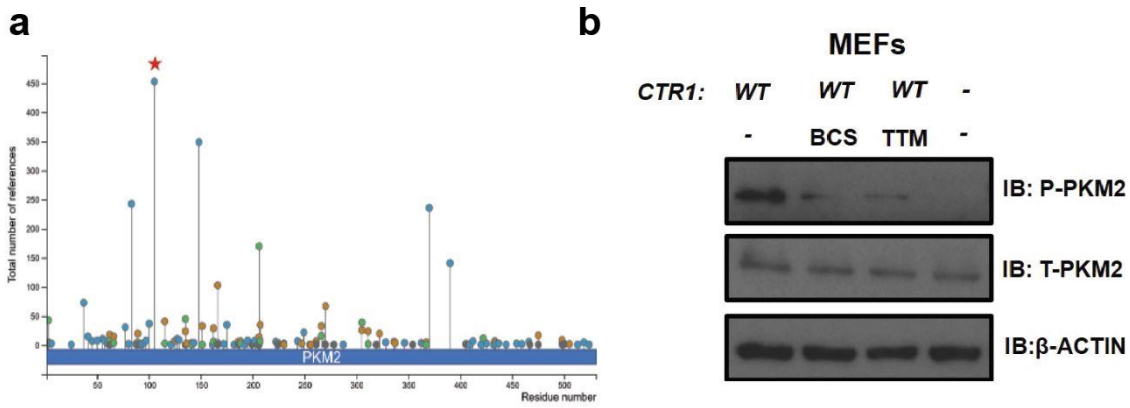

Figure 4.5 Cu availability reduces PKM2 tyrosine phosphorylation. (a) Representative post-translational modification map of human PKM2, adapted from PhosphoSitePlus® online database. Blue circles represent phosphorylation, green circles represent acetylation, orange-brown circles represent ubiquitylation, and all other modifications are represented by dark grey circles. A red star marks the phosphorylation event at Tyrosine105. (b) Immunoblot detection of Tyrosine105 phosphorylated PKM2 (P-PKM2), total PKM2 (T-PKM2), and β-Actin from MEFs, wild-type for the CTR1 transporter, that were treated with either vehicle (DMSO), 500 µM BCS, or 10 µM TTM for 48 hours. Representative immunoblot from *n* = 4 independent experiments.

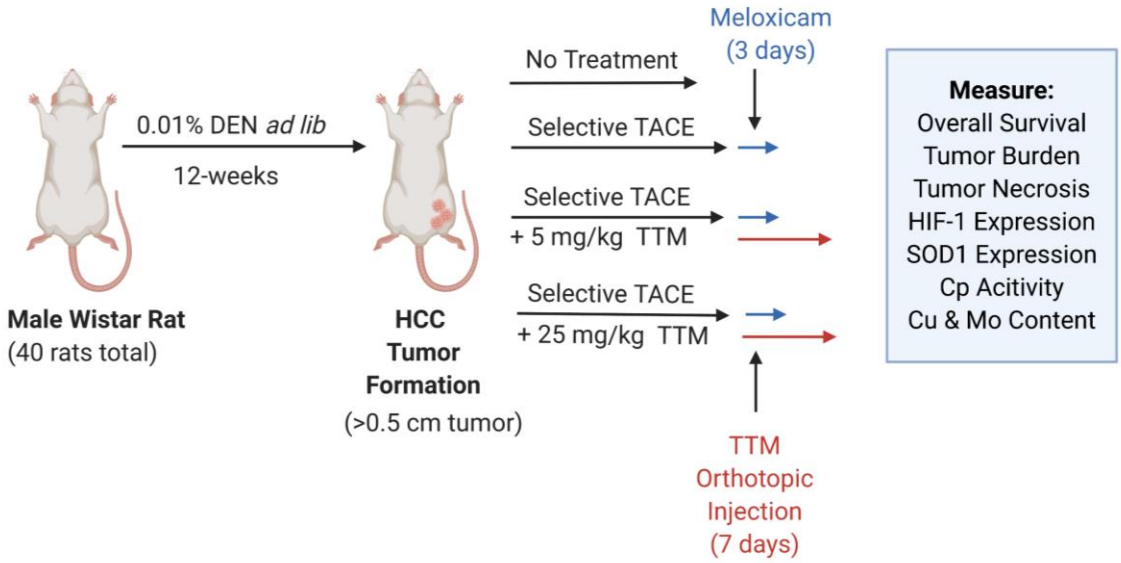

Figure 4.6 *In vivo* study design of TACE in combination with TTM as a potential treatment for advanced stage HCC.

BIBLIOGRAPHY

Ahn, S. M., Jang, S. J., Shim, J. H., Kim, D., Hong, S. M., Sung, C. O., Baek, D., Haq, F., Ansari, A. A., Lee, S. Y., Chun, S. M., Choi, S., Choi, H. J., Kim, J., Kim, S., Hwang, S., Lee, Y. J., Lee, J. E., Jung, W. R., … Kong, G. (2014). Genomic portrait of resectable hepatocellular carcinomas: Implications of RB1 and FGF19 aberrations for patient stratification. *Hepatology*, *60*(6), 1972–1982. https://doi.org/10.1002/hep.27198

Alison, M. R., & Lin, W.-R. (2011). Hepatocyte turnover and regeneration: Virtually a virtuoso performance. *Hepatology*, *53*(4), 1393–1396. https://doi.org/10.1002/hep.24252

Altekruse, S. F., Henley, S. J., Cucinelli, J. E., & McGlynn, K. A. (2014). Changing hepatocellular carcinoma incidence and liver cancer mortality rates in the United States. *American Journal of Gastroenterology*, *109*(4), 542–553. https://doi.org/10.1038/ajg.2014.11

Alvarez, H. M., Xue, Y., Robinson, C. D., Canalizo-Hernández, M. A., Marvin, R. G., Kelly, R. A., Mondragón, A., Penner-Hahn, J. E., & O'Halloran, T. V. (2010). Tetrathiomolybdate inhibits copper trafficking proteins through metal cluster formation. *Science*, *327*(5963), 331–334. https://doi.org/10.1126/science.1179907

Alvarez, L., Gonzalez-Iglesias, H., Garcia, M., Ghosh, S., Sanz-Medel, A., & Coca-Prados, M. (2012). The stoichiometric transition from Zn 6Cu 1- metallothionein to Zn 7-metallothionein underlies the up-regulation of metallothionein (MT) expression: Quantitative analysis of MT-metal load in eye cells. *Journal of Biological Chemistry*, *287*(34), 28456–28469. https://doi.org/10.1074/jbc.M112.365015

Amann, T., Maegdefrau, U., Hartmann, A., Agaimy, A., Marienhagen, J., Weiss, T. S., Stoeltzing, O., Warnecke, C., Schölmerich, J., Oefner, P. J., Kreutz, M., Bosserhoff, A. K., & Hellerbrand, C. (2009). GLUT1 expression is increased in hepatocellular carcinoma and promotes tumorigenesis. *American Journal of Pathology*, *174*(4), 1544–1552. https://doi.org/10.2353/ajpath.2009.080596

Andreini, C., Banci, L., Bertini, I., & Rosato, A. (2008). Occurrence of copper proteins through the three domains of life: A bioinformatic approach. *Journal of Proteome Research*, *7*(1), 209–216. https://doi.org/10.1021/pr070480u

Andreini, C., Bertini, I., Cavallaro, G., Holliday, G. L., & Thornton, J. M. (2008). Metal ions in biological catalysis: From enzyme databases to general principles. *Journal of Biological Inorganic Chemistry*, *13*(8), 1205–1218. https://doi.org/10.1007/s00775-008-0404-5

Arizumi, T., Ueshima, K., Iwanishi, M., Minami, T., Chishina, H., Kono, M., Takita, M., Yada, N., Hagiwara, S., Minami, Y., Ida, H., Komeda, Y., Takenaka, M., Sakurai, T., Watanabe, T., Nishida, N., & Kudo, M. (2017). The Overall Survival of Patients with Hepatocellular Carcinoma Correlates with the Newly Defined Time to Progression after Transarterial Chemoembolization. *Liver Cancer*, *6*(3), 227–235. https://doi.org/10.1159/000475777

Arnesano, F., Banci, L., Bertini, I., Ciofi-Baffoni, S., Molteni, E., Huffman, D. L., & O'Halloran, T. V. (2002). Metallochaperones and metal-transporting ATPases: A comparative analysis of sequences and structures. *Genome Research*, *12*(2), 255–271. https://doi.org/10.1101/gr.196802

Arredondo, M., Muñoz, P., Mura, C. V., & Núñez, M. T. (2003a). DMT1, a physiologically relevant apical Cu1+ transporter of intestinal cells. *American Journal of Physiology - Cell Physiology*, *284*(6 53-6). https://doi.org/10.1152/ajpcell.00480.2002

Arredondo, M., Muñoz, P., Mura, C. V., & Núñez, M. T. (2003b). DMT1, a physiologically relevant apical Cu1+ transporter of intestinal cells. *American Journal of Physiology - Cell Physiology*, *284*(6 53-6). https://doi.org/10.1152/ajpcell.00480.2002

Attar, N., Campos, O. A., Vogelauer, M., Cheng, C., Xue, Y., Schmollinger, S., Salwinski, L., Mallipeddi, N. V, Boone, B. A., Yen, L., Yang, S., Zikovich, S., Dardine, J., Carey, M. F., Merchant, S. S., & Kurdistani, S. K. (2020). The histone H3-H4 tetramer is a copper reductase enzyme. *Science*, *369*(6499), 59–64. https://doi.org/10.1126/SCIENCE.ABA8740

Attia, A. M., Attalla, S. M., Barakat, E. A. M. E., Zaki, M. E. S., & Elkhouly, N. Y. (2019). Role of copper, magnesium, and zinc in pathogenesis of hepatocellular carcinoma and cirrhosis. *Indian Journal of Forensic Medicine and Toxicology*, *13*(3), 398–404. https://doi.org/10.5958/0973-9130.2019.00230.5

Attwa, M. H., & El-Etreby, S. A. (2015). Guide for diagnosis and treatment of hepatocellular carcinoma. *World Journal of Hepatology*, *7*(12), 1632–1651. https://doi.org/10.4254/wjh.v7.i12.1632

Aubert, L., Nandagopal, N., Steinhart, Z., Lavoie, G., Nourreddine, S., Berman, J., Saba-El-Leil, M. K., Papadopoli, D., Lin, S., Hart, T., Macleod, G., Topisirovic, I., Gaboury, L., Fahrni, C. J., Schramek, D., Meloche, S., Angers, S., & Roux, P. P. (2020). Copper bioavailability is a KRAS-specific vulnerability in colorectal cancer. *Nature Communications*, *11*(1), 1–15. https://doi.org/10.1038/s41467-020-17549-y

Bakavayev, S., Chetrit, N., Zvagelsky, T., Mansour, R., Vyazmensky, M., Barak, Z., Israelson, A., & Engel, S. (2019). Cu/Zn-superoxide dismutase and wild-type like fALS SOD1 mutants produce cytotoxic quantities of H2O2 via cysteine-dependent redox short-circuit. *Scientific Reports*, *9*(1), 1–13. https://doi.org/10.1038/s41598-019-47326-x

Balamurugan, R., Palaniandavar, M., & Srinivasa Gopalan, R. (2001). Trigonal planar copper(I) complex: Synthesis, structure, and spectra of a redox pair of novel copper(II/I) complexes of tridentate bis(benzimidazol-2′-yl) ligand framework as models for electron-transfer copper proteins. *Inorganic Chemistry*, *40*(10), 2246–2255. https://doi.org/10.1021/ic0003372

Banci, L., Bertini, I., Ciofi-Baffoni, S., Hadjiloi, T., Martinelli, M., & Palumaa, P. (2008). Mitochondrial copper(I) transfer from Cox17 to Sco1 is coupled to electron transfer. *Proceedings of the National Academy of Sciences of the United States of America*, *105*(19), 6803–6808. https://doi.org/10.1073/pnas.0800019105

Banci, L., Bertini, I., Ciofi-Baffoni, S., Kozyreva, T., Zovo, K., & Palumaa, P. (2010). Affinity gradients drive copper to cellular destinations. *Nature*, *465*(7298), 645–648. https://doi.org/10.1038/nature09018

Bertinato, J., Iskandar, M., & L'Abbé, M. R. (2003). Copper deficiency induces the upregulation of the copper chaperone for Cu/Zn superoxide dismutase in weanling male rats. *The Journal of Nutrition*, *133*(1), 28–31. https://doi.org/10.1093/jn/133.1.28

Bertinato, J., Swist, E., Plouffe, L. J., Brooks, S. P. J., & L'Abbé, M. R. (2008). Ctr2 is partially localized to the plasma membrane and stimulates copper uptake in COS-7 cells. *Biochemical Journal*, *409*(3), 731–740. https://doi.org/10.1042/BJ20071025

Bhat, S. H., Azmi, A. S., & Hadi, S. M. (2007). Prooxidant DNA breakage induced by caffeic acid in human peripheral lymphocytes: Involvement of endogenous copper and a putative mechanism for anticancer properties. *Toxicology and Applied Pharmacology*, *218*(3), 249–255. https://doi.org/10.1016/j.taap.2006.11.022

Bhosale, P., Szklaruk, J., & Silverman, P. M. (2006). Current staging of hepatocellular carcinoma: Imaging implications. *Cancer Imaging*, *6*(1), 83–94. https://doi.org/10.1102/1470-7330.2006.0014

Blackman, R. K., Cheung-Ong, K., Gebbia, M., Proia, D. A., He, S., Kepros, J., Jonneaux, A., Marchetti, P., Kluza, J., Rao, P. E., Wada, Y., Giaever, G., & Nislow, C. (2012). Mitochondrial electron transport is the cellular target of the oncology drug Elesclomol. *PLoS ONE*, *7*(1). https://doi.org/10.1371/journal.pone.0029798

Bondanese, V. P., Lamboux, A., Simon, M., Lafont, J. E., Albalat, E., Pichat, S., Vanacker, J. M., Telouk, P., Balter, V., Oger, P., & Albarède, F. (2016). Hypoxia induces copper stable isotope fractionation in hepatocellular carcinoma, in a HIF-independent manner. *Metallomics*, *8*(11). https://doi.org/10.1039/c6mt00102e

Boult, J., Roberts, K., Brookes, M. J., Hughes, S., Bury, J. P., Cross, S. S., Anderson, G. J., Spychal, R., Iqbal, T., & Tselepis, C. (2008). Overexpression of cellular iron import proteins is associated with malignant progression of esophageal adenocarcinoma. *Clinical Cancer Research*, *14*(2), 379–387. https://doi.org/10.1158/1078-0432.CCR-07-1054

Brady, D. C., Crowe, M. S., Greenberg, D. N., & Counter, C. M. (2017). Copper chelation inhibits BRAFV600E-driven melanomagenesis and counters resistance to BRAFV600E and MEK1/2 inhibitors. *Cancer Research*, *77*(22), 6240–6252. https://doi.org/10.1158/0008-5472.CAN-16-1190

Brady, D. C., Crowe, M. S., Turski, M. L., Hobbs, G. A., Yao, X., Chaikuad, A., Knapp, S., Xiao, K., Campbell, S. L., Thiele, D. J., & Counter, C. M. (2014a). Copper is required for oncogenic BRAF signalling and tumorigenesis. *Nature*, *509*, 492–496. https://doi.org/10.1038/nature13180

Brady, D. C., Crowe, M. S., Turski, M. L., Hobbs, G. A., Yao, X., Chaikuad, A., Knapp, S., Xiao, K., Campbell, S. L., Thiele, D. J., & Counter, C. M. (2014b). Copper is required for oncogenic BRAF signalling and tumorigenesis. *Nature*, *509*(7501),

492–496. https://doi.org/10.1038/nature13180

Brady, G. F., Galban, S., Liu, X., Basrur, V., Gitlin, J. D., Elenitoba-Johnson, K. S. J., Wilson, T. E., & Duckett, C. S. (2010). Regulation of the Copper Chaperone CCS by XIAP-Mediated Ubiquitination. *Molecular and Cellular Biology*, *30*(8), 1923–1936. https://doi.org/10.1128/mcb.00900-09

Brady, Graham F., Galbán, S., Liu, X., Basrur, V., Gitlin, J. D., Elenitoba-Johnson, K. S. J., Wilson, T. E., & Duckett, C. S. (2010). Regulation of the Copper Chaperone CCS by XIAP-Mediated Ubiquitination. *Molecular and Cellular Biology*, *30*(8), 1923–1936. https://doi.org/10.1128/mcb.00900-09

Brem, S., Grossman, S. A., Carson, K. A., New, P., Phuphanich, S., Alavi, J. B., Mikkelsen, T., & Fisher, J. D. (2005). Phase 2 trial of copper depletion and penicillamine as antiangiogenesis therapy of glioblastoma. *Neuro-Oncology*, *7*(3), 246–253. https://doi.org/10.1215/S1152851704000869

Brewer, G. J. (2003). Copper in medicine. *Current Opinion in Chemical Biology*, *7*(2), 207–212. https://doi.org/10.1016/S1367-5931(03)00018-8

Brewer, G. J., Askari, F., Lorincz, M. T., Carlson, M., Schilsky, M., Kluin, K. J., Hedera, P., Moretti, P., Fink, J. K., Tankanow, R., Dick, R. B., & Sitterly, J. (2006). Treatment of Wilson disease with ammonium tetrathiomolybdate - IV. Comparison of tetrathiomolybdate and trientine in a double-blind study of treatment of the neurologic presentation of Wilson disease. *Archives of Neurology*, *63*(4), 521–527. https://doi.org/10.1001/archneur.63.4.521

Brewer, G. J., Dick, R. D., Grover, D. K., LeClaire, V., Tseng, M., Wicha, M., Pienta, K., Redman, B. G., Jahan, T., Sondak, V. K., Strawderman, M., LeCarpentier, G., & Merajver, S. D. (2000a). Treatment of metastatic cancer with tetrathiomolybdate, an anticopper, antiangiogenic agent: Phase I study. *Clinical Cancer Research*, *6*(1), 1–10.

Brewer, G. J., Dick, R. D., Grover, D. K., LeClaire, V., Tseng, M., Wicha, M., Pienta, K., Redman, B. G., Jahan, T., Sondak, V. K., Strawderman, M., LeCarpentier, G., & Merajver, S. D. (2000b). Treatment of metastatic cancer with tetrathiomolybdate, an anticopper, antiangiogenic agent: Phase I study. *Clinical Cancer Research*, *6*(1), 1–10.

Brewer, G. J., Ullenbruch, M. R., Dick, R., Olivarez, L., & Phan, S. H. (2003). Tetrathiomolybdate therapy protects against bleomycin-induced pulmonary fibrosis in mice. *Journal of Laboratory and Clinical Medicine*, *141*(3), 210–216. https://doi.org/10.1067/mlc.2003.20

Broderius, M., Mostad, E., Wendroth, K., & Prohaska, J. R. (2010). Levels of plasma ceruloplasmin protein are markedly lower following dietary copper deficiency in rodents. *Comparative Biochemistry and Physiology - C Toxicology and Pharmacology*, *151*(4), 473–479. https://doi.org/10.1016/j.cbpc.2010.02.005

Brooks, A. J., Eastwood, J., Beckingham, I. J., & Girling, K. J. (2004). Liver tissue partial pressure of oxygen and carbon dioxide during partial hepatectomy. *British Journal*

of Anaesthesia, *92*(5), 735–737. https://doi.org/10.1093/bja/aeh112

Brown, D. P. G., Chin-Sinex, H., Nie, B., Mendonca, M. S., & Wang, M. (2009). Targeting superoxide dismutase 1 to overcome cisplatin resistance in human ovarian cancer. *Cancer Chemotherapy and Pharmacology*, *63*(4), 723–730. https://doi.org/10.1007/s00280-008-0791-x

Bruick, R. K., & McKnight, S. L. (2001). A conserved family of prolyl-4-hydroxylases that modify HIF. *Science*, *294*(5545), 1337–1340. https://doi.org/10.1126/science.1066373

Bruix, J., Qin, S., Merle, P., Granito, A., Huang, Y. H., Bodoky, G., Pracht, M., Yokosuka, O., Rosmorduc, O., Breder, V., Gerolami, R., Masi, G., Ross, P. J., Song, T., Bronowicki, J. P., Ollivier-Hourmand, I., Kudo, M., Cheng, A. L., Llovet, J. M., … Han, G. (2017). Regorafenib for patients with hepatocellular carcinoma who progressed on sorafenib treatment (RESORCE): a randomised, double-blind, placebo-controlled, phase 3 trial. *The Lancet*, *389*(10064), 56–66. https://doi.org/10.1016/S0140-6736(16)32453-9

Bruix, J., & Sherman, M. (2011). Management of hepatocellular carcinoma: An update. *Hepatology*, *53*(3), 1020–1022.

Bruix, J., Sherman, M., Llovet, J. M., Beaugrand, M., Lencioni, R., Burroughs, A. K., Christensen, E., Pagliaro, L., Colombo, M., & Rodés, J. (2001). Clinical management of hepatocellular carcinoma. Conclusions of the barcelona-2000 EASL conference. *Journal of Hepatology*, *35*(3), 421–430. https://doi.org/10.1016/S0168-8278(01)00130-1

Buchanan, B. W., Lloyd, M. E., Engle, S. M., & Rubenstein, E. M. (2016). Cycloheximide chase analysis of protein degradation in Saccharomyces cerevisiae. *Journal of Visualized Experiments*, *2016*(110), 53975. https://doi.org/10.3791/53975

Bull, P C, Thomas, G. R., Rommens, J. M., Forbes, J. R., & Cox, D. W. (1993). The Wilson disease gene is a putative copper transporting P-type ATPase similar to the Menkes gene. *Nature Genetics*, *5*(4), 327–337.

Bull, Peter C., Thomas, G. R., Rommens, J. M., Forbes, J. R., & Cox, D. W. (1993). The Wilson disease gene is a putative copper transporting P-type ATPase similar to the menkes gene. *Nature Genetics*, *5*(4), 327–337. https://doi.org/10.1038/ng1293-327

Carpenter, A., Rassam, A., Jennings, M. H., Robinson-Jackson, S., Alexander, J. S., & Erkuran-Yilmaz, C. (2007). Effects of ammonium tetrathiomolybdate, an oncolytic/angiolytic drug on the viability and proliferation of endothelial and tumor cells. *Inflammation Research*, *56*(12), 515–519. https://doi.org/10.1007/s00011-007-7025-2

Carr, H. S., & Winge, D. R. (2003). Assembly of cytochrome c oxidase within the mitochondrion. *Accounts of Chemical Research*, *36*(5), 309–316. https://doi.org/10.1021/ar0200807

Carroll, M. C., Girouard, J. B., Ulloa, J. L., Subramaniam, J. R., Wong, P. C., Valentine,

J. S., & Culotta, V. C. (2004). Mechanisms for activating Cu- and Zn-containing superoxide dismutase in the absence of the CCS Cu chaperone. *Proceedings of the National Academy of Sciences of the United States of America*, *101*(16), 5964–5969. https://doi.org/10.1073/pnas.0308298101

Castaldo, G., Calcagno, G., Sibillo, R., Cuomo, R., Nardone, G., Castellano, L., Del Vecchio Blanco, C., Budillon, G., & Salvatore, F. (2000). Quantitative analysis of aldolase a mRNA in liver discriminates between hepatocellular carcinoma and cirrhosis. *Clinical Chemistry*, *46*(7). https://doi.org/10.1093/clinchem/46.7.901

Cen, D., Brayton, D., Shahandeh, B., Meyskens, F. L., & Farmer, P. J. (2004). Disulfiram facilitates intracellular Cu uptake and induces apoptosis in human melanoma cells. *Journal of Medicinal Chemistry*, *47*(27), 6914–6920. https://doi.org/10.1021/jm049568z

Chan, N., Willis, A., Kornhauser, N., Mward, M., Lee, S. B., Nackos, E., Seo, B. R., Chuang, E., Cigler, T., Moore, A., Donovan, D., Cobham, M. V., Fitzpatrick, V., Schneider, S., Wiener, A., Guillaume-Abraham, J., Aljom, E., Zelkowitz, R., Warren, J. D., … Vahdat, L. (2017). Influencing the tumor microenvironment: A Phase II study of copper depletion using tetrathiomolybdate in patients with breast cancer at high risk for recurrence and in preclinical models of lung metastases. *Clinical Cancer Research*, *23*(3), 666–676. https://doi.org/10.1158/1078-0432.CCR-16-1326

Chaneton, B., Hillmann, P., Zheng, L., Martin, A. C. L., Maddocks, O. D. K., Chokkathukalam, A., Coyle, J. E., Jankevics, A., Holding, F. P., Vousden, K. H., Frezza, C., O'Reilly, M., & Gottlieb, E. (2012). Serine is a natural ligand and allosteric activator of pyruvate kinase M2. *Nature*, *491*(7424), 458–462. https://doi.org/10.1038/nature11540

Chen, H., Huang, G., Su, T., Gao, H., Attieh, Z. K., McKie, A. T., Anderson, G. J., & Vulpe, C. D. (2006). Decreased Hephaestin Activity in the Intestine of Copper-Deficient Mice Causes Systemic Iron Deficiency. *The Journal of Nutrition*, *136*(5), 1236–1241. https://doi.org/10.1093/jn/136.5.1236

Chen, R., Xu, X., Tao, Y., Qian, Z., & Yu, Y. (2019). Exosomes in hepatocellular carcinoma: A new horizon. In *Cell Communication and Signaling* (Vol. 17, Issue 1, pp. 1–11). BioMed Central Ltd. https://doi.org/10.1186/s12964-018-0315-1

Chen, Z., Lu, X., Wang, Z., Jin, G., Wang, Q., Chen, D., Chen, T., Li, J., Fan, J., Cong, W., Gao, Q., & He, X. (2015). Co-expression of PKM2 and TRIM35 predicts survival and recurrence in hepatocellular carcinoma. *Oncotarget*, *6*(4), 2538–2548. https://doi.org/10.18632/oncotarget.2991

Christofk, H. R., Vander Heiden, M. G., Wu, N., Asara, J. M., & Cantley, L. C. (2008). Pyruvate kinase M2 is a phosphotyrosine-binding protein. *Nature*, *452*(7184), 181–186. https://doi.org/10.1038/nature06667

Chung, R. S., Howells, C., Eaton, E. D., Shabala, L., Zovo, K., Palumaa, P., Sillard, R., Woodhouse, A., Bennett, W. R., Ray, S., Vickers, J. C., & West, A. K. (2010). The Native Copper- and Zinc- Binding Protein Metallothionein Blocks Copper-Mediated

Aβ Aggregation and Toxicity in Rat Cortical Neurons. *PLoS ONE*, *5*(8), e12030. https://doi.org/10.1371/journal.pone.0012030

Church, S. J., Begley, P., Kureishy, N., McHarg, S., Bishop, P. N., Bechtold, D. A., Unwin, R. D., & Cooper, G. J. S. (2015). Deficient copper concentrations in dried-defatted hepatic tissue from ob/ob mice: A potential model for study of defective copper regulation in metabolic liver disease. *Biochemical and Biophysical Research Communications*, *460*(3), 549–554. https://doi.org/10.1016/j.bbrc.2015.03.067

Conticello, C., Martinetti, D., Adamo, L., Buccheri, S., Giuffrida, R., Parrinello, N., Lombardo, L., Anastasi, G., Amato, G., Cavalli, M., Chiarenza, A., De Maria, R., Giustolisi, R., Gulisano, M., & Di Raimondo, F. (2012). Disulfiram, an old drug with new potential therapeutic uses for human hematological malignancies. *International Journal of Cancer*, *131*(9), 2197–2203. https://doi.org/10.1002/ijc.27482

Cossack, Z. T., & Bouquet, J. (1986). The Treatment of Wilson's Disease in Paediatrics: Oral Zinc Thearpy Versus Penicillamine. *Acta Pharmacologica et Toxicologica*, *59*(7), 514–517. https://doi.org/10.1111/j.1600-0773.1986.tb02815.x

Cox, C., Teknos, T. N., Barrios, M., Brewer, G. J., Dick, R. D., & Merajver, S. D. (2001). The Role of Copper Suppression as an Antiangiogenic Strategy in Head and Neck Squamous Cell Carcinoma. *The Laryngoscope*, *111*(4), 696–701. https://doi.org/10.1097/00005537-200104000-00024

Crow, J. P., Sampson, J. B., Zhuang, Y., Thompson, J. A., & Beckman, J. S. (1997). Decreased Zinc Affinity of Amyotrophic Lateral Sclerosis-Associated Superoxide Dismutase Mutants Leads to Enhanced Catalysis of Tyrosine Nitration by Peroxynitrite. *Journal of Neurochemistry*, *69*(5), 1936–1944. https://doi.org/10.1046/j.1471-4159.1997.69051936.x

Dai, X. L., Sun, Y. X., & Jiang, Z. F. (2006). Cu(II) potentiation of Alzheimer Aβ1-40 cytotoxicity and transition on its secondary structure. *Acta Biochimica et Biophysica Sinica*, *38*(11), 765–772. https://doi.org/10.1111/j.1745-7270.2006.00228.x

Davies, P., Moualla, D., & Brown, D. R. (2011). Alpha-Synuclein Is a Cellular Ferrireductase. *PLoS ONE*, *6*(1), 15814. https://doi.org/10.1371/journal.pone.0015814

Davis, C. I., Gu, X., Kiefer, R. M., Ralle, M., Gade, T. P., & Brady, D. C. (2020). Altered copper homeostasis underlies sensitivity of hepatocellular carcinoma to copper chelation. *Metallomics*. https://doi.org/10.1039/D0MT00156B

De Berardinis, R. J., & Chandel, N. S. (2016). Fundamentals of cancer metabolism. *Science Advances*, *2*(5), e1600200. https://doi.org/10.1126/sciadv.1600200

De Feo, C. J., Aller, S. G., Siluvai, G. S., Blackburn, N. J., & Unger, V. M. (2009). Three-dimensional structure of the human copper transporter hCTR1. *Proceedings of the National Academy of Sciences of the United States of America*, *106*(11), 4237–4242. https://doi.org/10.1073/pnas.0810286106

De Matteis, S., Ragusa, A., Marisi, G., De Domenico, S., Casadei Gardini, A., Bonafè,

M., & Giudetti, A. M. (2018). Aberrant metabolism in hepatocellular carcinoma provides diagnostic and therapeutic opportunities. *Oxidative Medicine and Cellular Longevity*. https://doi.org/10.1155/2018/7512159

Dodani, S. C., Firl, A., Chan, J., Nam, C. I., Aron, A. T., Onak, C. S., Ramos-Torres, K. M., Paek, J., Webster, C. M., Feller, M. B., & Chang, C. J. (2014). Copper is an endogenous modulator of neural circuit spontaneous activity. *Proceedings of the National Academy of Sciences of the United States of America*, *111*(46), 16280–16285. https://doi.org/10.1073/pnas.1409796111

Dombrauckas, J. D., Santarsiero, B. D., & Mesecar, A. D. (2005). Structural basis for tumor pyruvate kinase M2 allosteric regulation and catalysis. *Biochemistry*, *44*(27), 9417–9429. https://doi.org/10.1021/bi0474923

Du, R., Lu, K. V., Petritsch, C., Liu, P., Ganss, R., Passegué, E., Song, H., VandenBerg, S., Johnson, R. S., Werb, Z., & Bergers, G. (2008). HIF1α Induces the Recruitment of Bone Marrow-Derived Vascular Modulatory Cells to Regulate Tumor Angiogenesis and Invasion. *Cancer Cell*, *13*(3), 206–220. https://doi.org/10.1016/j.ccr.2008.01.034

Eales, K. L., Hollinshead, K. E. R., & Tennant, D. A. (2016). Hypoxia and metabolic adaptation of cancer cells. *Oncogenesis*, *5*(1), e190–e190. https://doi.org/10.1038/oncsis.2015.50

Ebara, M., Fukuda, H., Hatano, R., Saisho, H., Nagato, Y., Suzuki, K., Nakajima, K., Yukawa, M., Kondo, F., Nakayama, A., & Sakurai, H. (2000). Relationship between copper, zinc and metallothionein in hepatocellular carcinoma and its surrounding liver parenchyma. *Journal of Hepatology*, *33*(3), 415–422. https://doi.org/10.1016/S0168-8278(00)80277-9

Ebara, M., Fukuda, H., Hatano, R., Yoshikawa, M., Sugiura, N., Saisho, H., Kondo, F., & Yukawa, M. (2003). Metal Contents in the Liver of Patients with Chronic Liver Disease Caused by Hepatitis C Virus. *Oncology*, *65*(4), 323–330. https://doi.org/10.1159/000074645

Eckerich, C., Zapf, S., Fillbrandt, R., Loges, S., Westphal, M., & Lamszus, K. (2007). Hypoxia can induce c-Met expression in glioma cells and enhance SF/HGF-induced cell migration. *International Journal of Cancer*, *121*(2), 276–283. https://doi.org/10.1002/ijc.22679

El-Serag, H. B. (2011). Hepatocellular Carcinoma. In *N Engl J Med* (Vol. 365).

El Fotouh, O. A., El Aziz, H. A., Galal, M., & El Nakeeb, N. (2012). Copper and zinc levels in serum and tissue in Egyptian patients with hepatocellular carcinoma and cirrhosis. *Egyptian Liver Journal*, *2*(1), 7–11. https://doi.org/10.1097/01.ELX.0000405290.36755.1c

Espinoza, A., Le Blanc, S., Olivares, M., Pizarro, F., Ruz, M., & Arredondo, M. (2012). Iron, copper, and zinc transport: Inhibition of divalent metal transporter 1 (DMT1) and human copper transporter 1 (hCTR1) by shRNA. *Biological Trace Element Research*, *146*(2), 281–286. https://doi.org/10.1007/s12011-011-9243-2

Feng, W., Ye, F., Xue, W., Zhou, Z., & Kang, Y. J. (2009). Copper regulation of hypoxia-inducible factor-1 activity. *Molecular Pharmacology*, *75*(1), 174–182. https://doi.org/10.1124/mol.108.051516

Fieten, H., Dirksen, K., van den Ingh, T. S. G. A. M., Winter, E. A., Watson, A. L., Leegwater, P. A. J., & Rothuizen, J. (2013). D-penicillamine treatment of copper-associated hepatitis in Labrador retrievers. *Veterinary Journal*, *196*(3), 522–527. https://doi.org/10.1016/j.tvjl.2012.12.013

Flowers, P., Neth, E. J., Robinson, W. R., Theopold, K., & Langley, R. (2019). Occurrence, Preparation, and Properties of Transition Metals and Their Compounds. In *Chemistry: Atoms First, 2E* (2nd ed.). OpenStax. https://openstax.org/details/books/chemistry-atoms-first-

Fodor, D., Jung, I., Turdean, S., Satala, C., & Gurzu, S. (2019). Angiogenesis of hepatocellular carcinoma: An immunohistochemistry study. *World Journal of Hepatology*, *11*(3), 294–304. https://doi.org/10.4254/wjh.v11.i3.294

Frazer, D. M., Vulpe, C. D., McKie, A. T., Wilkins, S. J., Trinder, D., Cleghorn, G. J., & Anderson, G. J. (2001). Cloning and gastrointestinal expression of rat hephaestin: Relationship to other iron transport proteins. *American Journal of Physiology - Gastrointestinal and Liver Physiology*, *281*(4 44-4). https://doi.org/10.1152/ajpgi.2001.281.4.g931

Furuyama, K., Kawaguchi, Y., Akiyama, H., Horiguchi, M., Kodama, S., Kuhara, T., Hosokawa, S., Elbahrawy, A., Soeda, T., Koizumi, M., Masui, T., Kawaguchi, M., Takaori, K., Doi, R., Nishi, E., Kakinoki, R., Deng, J. M., Behringer, R. R., Nakamura, T., & Uemoto, S. (2011). Continuous cell supply from a Sox9-expressing progenitor zone in adult liver, exocrine pancreas and intestine. *Nature Genetics*, *43*(1), 34–41. https://doi.org/10.1038/ng.722

Gaballah, A. H., Jensen, C. T., Palmquist, S., Pickhardt, P. J., Duran, A., Broering, G., & Elsayes, K. M. (2017). Angiosarcoma: Clinical and imaging features from head to toe. *British Journal of Radiology*, *90*(1075). https://doi.org/10.1259/bjr.20170039

Gade, T. P. F., Hunt, S. J., Harrison, N., Nadolski, G. J., Weber, C., Pickup, S., Furth, E. E., Schnall, M. D., Soulen, M. C., & Celeste Simon, M. (2015). Segmental transarterial embolization in a translational rat model of hepatocellular carcinoma. *Journal of Vascular and Interventional Radiology*, *26*(8), 1229–1237. https://doi.org/10.1016/j.jvir.2015.02.006

Gade, T. P. F., Tucker, E., Nakazawa, M. S., Hunt, S. J., Wong, W., Krock, B., Weber, C. N., Nadolski, G. J., Clark, T. W. I., Soulen, M. C., Furth, E. E., Winkler, J. D., Amaravadi, R. K., & Simon, M. C. (2017). Ischemia Induces Quiescence and Autophagy Dependence in Hepatocellular Carcinoma. *Radiology*, *000*(0), 160728. https://doi.org/10.1148/radiol.2017160728

Gao, C., Zhu, L., Zhu, F., Sun, J., & Zhu, Z. (2014). Effects of different sources of copper on Ctr1, ATP7A, ATP7B, MT and DMT1 protein and gene expression in Caco-2 cells. *Journal of Trace Elements in Medicine and Biology*, *28*(3), 344–350. https://doi.org/10.1016/j.jtemb.2014.04.004

Gartner, E. M., Griffith, K. A., Pan, Q., Brewer, G. J., Henja, G. F., Merajver, S. D., & Zalupski, M. M. (2009). A pilot trial of the anti-angiogenic copper lowering agent tetrathiomolybdate in combination with irinotecan, 5-flurouracil, and leucovorin for metastatic colorectal cancer. *Investigational New Drugs*, *27*(2), 159–165. https://doi.org/10.1007/s10637-008-9165-9

Genoud, S., Roberts, B. R., Gunn, A. P., Halliday, G. M., Lewis, S. J. G., Ball, H. J., Hare, D. J., & Double, K. L. (2017). Subcellular compartmentalisation of copper, iron, manganese, and zinc in the Parkinson's disease brain. *Metallomics*, *9*(10), 1447–1455. https://doi.org/10.1039/c7mt00244k

George, G. N., Pickering, I. J., Harris, H. H., Gailer, J., Klein, D., Lichtmannegger, J., & Summer, K. H. (2003). Tetrathiomolybdate causes formation of hepatic copper-molybdenum clusters in an animal model of Wilson's disease. *Journal of the American Chemical Society*, *125*(7), 1704–1705. https://doi.org/10.1021/ja029054u

González, M., Reyes-Jara, A., Suazo, M., Jo, W. J., & Vulpe, C. (2008). Expression of copper-related genes in response to copper load. *The American Journal of Clinical Nutrition*, *88*(3), 830S-834S. https://doi.org/10.1093/ajcn/88.3.830S

Guichard, C., Amaddeo, G., Imbeaud, S., Ladeiro, Y., Pelletier, L., Maad, I. Ben, Calderaro, J., Bioulac-Sage, P., Letexier, M., Degos, F., Clément, B., Balabaud, C., Chevet, E., Laurent, A., Couchy, G., Letouzé, E., Calvo, F., & Zucman-Rossi, J. (2012). Integrated analysis of somatic mutations and focal copy-number changes identifies key genes and pathways in hepatocellular carcinoma. *Nature Genetics*, *44*(6), 694–698. https://doi.org/10.1038/ng.2256

Günther, V., Lindert, U., & Schaffner, W. (2012). The taste of heavy metals: Gene regulation by MTF-1. *Biochimica et Biophysica Acta - Molecular Cell Research*, *1823*(9), 1416–1425. https://doi.org/10.1016/j.bbamcr.2012.01.005

Guo, Y., Smith, K., Lee, J., Thiele, D. J., & Petris, M. J. (2004). Identification of Methionine-rich Clusters That Regulate Copper-stimulated Endocytosis of the Human Ctr1 Copper Transporter. *Journal of Biological Chemistry*, *279*(17), 17428–17433. https://doi.org/10.1074/jbc.M401493200

Gupte, A., & Mumper, R. J. (2009). Elevated copper and oxidative stress in cancer cells as a target for cancer treatment. *Cancer Treatment Reviews*, *35*(1), 32–46. https://doi.org/10.1016/j.ctrv.2008.07.004

Guzman, G., Chennuri, R., Chan, A., Rea, B., Quintana, A., Patel, R., Xu, P. Z., Xie, H., & Hay, N. (2015). Evidence for Heightened Hexokinase II Immunoexpression in Hepatocyte Dysplasia and Hepatocellular Carcinoma. *Digestive Diseases and Sciences*, *60*(2), 420–426. https://doi.org/10.1007/s10620-014-3364-3

Ha, W.-S., Kim, C.-K., Song, S.-H., & Kang, C.-B. (2001). Study on mechanism of multistep hepatotumorigenesis in rat: development of hepatotumorigenesis. *J. Vet. Sci*, *2*(1), 53–58.

Hara, S., Nakashiro, K. ichi, Klosek, S. K., Ishikawa, T., Shintani, S., & Hamakawa, H. (2006). Hypoxia enhances c-Met/HGF receptor expression and signaling by

activating HIF-1α in human salivary gland cancer cells. *Oral Oncology*, *42*(6), 593–598. https://doi.org/10.1016/j.oraloncology.2005.10.016

Harris, E. D. (2001). Copper Homeostasis: The Role of Cellular Transporters. *Nutrition Reviews*, *59*(9), 281–285. https://doi.org/10.1111/j.1753-4887.2001.tb07017.x

Harris, Z. L., Klomp, L. W., & Gitlin, J. D. (1998). Aceruloplasminemia: an inherited neurodegenerative disease with impairment of iron homeostasis. *The American Journal of Clinical Nutrition*, *67*(5 Suppl), 972S-977S. https://doi.org/10.1093/ajcn/67.5.972S

Hasan, N. M., Gupta, A., Polishchuks, E., Yu, C. H., Polishchuks, R., Dmitriev, O. Y., & Lutsenko, S. (2012). Molecular events initiating exit of a copper-transporting ATPase ATP7B from the trans-Golgi network. *Journal of Biological Chemistry*, *287*(43), 36041–36050. https://doi.org/10.1074/jbc.M112.370403

Hasinoff, B. B., Yadav, A. A., Patel, D., & Wu, X. (2014). The cytotoxicity of the anticancer drug elesclomol is due to oxidative stress indirectly mediated through its complex with Cu(II). *Journal of Inorganic Biochemistry*, *137*. https://doi.org/10.1016/j.jinorgbio.2014.04.004

Hay, N. (2016). Reprogramming glucose metabolism in cancer: Can it be exploited for cancer therapy? *Nature Reviews Cancer*, *16*(10), 635–649. https://doi.org/10.1038/nrc.2016.77

Hayashi, M., Nishiya, H., Chiba, T., Endoh, D., Kon, Y., & Okui, T. (2007). Trientine, a Copper-Chelating Agent, Induced Apoptosis in Murine Fibrosarcoma Cells In Vivo and In Vitro. *Journal of Veterinary Medical Science*, *69*(2), 137–142. https://doi.org/10.1292/jvms.69.137

Hedley, D., Shamas-Din, A., Chow, S., Sanfelice, D., Schuh, A. C., Brandwein, J. M., Seftel, M. D., Gupta, V., Yee, K. W. L., & Schimmer, A. D. (2016). A phase I study of elesclomol sodium in patients with acute myeloid leukemia. *Leukemia and Lymphoma*, *57*(10). https://doi.org/10.3109/10428194.2016.1138293

Heimbach, J. K., Kulik, L. M., Finn, R. S., Sirlin, C. B., Abecassis, M. M., Roberts, L. R., Zhu, A. X., Murad, M. H., & Marrero, J. A. (2018). AASLD guidelines for the treatment of hepatocellular carcinoma. *Hepatology*, *67*(1), 358–380. https://doi.org/10.1002/hep.29086

Henry, N. L., Dunn, R., Merjaver, S., Pan, Q., Pienta, K. J., Brewer, G., & Smith, D. C. (2006). Phase II Trial of Copper Depletion with Tetrathiomolybdate as an Antiangiogenesis Strategy in Patients with Hormone-Refractory Prostate Cancer. *Oncology*, *71*(3–4), 168–175. https://doi.org/10.1159/000106066

Hernandez, S., Tsuchiya, Y., García-Ruiz, J. P., Lalioti, V., Nielsen, S., Cassio, D., & Sandoval, I. V. (2008). ATP7B Copper-Regulated Traffic and Association With the Tight Junctions: Copper Excretion Into the Bile. *Gastroenterology*, *134*(4), 1215–1223. https://doi.org/10.1053/j.gastro.2008.01.043

Higgins, D. F., Kimura, K., Bernhardt, W. M., Shrimanker, N., Akai, Y., Hohenstein, B.,

Saito, Y., Johnson, R. S., Kretzler, M., Cohen, C. D., Eckardt, K. U., Iwano, M., & Haase, V. H. (2007). Hypoxia promotes fibrogenesis in vivo via HIF-1 stimulation of epithelial-to-mesenchymal transition. *Journal of Clinical Investigation*, *117*(12), 3810–3820. https://doi.org/10.1172/JCI30487

Himoto, T., Fujita, K., Nomura, T., Tani, J., Miyoshi, H., Morishita, A., Yoneyama, H., Kubota, S., Haba, R., Suzuki, Y., & Masaki, T. (2016). Roles of Copper in Hepatocarcinogenesis via the Activation of Hypoxia-Inducible Factor-1α. *Biological Trace Element Research*, *174*(1), 58–64. https://doi.org/10.1007/s12011-016-0702-7

Hitosugi, T., Kang, S., Vander Heiden, M. G., Chung, T. W., Elf, S., Lythgoe, K., Dong, S., Lonial, S., Wang, X., Chen, G. Z., Xie, J., Gu, T. L., Polakiewicz, R. D., Roesel, J. L., Boggon, T. J., Khuri, F. R., Gilliland, D. G., Cantley, L. C., Kaufman, J., & Chen, J. (2009). Tyrosine phosphorylation inhibits PKM2 to promote the warburg effect and tumor growth. *Science Signaling*, *2*(97), ra73–ra73. https://doi.org/10.1126/scisignal.2000431

Hopkins, R. G., & Failla, M. L. (1997). Copper deficiency reduces interleukin-2 (IL-2) production and IL-2 mRNA in human T-lymphocytes. *Journal of Nutrition*, *127*(2). https://doi.org/10.1093/jn/127.2.257

Horn, N., Møller, L. B., Nurchi, V. M., & Aaseth, J. (2019). Chelating principles in Menkes and Wilson diseases: Choosing the right compounds in the right combinations at the right time. *Journal of Inorganic Biochemistry*, *190*, 98–112. https://doi.org/10.1016/j.jinorgbio.2018.10.009

Hou, G., Dick, R., Abrams, G. D., & Brewer, G. J. (2005). Tetrathiomolybdate protects against cardiac damage by doxorubicin in mice. *Journal of Laboratory and Clinical Medicine*, *146*(5), 299–303. https://doi.org/10.1016/j.lab.2005.07.004

Hu, W., Lu, S. X., Li, M., Zhang, C., Liu, L. L., Fu, J., Jin, J. T., Luo, R. Z., Zhang, C. Z., & Yun, J. P. (2015). Pyruvate kinase M2 prevents apoptosis via modulating Bim stability and associates with poor outcome in hepatocellular carcinoma. *Oncotarget*, *6*(9), 6570–6583. https://doi.org/10.18632/oncotarget.3262

Huang, Z. L., & Failla, M. L. (2000). Copper Deficiency Suppresses Effector Activities of Differentiated U937 Cells. *The Journal of Nutrition*, *130*(6). https://doi.org/10.1093/jn/130.6.1536

Huster, D. (2014). Structural and metabolic changes in Atp7b−/− mouse liver and potential for new interventions in Wilson's disease. *Annals of the New York Academy of Sciences*, *1315*(1), 37–44.

Huster, D., Purnat, T. D., Burkhead, J. L., Ralle, M., Fiehn, O., Stuckert, F., Olson, N. E., Teupser, D., & Lutsenko, S. (2007). High copper selectively alters lipid metabolism and cell cycle machinery in the mouse model of Wilson disease. *J Biol Chem*, *282*(11), 8343–8355.

Ikeda, K., Saitoh, S., Koida, I., Tsubota, A., Arase, Y., Chayama, K., & Kumada, H. (1994). Imaging diagnosis of small hepatocellular carcinoma. *Hepatology*, *20*(1),

82–87. https://doi.org/10.1002/hep.1840200113

Ishida, S., Andreux, P., Poitry-Yamate, C., Auwerx, J., & Hanahan, D. (2013). Bioavailable copper modulates oxidative phosphorylation and growth of tumors. *Proc Natl Acad Sci U S A*, *110*(48), 19507–19512.

Ishigami, I., Zatsepin, N. A., Hikita, M., Conrad, C. E., Nelson, G., Coe, J. D., Basu, S., Grant, T. D., Seaberg, M. H., Sierra, R. G., Hunter, M. S., Fromme, P., Fromme, R., Yeh, S. R., & Rousseau, D. L. (2017). Crystal structure of CO-bound cytochrome c oxidase determined by serial femtosecond X-ray crystallography at room temperature. *Proceedings of the National Academy of Sciences of the United States of America*, *114*(30), 8011–8016. https://doi.org/10.1073/pnas.1705628114

Iwadate, H., Ohira, H., Suzuki, T., Abe, K., Yokokawa, J., Takiguchi, J., Rai, T., Orikasa, H., Irisawa, A., Obara, K., Kasukawa, R., & Sato, Y. (2004). Hepatocellular Carcinoma Associated with Wilson's Disease. *Internal Medicine*, *43*(11), 1042–1045. https://doi.org/10.2169/internalmedicine.43.1042

Jain, M., Nilsson, R., Sharma, S., Madhusudhan, N., Kitami, T., Souza, A. L., Kafri, R., Kirschner, M. W., Clish, C. B., & Mootha, V. K. (2012). Metabolite profiling identifies a key role for glycine in rapid cancer cell proliferation. *Science*, *336*(6084), 1040–1044. https://doi.org/10.1126/science.1218595

Jain, S., Cohen, J., Ward, M. M., Kornhauser, N., Chuang, E., Cigler, T., Moore, A., Donovan, D., Lam, C., Cobham, M. V., Schneider, S., Hurtado Rúa, S. M., Benkert, S., Mathijsen Greenwood, C., Zelkowitz, R., Warren, J. D., Lane, M. E., Mittal, V., Rafii, S., & Vahdat, L. T. (2013). Tetrathiomolybdate-associated copper depletion decreases circulating endothelial progenitor cells in women with breast cancer at high risk of relapse. *Annals of Oncology*, *24*(6), 1491–1498. https://doi.org/10.1093/annonc/mds654

Jiang, J., Nadas, I. A., Kim, M. A., & Franz, K. J. (2005). A Mets motif peptide found in copper transport proteins selectively binds Cu(I) with methionine-only coordination. *Inorganic Chemistry*, *44*(26), 9787–9794. https://doi.org/10.1021/ic051180m

Jiang, L., Garrick, M. D., Garrick, L. M., Zhao, L., & Collins, J. F. (2013). Divalent metal transporter 1 (Dmt1) Mediates Copper Transport in the Duodenum of Iron-Deficient Rats and When Overexpressed in Iron-Deprived HEK-293 Cells. *The Journal of Nutrition*, *143*(12), 1927–1933. https://doi.org/10.3945/jn.113.181867

Jiang, Y., Dai, A., Li, Q., & Hu, R. (2007). Hypoxia Induces Transforming Growth Factor-β1 Gene Expression in the Pulmonary Artery of Rats via Hypoxia-inducible Factor-1α. *Acta Biochimica et Biophysica Sinica*, *39*(1), 73–80. https://doi.org/10.1111/j.1745-7270.2007.00249.x

Jie, J., Hao, S., Hongxiu, Y., Huiying, Y., Jun, M., Chenji, W., Mingjie, Y., & Yong, M. (2007). Evaluation of Cu in hepatocellular carcinoma by particle induced X-ray emission. *Journal of Trace Elements in Medicine and Biology*, *21*(4), 255–260. https://doi.org/10.1016/j.jtemb.2007.06.004

Jin, N., Zhu, X., Cheng, F., & Zhang, L. (2018). Disulfiram/copper targets stem cell-like

ALDH $^{+}$ population of multiple myeloma by inhibition of ALDH1A1 and Hedgehog pathway. *Journal of Cellular Biochemistry*, *119*(8), 6882–6893. https://doi.org/10.1002/jcb.26885

Jung, H. R., Kang, H. M., Ryu, J. W., Kim, D. S., Noh, K. H., Kim, E. S., Lee, H. J., Chung, K. S., Cho, H. S., Kim, N. S., Im, D. S., Lim, J. H., & Jung, C. R. (2017). Cell Spheroids with Enhanced Aggressiveness to Mimic Human Liver Cancer in Vitro and in Vivo. *Scientific Reports*, *7*(1), 1–14. https://doi.org/10.1038/s41598-017-10828-7

Kaelin, W. G. (2008). The von Hippel-Lindau tumour suppressor protein: O2 sensing and cancer. *Nature Reviews Cancer*, *8*(11), 865–873. https://doi.org/10.1038/nrc2502

Kahra, D., Kovermann, M., & Wittung-Stafshede, P. (2016). The C-Terminus of Human Copper Importer Ctr1 Acts as a Binding Site and Transfers Copper to Atox1. *Biophysical Journal*, *110*(1), 95–102. https://doi.org/10.1016/j.bpj.2015.11.016

Kalaiarasan, P., Subbarao, N., & Bamezai, R. N. K. (2014). Molecular simulation of Tyr105 phosphorylated pyruvate kinase M2 to understand its structure and dynamics. *Journal of Molecular Modeling*, *20*(9), 1–12. https://doi.org/10.1007/s00894-014-2447-6

Kang, Y. B. A., Eo, J., Mert, S., Yarmush, M. L., & Usta, O. B. (2018). Metabolic Patterning on a Chip: Towards in vitro Liver Zonation of Primary Rat and Human Hepatocytes. *Scientific Reports*, *8*(1), 1–13. https://doi.org/10.1038/s41598-018-27179-6

Kapitsinou, P. P., Liu, Q., Unger, T. L., Rha, J., Davidoff, O., Keith, B., Epstein, J. A., Moores, S. L., Erickson-Miller, C. L., & Haase, V. H. (2010). Hepatic HIF-2 regulates erythropoietic responses to hypoxia in renal anemia. *Blood*, *116*(16), 3039–3048. https://doi.org/10.1182/blood-2010-02-270322

Karim, S., Adams, D. H., & Lalor, P. F. (2012). Hepatic expression and cellular distribution of the glucose transporter family. *World Journal of Gastroenterology*, *18*(46), 6771–6781. https://doi.org/10.3748/wjg.v18.i46.6771

Kato, N., Nakamura, M., & Uchiyama, T. (1999). 1H NMR studies of the reactions of copper(I) and copper(II) with D- penicillamine and glutathione. *Journal of Inorganic Biochemistry*, *75*(2), 117–121. https://doi.org/10.1016/S0162-0134(99)00044-6

Keith, B., Johnson, R. S., & Simon, M. C. (2012). HIF1 α and HIF2 α: sibling rivalry in hypoxic tumour growth and progression. *Nature Reviews Cancer*, *12*(1), 9–22. https://doi.org/10.1038/nrc3183

Kiefer, R. M., Hunt, S. J., Pulido, S., Pickup, S., Furth, E. E., Soulen, M. C., Nadolski, G. J., & Gade, T. P. (2017). Relative Initial Weight Is Associated with Improved Survival without Altering Tumor Latency in a Translational Rat Model of Diethylnitrosamine-Induced Hepatocellular Carcinoma and Transarterial Embolization. *Journal of Vascular and Interventional Radiology*, *28*(7), 1043-1050.e2. https://doi.org/10.1016/j.jvir.2017.03.037

Kim, H. seok, & El-Serag, H. B. (2019). The Epidemiology of Hepatocellular Carcinoma in the USA. *Current Gastroenterology Reports*, *21*(4), 1–8. https://doi.org/10.1007/s11894-019-0681-x

Kim, K. K., Abelman, S., Yano, N., Ribeiro, J. R., Singh, R. K., Tipping, M., & Moore, R. G. (2015). Tetrathiomolybdate inhibits mitochondrial complex IV and mediates degradation of hypoxia-inducible factor-1α in cancer cells. *Scientific Reports*, *5*(1), 14296. https://doi.org/10.1038/srep14296

Kim, Y. J., Tsang, T., Anderson, G. R., Posimo, J. M., & Brady, D. C. (2020). Inhibition of BCL2 family members increases the efficacy of copper chelation in BRAFV600E-driven melanoma. *Cancer Research*, *80*(7), 1387–1400. https://doi.org/10.1158/0008-5472.CAN-19-1784

Kimber, R. L., Parmeggiani, F., Joshi, N., Rakowski, A. M., Haigh, S. J., Turner, N. J., & Lloyd, J. R. (2019). Synthesis of copper catalysts for click chemistry from distillery wastewater using magnetically recoverable bionanoparticles. *Green Chemistry*, *21*(15), 4020–4024. https://doi.org/10.1039/c9gc00270g

Kirshner, J. R., He, S., Balasubramanyam, V., Kepros, J., Yang, C. Y., Zhang, M., Du, Z., Barsoum, J., & Bertin, J. (2008). Elesclomol induces cancer cell apoptosis through oxidative stress. *Molecular Cancer Therapeutics*, *7*(8). https://doi.org/10.1158/1535-7163.MCT-08-0298

Krishnamachary, B., Berg-Dixon, S., Kelly, B., Agani, F., Feldser, D., Ferreira, G., Iyer, N., LaRusch, J., Pak, B., Taghavi, P., & Semenza, G. L. (2003). Regulation of colon carcinoma cell invasion by hypoxia-inducible factor 1. *Cancer Research*, *63*(5), 1138–1143. https://cancerres.aacrjournals.org/content/63/5/1138.long

Krishnamoorthy, L., Cotruvo, J. A., Chan, J., Kaluarachchi, H., Muchenditsi, A., Pendyala, V. S., Jia, S., Aron, A. T., Ackerman, C. M., Wal, M. N. V., Guan, T., Smaga, L. P., Farhi, S. L., New, E. J., Lutsenko, S., & Chang, C. J. (2016). Copper regulates cyclic-AMP-dependent lipolysis. *Nature Chemical Biology*, *12*(8), 586–592. https://doi.org/10.1038/nchembio.2098

Kumagi, T., Horiike, N., Abe, M., Kurose, K., Iuchi, H., Masumoto, T., Joko, K., Akbar, S. M. F., Michitaka, K., & Onji, M. (2005). Small Hepatocellular Carcinoma Associated with Wilson's Disease. *Internal Medicine*, *44*(5), 439–443. https://doi.org/10.2169/internalmedicine.44.439

Kumagi, T., Horiike, N., Michitaka, K., Hasebe, A., Kawai, K., Tokumoto, Y., Nakanishi, S., Furukawa, S., Hiasa, Y., Matsui, H., Kurose, K., Matsuura, B., & Onji, M. (2004). Recent clinical features of Wilson's disease with hepatic presentation. *Journal of Gastroenterology*, *39*(12), 1165–1169. https://doi.org/10.1007/s00535-004-1466-y

Kumcu, E. K., Büyüknacar, H. S. G., Göçmen, C., Evrüke, I. C., & Önder, S. (2009). Differential effect of neocuproine, a copper(I) chelator, on contractile activity in isolated ovariectomized non-pregnant rat, pregnant rat and pregnant human uterus. *European Journal of Pharmacology*, *605*(1–3), 158–163. https://doi.org/10.1016/j.ejphar.2009.01.008

Kung-Chun Chiu, D., Pui-Wah Tse, A., Law, C. T., Ming-Jing Xu, I., Lee, D., Chen, M., Kit-Ho Lai, R., Wai-Hin Yuen, V., Wing-Sum Cheu, J., Wai-Hung Ho, D., Wong, C. M., Zhang, H., Oi-Lin Ng, I., & Chak-Lui Wong, C. (2019). Hypoxia regulates the mitochondrial activity of hepatocellular carcinoma cells through HIF/HEY1/PINK1 pathway. *Cell Death and Disease*, *10*(12), 1–16. https://doi.org/10.1038/s41419-019-2155-3

Kuo, Y. M., Zhou, B., Cosco, D., & Gitschier, J. (2001). The copper transporter CTR1 provides an essential function in mammalian embryonic development. *Proceedings of the National Academy of Sciences of the United States of America*, *98*(12), 6836–6841. https://doi.org/10.1073/pnas.111057298

Laitinen, R., Vuori, E., & Viikari, J. (1989). Serum Zinc and Copper: Associations with Cholesterol and Triglycride Levels in Children and Adolescents. Cardiovascular Risk in Young Finns. *Journal of the American College of Nutrition*, *8*(5), 400–406. https://doi.org/10.1080/07315724.1989.10720314

Leary, T. S., Klinck, J. R., Hayman, G., Friend, P., Jamieson, N. V., & Gupta, A. K. (2002). Measurement of liver tissue oxygenation after orthotopic liver transplantation using a multiparameter sensor. *Anaesthesia*, *57*(11), 1128–1133. https://doi.org/10.1046/j.1365-2044.2002.02782_5.x

Lee, J.-W., Eo Ng-H U I B Ae, S., On Jeong, J.-W., Im, S. E.-H. E. K., & Im, K. Y.-W. O. K. (2004). Hypoxia-inducible factor (HIF-1)α: its protein stability and biological functions. *EXPERIMENTAL and MOLECULAR MEDICINE*, *36*(1), 1–12.

Lee, J., Prohaska, J. R., & Thiele, D. J. (2001). Essential role for mammalian copper transporter Ctr1 in copper homeostasis and embryonic development. *Proceedings of the National Academy of Sciences of the United States of America*, *98*(12), 6842–6847. https://doi.org/10.1073/pnas.111058698

Lee, J. S. (2015). The mutational landscape of hepatocellular carcinoma. *Clinical and Molecular Hepatology*, *21*(3), 220–229. https://doi.org/10.3350/cmh.2015.21.3.220

Lee, S. E., Chang, S. H., Kim, W. Y., Lim, S. D., Kim, W. S., Hwang, T. S., & Han, H. S. (2016). Frequent somatic TERT promoter mutations and CTNNB1 mutations in hepatocellular carcinoma. *Oncotarget*, *7*(43), 69267–69275. https://doi.org/10.18632/oncotarget.12121

Lee, V. S., Halabi, C. M., Broekelmann, T. J., Trackman, P. C., Stitziel, N. O., & Mecham, R. P. (2019). Intracellular retention of mutant lysyl oxidase leads to aortic dilation in response to increased hemodynamic stress. *JCI Insight*, *4*(15). https://doi.org/10.1172/jci.insight.127748

Leinartaitè, L., Saraboji, K., Nordlund, A., Logan, D. T., & Oliveberg, M. (2010). Folding catalysis by transient coordination of Zn2+ to the Cu ligands of the als-associated enzyme Cu/Zn superoxide dismutase 1. *Journal of the American Chemical Society*, *132*(38), 13495–13504. https://doi.org/10.1021/ja1057136

Lenartowicz, M., Wieczerzak, K., Krzeptowski, W., Dobosz, P., Grzmil, P., Starzyn, R., & Lipin, P. (2010). Developmental Changes in the Expression of the Atp7a Gene in

the Liver of Mice During the Postnatal Period. *J. Exp. Zool*, *313*, 209–217. https://doi.org/10.1002/jez.586

Lencioni, R., & Crocetti, L. (2007). Radiofrequency Ablation of Liver Cancer. *Techniques in Vascular and Interventional Radiology*, *10*(1), 38–46. https://doi.org/10.1053/j.tvir.2007.08.006

Lencioni, R., Crocetti, L., De Simone, P., & Filipponi, F. (2010). Loco-regional interventional treatment of hepatocellular carcinoma: techniques, outcomes, and future prospects. *Transplant International*, *23*(7), 698–703. https://doi.org/10.1111/j.1432-2277.2010.01109.x

Lerner, A. B., & Fitzpatrick, T. B. (1950). Biochemistry of melanin formation. *Physiological Reviews*, *30*(1), 91–126. https://doi.org/10.1152/physrev.1950.30.1.91

Lewis, C. A., Parker, S. J., Fiske, B. P., McCloskey, D., Gui, D. Y., Green, C. R., Vokes, N. I., Feist, A. M., Vander Heiden, M. G., & Metallo, C. M. (2014). Tracing Compartmentalized NADPH Metabolism in the Cytosol and Mitochondria of Mammalian Cells. *Molecular Cell*, *55*(2), 253–263. https://doi.org/10.1016/j.molcel.2014.05.008

Li, T., Zhong, J., Dong, X., Xiu, P., Wang, F., Wei, H., Wang, X., Xu, Z., Liu, F., Sun, X., & Li, J. (2016). Meloxicam suppresses hepatocellular carcinoma cell proliferation and migration by targeting COX-2/PGE2-regulated activation of the β-catenin signaling pathway. *Oncology Reports*, *35*(6), 3614–3622. https://doi.org/10.3892/or.2016.4764

Liang, J., Cao, R., Wang, X., Zhang, Y., Wang, P., Gao, H., Li, C., Yang, F., Zeng, R., Wei, P., Li, D., Li, W., & Yang, W. (2017). Mitochondrial PKM2 regulates oxidative stress-induced apoptosis by stabilizing Bcl2. *Cell Research*, *27*(3), 329–351. https://doi.org/10.1038/cr.2016.159

Liao, Y., Zhao, J., Bulek, K., Tang, F., Chen, X., Cai, G., Jia, S., Fox, P. L., Huang, E., Pizarro, T. T., Kalady, M. F., Jackson, M. W., Bao, S., Sen, G. C., Stark, G. R., Chang, C. J., & Li, X. (2020). Inflammation mobilizes copper metabolism to promote colon tumorigenesis via an IL-17-STEAP4-XIAP axis. *Nature Communications*, *11*(1), 1–15. https://doi.org/10.1038/s41467-020-14698-y

Lin, C., Song, W., Bi, X., Zhao, J., Huang, Z., Li, Z., Zhou, J., Cai, J., & Zhao, H. (2014). Recent advances in the ARID family: Focusing on roles in human cancer. *OncoTargets and Therapy*, *7*, 315–324. https://doi.org/10.2147/OTT.S57023

Lin, C., Zhang, Z., Wang, T., Chen, C., & James Kang, Y. (2015). Copper uptake by DMT1: A compensatory mechanism for CTR1 deficiency in human umbilical vein endothelial cells. *Metallomics*, *7*(8), 1285–1289. https://doi.org/10.1039/c5mt00097a

Linden, A. G., Li, S., Choi, H. Y., Fang, F., Fukasawa, M., Uyeda, K., Hammer, R. E., Horton, J. D., Engelking, L. J., & Liang, G. (2018). Interplay between ChREBP and SREBP-1c coordinates postprandial glycolysis and lipogenesis in livers of mice. *Journal of Lipid Research*, *59*(3), 475–487. https://doi.org/10.1194/jlr.M081836

Liu, M., Galli, G., Wang, Y., Fan, Q., Wang, Z., Wang, X., & Xiao, W. (2020). Novel Therapeutic Targets for Hypoxia-Related Cardiovascular Diseases: The Role of HIF-1. *Frontiers in Physiology*, *11*, 774. https://doi.org/10.3389/fphys.2020.00774

Liu, Q., Davidoff, O., Niss, K., & Haase, V. H. (2012). Hypoxia-inducible factor regulates hepcidin via erythropoietin-induced erythropoiesis. *Journal of Clinical Investigation*, *122*(12), 4635–4644. https://doi.org/10.1172/JCI63924

Liu, W. R., Tian, M. X., Yang, L. X., Lin, Y. L., Jin, L., Ding, Z. Bin, Shen, Y. H., Peng, Y. F., Gao, D. M., Zhou, J., Qiu, S. J., Dai, Z., He, R., Fan, J., & Shi, Y. H. (2015). PKM2 promotes metastasis by recruiting myeloid-derived suppressor cells and indicates poor prognosis for hepatocellular carcinoma. *Oncotarget*, *6*(2), 846–861. https://doi.org/10.18632/oncotarget.2749

Liu, X., Zhang, W., Wu, Z., Yang, Y., & Kang, Y. J. (2018). Copper levels affect targeting of hypoxia-inducible factor 1 to the promoters of hypoxia-regulated genes. *Journal of Biological Chemistry*, *293*(38). https://doi.org/10.1074/jbc.RA118.001764

Llovet, J. M., Ricci, S., Mazzaferro, V., Hilgard, P., Gane, E., Blanc, J.-F., de Oliveira, A. C., Santoro, A., Raoul, J.-L., Forner, A., Schwartz, M., Porta, C., Zeuzem, S., Bolondi, L., Greten, T. F., Galle, P. R., Seitz, J.-F., Borbath, I., Häussinger, D., … Bruix, J. (2008). Sorafenib in Advanced Hepatocellular Carcinoma. *New England Journal of Medicine*, *359*(4), 378–390. https://doi.org/10.1056/NEJMoa0708857

Losman, J. A., & Kaelin, W. G. (2013). What a difference a hydroxyl makes: Mutant IDH, (R)-2-hydroxyglutarate, and cancer. *Genes and Development*, *27*(8), 836–852. https://doi.org/10.1101/gad.217406.113

Lu, J. (2010). Triethylenetetramine pharmacology and its clinical applications. *Molecular Cancer Therapeutics*, *9*(9), 2458–2467. https://doi.org/10.1158/1535-7163.MCT-10-0523

Luo, W., Hu, H., Chang, R., Zhong, J., Knabel, M., O'Meally, R., Cole, R. N., Pandey, A., & Semenza, G. L. (2011). Pyruvate kinase M2 is a PHD3-stimulated coactivator for hypoxia-inducible factor 1. *Cell*, *145*(5), 732–744. https://doi.org/10.1016/j.cell.2011.03.054

Lutsenko, S., Barnes, N. L., Bartee, M. Y., & Dmitriev, O. Y. (2007). Function and regulation of human copper-transporting ATPases. *Physiological Reviews*, *87*(3), 1011–1046. https://doi.org/10.1152/physrev.00004.2006

Lv, L., Li, D., Zhao, D., Lin, R., Chu, Y., Zhang, H., Zha, Z., Liu, Y., Li, Z., Xu, Y., Wang, G., Huang, Y., Xiong, Y., Guan, K. L., & Lei, Q. Y. (2011). Acetylation Targets the M2 Isoform of Pyruvate Kinase for Degradation through Chaperone-Mediated Autophagy and Promotes Tumor Growth. *Molecular Cell*, *42*(6), 719–730. https://doi.org/10.1016/j.molcel.2011.04.025

Malato, Y., Naqvi, S., Schürmann, N., Ng, R., Wang, B., Zape, J., Kay, M. A., Grimm, D., & Willenbring, H. (2011). Fate tracing of mature hepatocytes in mouse liver homeostasis and regeneration. *Journal of Clinical Investigation*, *121*(12), 4850–4860. https://doi.org/10.1172/JCI59261

Mandinov, L., Mandinova, A., Kyurkchiev, S., Kyurkchiev, D., Kehayov, I., Kolev, V., Soldi, R., Bagala, C., De Muinck, E. D., Lindner, V., Post, M. J., Simons, M., Bellum, S., Prudovsky, I., & Maciag, T. (2003). Copper chelation represses the vascular response to injury. *Proceedings of the National Academy of Sciences of the United States of America*, *100*(11), 6700–6705. https://doi.org/10.1073/pnas.1231994100

Marchetto, A., Ohmura, S., Orth, M. F., Knott, M. M. L., Colombo, M. V., Arrigoni, C., Bardinet, V., Saucier, D., Wehweck, F. S., Li, J., Stein, S., Gerke, J. S., Baldauf, M. C., Musa, J., Dallmayer, M., Romero-Pérez, L., Hölting, T. L. B., Amatruda, J. F., Cossarizza, A., … Grünewald, T. G. P. (2020). Oncogenic hijacking of a developmental transcription factor evokes vulnerability toward oxidative stress in Ewing sarcoma. *Nature Communications*, *11*(1). https://doi.org/10.1038/s41467-020-16244-2

Martin, F., Linden, T., Katschinski, D. M., Oehme, F., Flamme, I., Mukhopadhyay, C. K., Eckhardt, K., Tröger, J., Barth, S., Camenisch, G., & Wenger, R. H. (2005). Copper-dependent activation of hypoxia-inducible factor (HIF)-1: Implications for ceruloplasmin regulation. *Blood*, *105*(12), 4613–4619. https://doi.org/10.1182/blood-2004-10-3980

Matak, P., Zumerle, S., Mastrogiannaki, M., El Balkhi, S., Delga, S., Mathieu, J. R. R., Canonne-Hergaux, F., Poupon, J., Sharp, P. A., Vaulont, S., & Peyssonnaux, C. (2013). Copper Deficiency Leads to Anemia, Duodenal Hypoxia, Upregulation of HIF-2α and Altered Expression of Iron Absorption Genes in Mice. *PLoS ONE*, *8*(3), e59538. https://doi.org/10.1371/journal.pone.0059538

Matoba, Y., Kumagai, T., Yamamoto, A., Yoshitsu, H., & Sugiyama, M. (2006). Crystallographic evidence that the dinuclear copper center of tyrosinase is flexible during catalysis. *Journal of Biological Chemistry*, *281*(13), 8981–8990. https://doi.org/10.1074/jbc.M509785200

Mazzaferro, V., Regalia, E., Doci, R., Andreola, S., Pulvirenti, A., Bozzetti, F., Montalto, F., Ammatuna, M., Morabito, A., & Gennari, L. (1996). Liver Transplantation for the Treatment of Small Hepatocellular Carcinomas in Patients with Cirrhosis. *New England Journal of Medicine*, *334*(11), 693–700. https://doi.org/10.1056/NEJM199603143341104

Mendez-Lucas, A., Li, X., Hu, J., Che, L., Song, X., Jia, J., Wang, J., Xie, C., Driscoll, P. C., Tschaharganeh, D. F., Calvisi, D. F., Yuneva, M., & Chen, X. (2017). Glucose catabolism in liver tumors induced by c-MYC can be sustained by various PKM1/PKM2 ratios and pyruvate kinase activities. *Cancer Research*, *77*(16). https://doi.org/10.1158/0008-5472.CAN-17-0498

Miller, L. M., Wang, Q., Telivala, T. P., Smith, R. J., Lanzirotti, A., & Miklossy, J. (2006). Synchrotron-based infrared and X-ray imaging shows focalized accumulation of Cu and Zn co-localized with β-amyloid deposits in Alzheimer's disease. *Journal of Structural Biology*, *155*(1), 30–37. https://doi.org/10.1016/j.jsb.2005.09.004

Min, O. S., Li, J., & Freedman, J. H. (2009). Physiological and toxicological

transcriptome changes in HepG2 cells exposed to copper. *Physiological Genomics*, *38*(3), 386–401. https://doi.org/10.1152/physiolgenomics.00083.2009

Minchenko, D. O., Kharkova, A. P., Karbovskyi, L. L., & Minchenko, O. H. (2015). Expression of insulin-like growth factor binding protein genes and its hypoxic regulation in U87 glioma cells depends on ERN1 mediated signaling pathway of endoplasmic reticulum stress. *Endocrine Regulations*, *49*(2), 73–83. https://doi.org/10.4149/endo_2015_02_73

Miranda-Gonçalves, V., Granja, S., Martinho, O., Honavar, M., Pojo, M., Costa, B. M., Pires, M. M., Pinheiro, C., Cordeiro, M., Bebiano, G., Costa, P., Reis, R. M., & Baltazar, F. (2016). Hypoxia-mediated upregulation of MCT1 expression supports the glycolytic phenotype of glioblastomas. *Oncotarget*, *7*(29), 46335–46353. https://doi.org/10.18632/oncotarget.10114

Mitteregger, G., Korte, S., Shakarami, M., Herms, J., & Kretzschmar, H. A. (2009). Role of copper and manganese in prion disease progression. *Brain Research*, *1292*, 155–164. https://doi.org/10.1016/j.brainres.2009.07.051

Moriguchi, M., Nakajima, T., Kimura, H., Watanabe, T., Takashima, H., Mitsumoto, Y., Katagishi, T., Okanoue, T., & Kagawa, K. (2002). The copper chelator trientine has an antiangiogenic effect against hepatocellular carcinoma, possibly through inhibition of interleukin-8 production. *International Journal of Cancer*, *102*(5), 445–452. https://doi.org/10.1002/ijc.10740

Motterlini, R., Foresti, R., Bassi, R., Calabrese, V., Clark, J. E., & Green, C. J. (2000). Endothelial heme oxygenase-1 induction by hypoxia. Modulation by inducible nitric-oxide synthase and S-nitrosothiols. *Journal of Biological Chemistry*, *275*(18), 13613–13620. https://doi.org/10.1074/jbc.275.18.13613

Mu, X., Español-Suñer, R., Mederacke, I., Affò, S., Manco, R., Sempoux, C., Lemaigre, F. P., Adili, A., Yuan, D., Weber, A., Unger, K., Heikenwälder, M., Leclercq, I. A., & Schwabe, R. F. (2015). Hepatocellular carcinoma originates from hepatocytes and not from the progenitor/biliary compartment. *Journal of Clinical Investigation*, *125*(10), 3891–3903. https://doi.org/10.1172/JCI77995

Mufti, A. R., Burstein, E., Csomos, R. A., Graf, P. C. F., Wilkinson, J. C., Dick, R. D., Challa, M., Son, J. K., Bratton, S. B., Su, G. L., Brewer, G. J., Jakob, U., & Duckett, C. S. (2006). XIAP is a copper binding protein deregulated in Wilson's disease and other copper toxicosis disorders. *Molecular Cell*, *21*(6), 775–785. https://doi.org/10.1016/j.molcel.2006.01.033

Mukhopadhyay, C. K., Mazumder, B., & Fox, P. L. (2000). Role of hypoxia-inducible factor-1 in transcriptional activation of ceruloplasmin by iron deficiency. *Journal of Biological Chemistry*, *275*(28), 21048–21054. https://doi.org/10.1074/jbc.M000636200

Muller, P., Van Bakel, H., Van De Sluis, B., Holstege, F., Wijmenga, C., & Klomp, L. W. J. (2007). Gene expression profiling of liver cells after copper overload in vivo and in vitro reveals new copper-regulated genes. *Journal of Biological Inorganic Chemistry*, *12*(4), 495–507. https://doi.org/10.1007/s00775-006-0201-y

Muz, B., de la Puente, P., Azab, F., & Azab, A. K. (2015). The role of hypoxia in cancer progression, angiogenesis, metastasis, and resistance to therapy. *Hypoxia*, *3*, 83. https://doi.org/10.2147/hp.s93413

Nagai, M., Vo, N. H., Ogawa, L. S., Chimmanamada, D., Inoue, T., Chu, J., Beaudette-Zlatanova, B. C., Lu, R., Blackman, R. K., Barsoum, J., Koya, K., & Wada, Y. (2012). The oncology drug elesclomol selectively transports copper to the mitochondria to induce oxidative stress in cancer cells. *Free Radical Biology and Medicine*, *52*(10). https://doi.org/10.1016/j.freeradbiomed.2012.03.017

Namdarghanbari, M. A., Meeusen, J., Bachowski, G., Giebel, N., Johnson, J., & Petering, D. H. (2010). Reaction of the zinc sensor FluoZin-3 with Zn7-metallothionein: Inquiry into the existence of a proposed weak binding site. *Journal of Inorganic Biochemistry*, *104*(3), 224–231. https://doi.org/10.1016/j.jinorgbio.2009.11.003

Nault, J. C., Mallet, M., Pilati, C., Calderaro, J., Bioulac-Sage, P., Laurent, C., Laurent, A., Cherqui, D., Balabaud, C., & Rossi, J. Z. (2013). High frequency of telomerase reverse-transcriptase promoter somatic mutations in hepatocellular carcinoma and preneoplastic lesions. *Nature Communications*, *4*(1), 1–7. https://doi.org/10.1038/ncomms3218

Nguyen, M., Robert, A., Sournia-Saquet, A., Vendier, L., & Meunier, B. (2014). Characterization of new specific copper chelators as potential drugs for the treatment of alzheimer's disease. *Chemistry - A European Journal*, *20*(22), 6771–6785. https://doi.org/10.1002/chem.201402143

Niizeki, H., Kobayashi, M., Horiuchi, I., Akakura, N., Chen, J., Wang, J., Hamada, J. I., Seth, P., Katoh, H., Watanabe, H., Raz, A., & Hosokawa, M. (2002). Hypoxia enhances the expression of autocrine motility factor and the motility of human pancreatic cancer cells. *British Journal of Cancer*, *86*(12), 1914–1919. https://doi.org/10.1038/sj.bjc.6600331

Nishimura, R., Hasegawa, Hiroki Yamshita, M., Ito, N., Okamoto, Y., Takeuchi, T., Kubo, T., Iga, K., Kimura, K., Hishinuma, M., & Okuda, K. (2017). Hypoxia increases glucose transporter 1 expression in bovine corpus luteum at the early luteal stage. *Journal of Veterinary Medical Science*, *79*(11), 1878–1883. https://doi.org/10.1292/jvms.17-0284

Nobili, V., Siotto, M., Bedogni, G., Ravà, L., Pietrobattista, A., Panera, N., Alisi, A., & Squitti, R. (2013). Levels of Serum Ceruloplasmin Associate With Pediatric Nonalcoholic Fatty Liver Disease. *Journal of Pediatric Gastroenterology and Nutrition*, *56*(4), 370–375. https://doi.org/10.1097/MPG.0b013e31827aced4

Nyasae, L., Bustos, R., Braiterman, L., Eipper, B., & Hubbard, A. (2007). Dynamics of endogenous ATP7A (Menkes protein) in intestinal epithelial cells: copper-dependent redistribution between two intracellular sites. *American Journal of Physiology-Gastrointestinal and Liver Physiology*, *292*(4), G1181–G1194. https://doi.org/10.1152/ajpgi.00472.2006

O'Day, S., Gonzalez, R., Lawson, D., Weber, R., Hutchins, L., Anderson, C., Haddad, J.,

Kong, S., Williams, A., & Jacobson, E. (2009). Phase II, randomized, controlled, double-blinded trial of weekly elesclomol plus paclitaxel versus paclitaxel alone for stage IV metastatic melanoma. *Journal of Clinical Oncology*, *27*(32). https://doi.org/10.1200/JCO.2008.17.1579

O'Day, S. J., Eggermont, A. M. M., Chiarion-Sileni, V., Kefford, R., Grob, J. J., Mortier, L., Robert, C., Schachter, J., Testori, A., Mackiewicz, J., Friedlander, P., Garbe, C., Ugurel, S., Collichio, F., Guo, W., Lufkin, J., Bahcall, S., Vukovic, V., & Hauschild, A. (2013). Final results of phase III SYMMETRY study: Randomized, double-blind trial of elesclomol plus paclitaxel versus paclitaxel alone as treatment for chemotherapy-naive patients with advanced melanoma. *Journal of Clinical Oncology*, *31*(9). https://doi.org/10.1200/JCO.2012.44.5585

Ogra, Y., & Suzuki, K. T. (1998). Targeting of tetrathiomolybdate on the copper accumulating in the liver of LEC rats. *Journal of Inorganic Biochemistry*, *70*(1), 49–55. https://doi.org/10.1016/S0162-0134(98)00012-9

Ohgami, R. S., Campagna, D. R., McDonald, A., & Fleming, M. D. (2006). The Steap proteins are metalloreductases. *Blood*, *108*(4), 1388–1394. https://doi.org/10.1182/blood-2006-02-003681

Ohki, T., Tateishi, R., Akahane, M., Mikami, S., Sato, M., Uchino, K., Arano, T., Enooku, K., Kondo, Y., Yamashiki, N., Goto, T., Shiina, S., Yoshida, H., Matsuyama, Y., Omata, M., Ohtomo, K., & Koike, K. (2013). CT with hepatic arterioportography as a pretreatment examination for hepatocellular carcinoma patients: A randomized controlled trial. *American Journal of Gastroenterology*, *108*(8), 1305–1313. https://doi.org/10.1038/ajg.2013.109

Öhrvik, H., Nose, Y., Wood, L. K., Kim, B. E., Gleber, S. C., Ralle, M., & Thiele, D. J. (2013). Ctr2 regulates biogenesis of a cleaved form of mammalian Ctr1 metal transporter lacking the copper- And cisplatin-binding ecto-domain. *Proceedings of the National Academy of Sciences of the United States of America*, *110*(46), E4279–E4288. https://doi.org/10.1073/pnas.1311749110

Omoto, A., Kawahito, Y., Prudovsky, I., Tubouchi, Y., Kimura, M., Ishino, H., Wada, M., Yoshida, M., Kohno, M., Yoshimura, R., Yoshikawa, T., & Sano, H. (2005). Copper chelation with tetrathiomolybdate suppresses adjuvant-induced arthritis and inflammation-associated cachexia in rats. *Arthritis Research & Therapy*, *7*(6). https://doi.org/10.1186/ar1801

Pacold, M. E., Brimacombe, K. R., Chan, S. H., Rohde, J. M., Lewis, C. A., Swier, L. J. Y. M., Possemato, R., Chen, W. W., Sullivan, L. B., Fiske, B. P., Cho, S., Freinkman, E., Birsoy, K., Abu-Remaileh, M., Shaul, Y. D., Liu, C. M., Zhou, M., Koh, M. J., Chung, H., … Sabatini, D. M. (2016). A PHGDH inhibitor reveals coordination of serine synthesis and one-carbon unit fate. *Nature Chemical Biology*, *12*(6), 452–458. https://doi.org/10.1038/nchembio.2070

Paik, S. R., Shin, H.-J., Lee, J.-H., Chang, C.-S., & Kim, J. (1999). Copper(II)-induced self-oligomerization of α-synuclein. *Biochemical Journal*, *340*(3), 821–828. https://doi.org/10.1042/bj3400821

Palmer, M. K., & Toth, P. P. (2019). Trends in Lipids, Obesity, Metabolic Syndrome, and Diabetes Mellitus in the United States: An NHANES Analysis (2003-2004 to 2013-2014). *Obesity*, *27*(2), 309–314. https://doi.org/10.1002/oby.22370

Pan, Q., Bao, L. W., & Merajver, S. D. (2003). Tetrathiomolybdate inhibits angiogenesis and metastasis through suppression of the NFκB signaling cascade. *Molecular Cancer Research*, *1*(10), 701–706.

Pan, Q., Kleer, C. G., Van Golen, K. L., Irani, J., Bottema, K. M., Bias, C., De Carvalho, M., Mesri, E. A., Robins, D. M., Dick, R. D., Brewer, G. J., & Merajver, S. D. (2002a). Copper deficiency induced by tetrathiomolybdate suppresses tumor growth and angiogenesis. *Cancer Research*, *62*(17), 4854–4859.

Pan, Q., Kleer, C. G., Van Golen, K. L., Irani, J., Bottema, K. M., Bias, C., De Carvalho, M., Mesri, E. A., Robins, D. M., Dick, R. D., Brewer, G. J., & Merajver, S. D. (2002b). Copper deficiency induced by tetrathiomolybdate suppresses tumor growth and angiogenesis. *Cancer Research*, *62*(17), 4854–4859.

Pase, L., Voskoboinik, I., Greenough, M., & Camakaris, J. (2004). Copper stimulates trafficking of a distinct pool of the Menkes copper ATPase (ATP7A) to the plasma membrane and diverts it into a rapid recycling pool. *Biochemical Journal*, *378*(3), 1031–1037. https://doi.org/10.1042/BJ20031181

Patel, R. P., Svistunenko, D., Wilson, M. T., & Darley-Usmar, V. M. (1997). Reduction of Cu(II) by lipid hydroperoxides: implications for the copper-dependent oxidation of low-density lipoprotein. *Biochem. J*, *322*, 425–433.

Paul, S. B., Gamanagatti, S., Sreenivas, V., Chandrashekhara, S. H., Mukund, A., Gulati, M. S., Gupta, A. K., & Acharya, S. K. (2011). Trans-arterial chemoembolization (TACE) in patients with unresectable hepatocellular carcinoma: Experience from a Tertiary Care Centre in India. *Indian Journal of Radiology and Imaging*, *21*(2), 113–120. https://doi.org/10.4103/0971-3026.82294

Peisach, J., & Blumberg, W. E. (1969). A Mechanism for the Action of Penicillamine in the Treatment of Wilson's Disease. *Molecular Pharmacology*, *5*(2), 200–209.

Perkons, N., Kiefer, R., Noji, M., Pourfathi, M., Ackerman, D., Siddiqui, S., Tischfield, D., Profka, E., Johnson, O., Pickup, S., Mancuso, A., Pantel, A., Denburg, MR Nadolski, G., Hunt, S., Furth, E., Kadlecek, S., & Gade, T. (2019). Hyperpolarized Metabolic Imaging Detects Latent Hepatocellular Carcinoma Domains Surviving Locoregional Therapy. *Hepatology*, Epub.

Petris, M. J., Mercer, J. F., Culvenor, J. G., Lockhart, P., Gleeson, P. A., & Camakaris, J. (1996). Ligand-regulated transport of the Menkes copper P-type ATPase efflux pump from the Golgi apparatus to the plasma membrane: a novel mechanism of regulated trafficking. *The EMBO Journal*, *15*(22), 6084–6095. https://doi.org/10.1002/j.1460-2075.1996.tb00997.x

Petris, Michael J., Smith, K., Lee, J., & Thiele, D. J. (2003). Copper-stimulated endocytosis and degradation of the human copper transporter, hCtr1. *Journal of Biological Chemistry*, *278*(11), 9639–9646. https://doi.org/10.1074/jbc.M209455200

Pfeiffenberger, J., Lohse, C. M., Gotthardt, D., Rupp, C., Weiler, M., Teufel, U., Weiss, K. H., & Gauss, A. (2018). Long-term evaluation of urinary copper excretion and non-caeruloplasmin associated copper in Wilson disease patients under medical treatment. *Journal of Inherited Metabolic Disease*, 1–9. https://doi.org/10.1007/s10545-018-0218-8

Pfeiffenberger, J., Mogler, C., Gotthardt, D. N., Schulze-Bergkamen, H., Litwin, T., Reuner, U., Hefter, H., Huster, D., Schemmer, P., Członkowska, A., Schirmacher, P., Stremmel, W., Cassiman, D., & Weiss, K. H. (2015). Hepatobiliary malignancies in Wilson disease. *Liver International*, *35*, 1615–1622. https://doi.org/10.1111/liv.12727

Pfeiffer, R. F. (2011). Wilson's disease. In *Handbook of Clinical Neurology* (Vol. 100). Elsevier. https://doi.org/10.1016/B978-0-444-52014-2.00049-5

Poo, J. L., Rosas-Romero, R., Montemayor, A. C., Isoard, F., & Uribe, M. (2003). Diagnostic value of the copper/zinc ratio in hepatocellular carcinoma: A case control study. *Journal of Gastroenterology*, *38*(1), 45–51. https://doi.org/10.1007/s005350300005

Porcu, C., Antonucci, L., Barbaro, B., Illi, B., Nasi, S., Martini, M., Licata, A., Miele, L., Grieco, A., & Balsano, C. (2018). Copper/MYC/CTR1 interplay: a dangerous relationship in hepatocellular carcinoma. *Oncotarget*, *9*(10), 9325–9343. www.impactjournals.com/oncotarget

Pourvali, K., Matak, P., Latunde-Dada, G. O., Solomou, S., Mastrogiannaki, M., Peyssonnaux, C., & Sharp, P. A. (2012). Basal expression of copper transporter 1 in intestinal epithelial cells is regulated by hypoxia-inducible factor 2α. *FEBS Letters*, *586*(16), 2423–2427. https://doi.org/10.1016/j.febslet.2012.05.058

Prakasam, G., Iqbal, M. A., Bamezai, R. N. K., & Mazurek, S. (2018). Posttranslational modifications of pyruvate kinase M2: Tweaks that benefit cancer. *Frontiers in Oncology*, *8*(FEB), 1. https://doi.org/10.3389/fonc.2018.00022

Qian, G. S., Ross, R. K., Yu, M. C., Yuan, J. M., Gao, Y. T., Henderson, B. E., Wogan, G. N., & Groopman, J. D. (1994). A Follow-Up Study of Urinary Markers of Aflatoxin Exposure and Liver Cancer Risk in Shanghai, People's Republic of China. *Cancer Epidemiology Biomarkers and Prevention*, *3*(1), 3–10.

Ranganathan, P. N., Lu, Y., Jiang, L., Kim, C., & Collins, J. F. (2011). Serum ceruloplasmin protein expression and activity increases in iron-deficient rats and is further enhanced by higher dietary copper intake. *Blood*, *118*(11), 3146–3153. https://doi.org/10.1182/blood-2011-05-352112

Rapisarda, V. A., Volentini, S. I., Farías, R. N., & Massa, E. M. (2002). Quenching of bathocuproine disulfonate fluorescence by Cu(I) as a basis for copper quantification. *Analytical Biochemistry*, *307*(1), 105–109. https://doi.org/10.1016/S0003-2697(02)00031-3

Rasoloson, D., Shi, L., Chong, C. R., Kafsack, B. F., & Sullivan, D. J. (2004). Copper pathways in Plasmodium falciparum infected erythrocytes indicate an efflux role for

the copper P-ATPase. *Biochemical Journal*, *381*(3), 803–811. https://doi.org/10.1042/BJ20040335

Razumilava, N., & Gores, G. J. (2014). Cholangiocarcinoma. In *The Lancet* (Vol. 383, Issue 9935, pp. 2168–2179). Lancet Publishing Group. https://doi.org/10.1016/S0140-6736(13)61903-0

Redman, B. G., Esper, P., Pan, Q., Dunn, R. L., Hussain, H. K., Chenevert, T., Brewer, G. J., & Merajver, S. D. (2003). Phase II trial of tetrathiomolybdate in patients with advanced kidney cancer. *Clinical Cancer Research*, *9*(5), 1666–1672.

Rees, E. M., Lee, J., & Thiele, D. J. (2004). Mobilization of intracellular copper stores by the Ctr2 vacuolar copper transporter. *Journal of Biological Chemistry*, *279*(52), 54221–54229. https://doi.org/10.1074/jbc.M411669200

Reyes, C. V. (2008). Hepatocellular Carcinoma in Wilson Disease-related Liver Cirrhosis. *Gastroenterology & Hepatology*, *4*(6), 435–437. http://www.ncbi.nlm.nih.gov/pubmed/21904521

Rigiracciolo, D. C., Scarpelli, A., Lappano, R., Pisano, A., Santolla, M. F., Marco, P. De, Cirillo, F., Cappello, A. R., Dolce, V., Belfiore, A., Maggiolini, M., & De Francesco, E. M. (2015). Copper activates HIF-1α/GPER/VEGF signalling in cancer cells. *Oncotarget*, *6*(33). https://doi.org/10.18632/oncotarget.5779

Rizvi, S., Khan, S. A., Hallemeier, C. L., Kelley, R. K., & Gores, G. J. (2018). Cholangiocarcinoma-evolving concepts and therapeutic strategies. *Nature Reviews Clinical Oncology*, *15*(2), 95–111. https://doi.org/10.1038/nrclinonc.2017.157

Rolfs, A., Kvietikova, I., Gassmann, M., & Wenger, R. H. (1997). Oxygen-regulated transferrin expression is mediated by hypoxia-inducible factor-1. *Journal of Biological Chemistry*, *272*(32), 20055–20062. https://doi.org/10.1074/jbc.272.32.20055

Rorabacher, D. B. (1999). Influence of coordination geometry upon copper(II/I) redox potentials. Physical parameters for twelve copper tripodal ligand complexes. *Inorganic Chemistry*, *38*(19), 4233–4242. https://doi.org/10.1021/ic990334t

Rose, F., Hodak, M., & Bernholc, J. (2011). Mechanism of copper(II)-induced misfolding of Parkinson's disease protein. *Scientific Reports*, *1*(1), 1–5. https://doi.org/10.1038/srep00011

Rupp, C., Scherzer, M., Rudisch, A., Unger, C., Haslinger, C., Schweifer, N., Artaker, M., Nivarthi, H., Moriggl, R., Hengstschläger, M., Kerjaschki, D., Sommergruber, W., Dolznig, H., & Garin-Chesa, P. (2015). IGFBP7, a novel tumor stroma marker, with growth-promoting effects in colon cancer through a paracrine tumor-stroma interaction. *Oncogene*, *34*(7), 815–825. https://doi.org/10.1038/onc.2014.18

Rupp, Christian, & Weiss, K. H. (2019). Part V: Treatment Decisions. In K. H. Weiss & M. Schilsky (Eds.), *Wilson Disease: Pathogenesis, Molecular Mechanisms, Diagnosis, Treatment and Monitoring.* (pp. 197–203). Academic Press.

Sanoff, H. K., Chang, Y., Lund, J. L., O'Neil, B. H., & Dusetzina, S. B. (2016). Sorafenib Effectiveness in Advanced Hepatocellular Carcinoma. *The Oncologist*, *21*(9), 1113–1120. https://doi.org/10.1634/theoncologist.2015-0478

Sanyal, A., Poklepovic, A., Moyneur, E., & Barghout, V. (2010). Population-based risk factors and resource utilization for HCC: US perspective. *Current Medical Research and Opinion*, *26*(9), 2183–2191. https://doi.org/10.1185/03007995.2010.506375

Sarell, C. J., Syme, C. D., Rigby, S. E. J., & Viles, J. H. (2009). Copper(II) binding to amyloid-β fibrils of Alzheimer's disease reveals a picomolar affinity: Stoichiometry and coordination geometry are independent of Aβ oligomeric form. *Biochemistry*, *48*(20), 4388–4402. https://doi.org/10.1021/bi900254n

Sarkar, B., Sass-Kortsak, A., Clarke, R., Laurie, S. H., & Wei, P. (1977). A comparative study of in vitro and in vivo interaction of D-penicillamine and triethylenetetramine with copper. *Proceedings of the Royal Society of Medicine*, *70 Suppl 3*(Suppl 3), 13–18. https://doi.org/10.1177/00359157770700s307

Schmittgen, T. D., & Livak, K. J. (2008). Analyzing real-time PCR data by the comparative CT method. *Nature Protocols*, *3*(6), 1101–1108. https://doi.org/10.1038/nprot.2008.73

Schneider, B. J., Lee, J. S. J., Hayman, J. A., Chang, A. C., Orringer, M. B., Pickens, A., Pan, C. C., Merajver, S. D., & Urba, S. G. (2013). Pre-operative chemoradiation followed by post-operative adjuvant therapy with tetrathiomolybdate, a novel copper chelator, for patients with resectable esophageal cancer. *Investigational New Drugs*, *31*(2), 435–442. https://doi.org/10.1007/s10637-012-9864-0

Schönenberger, M. J., & Kovacs, W. J. (2015). Hypoxia signaling pathways: Modulators of oxygen-related organelles. In *Frontiers in Cell and Developmental Biology* (Vol. 3, Issue JUL, p. 42). Frontiers Media S.A. https://doi.org/10.3389/fcell.2015.00042

Schulze, K., Imbeaud, S., Letouzé, E., Alexandrov, L. B., Calderaro, J., Rebouissou, S., Couchy, G., Meiller, C., Shinde, J., Soysouvanh, F., Calatayud, A.-L., Pinyol, R., Pelletier, L., Balabaud, C., Laurent, A., Blanc, J.-F., Mazzaferro, V., Calvo, F., Villanueva, A., … Zucman-Rossi, J. (2015). Exome sequencing of hepatocellular carcinomas identifies new mutational signatures and potential therapeutic targets. *Nat Genet*, *47*(5), 505–511.

Schweizer, M. T., Lin, J., Blackford, A., Bardia, A., King, S., Armstrong, A. J., Rudek, M. A., Yegnasubramanian, S., & Carducci, M. A. (2013). Pharmacodynamic study of disulfiram in men with non-metastatic recurrent prostate cancer. *Prostate Cancer and Prostatic Diseases*, *16*(4), 357–361. https://doi.org/10.1038/pcan.2013.28

Scott, R. A. (1995). Functional significance of cytochrome c oxidase structure. *Structure*, *3*(10), 981–986. https://doi.org/10.1016/S0969-2126(01)00233-7

Semenza, G. L. (2007). Life with oxygen. *Science*, *318*(5847), 62–64. https://doi.org/10.1126/science.1147949

Semenza, G. L. (2012). Hypoxia-inducible factors: Mediators of cancer progression and

targets for cancer therapy. *Trends in Pharmacological Sciences*, *33*(4), 207–214. https://doi.org/10.1016/j.tips.2012.01.005

Seng, H. L., Tan, K. W., Maah, M. J., Tan, W. T., Hamada, H., Chikira, M., & Ng, C. H. (2009). Copper(II) complexes of methylated glycine derivatives: Effect of methyl substituent on their DNA binding and nucleolytic property. *Polyhedron*, *28*(11), 2219–2227. https://doi.org/10.1016/j.poly.2009.03.022

Sensi, S. L., Paoletti, P., Bush, A. I., & Sekler, I. (2009). Zinc in the physiology and pathology of the CNS. *Nature Reviews Neuroscience*, *10*(11), 780–791. https://doi.org/10.1038/nrn2734

Sesham, R., Choi, D., Balaji, A., Cheruku, S., Ravichetti, C., Alshahrani, A. A., Nasani, M., & Angel, L. A. (2013). The pH Dependent Cu(II) and Zn(II) Binding Behavior of an Analog Methanobactin Peptide. *European Journal of Mass Spectrometry*, *19*(6), 463–473. https://doi.org/10.1255/ejms.1249

She, Y. M., Narindrasorasak, S., Yang, S., Spitale, N., Roberts, E. A., & Sarkar, B. (2003). Identification of metal-binding proteins in human hepatoma lines by immobilized metal affinity chromatography and mass spectrometry. *Molecular & Cellular Proteomics : MCP*, *2*(12), 1306–1318. https://doi.org/10.1074/mcp.M300080-MCP200

Shen, Q., Fan, J., Yang, X. R., Tan, Y., Zhao, W., Xu, Y., Wang, N., Niu, Y., Wu, Z., Zhou, J., Qiu, S. J., Shi, Y. H., Yu, B., Tang, N., Chu, W., Wang, M., Wu, J., Zhang, Z., Yang, S., … Qin, W. (2012). Serum DKK1 as a protein biomarker for the diagnosis of hepatocellular carcinoma: A large-scale, multicentre study. *The Lancet Oncology*, *13*(8), 817–826. https://doi.org/10.1016/S1470-2045(12)70233-4

Sheng, Y., Chattopadhyay, M., Whitelegge, J., & Selverstone Valentine, J. (2013). SOD1 Aggregation and ALS: Role of Metallation States and Disulfide Status. *Current Topics in Medicinal Chemistry*, *12*(22), 2560–2572. https://doi.org/10.2174/1568026611212220010

Si-Tayeb, K., Lemaigre, F. P., & Duncan, S. A. (2010). Organogenesis and Development of the Liver. *Developmental Cell*, *18*(2), 175–189. https://doi.org/10.1016/j.devcel.2010.01.011

Siegel, R. L., Miller, K. D., & Jemal, A. (2019). Cancer statistics, 2019. *CA: A Cancer Journal for Clinicians*, *69*(1), 7–34. https://doi.org/10.3322/caac.21551

Siegel, R. L., Miller, K. D., & Jemal, A. (2020). Cancer statistics, 2020. *CA: A Cancer Journal for Clinicians*, *70*(1), 7–30. https://doi.org/10.3322/caac.21590

Simmons, O. L., Feng, Y., Parikh, N. D., & Singal, A. G. (2019). Primary Care Provider Practice Patterns and Barriers to Hepatocellular Carcinoma Surveillance. *Clinical Gastroenterology and Hepatology*, *17*(4), 766–773. https://doi.org/10.1016/j.cgh.2018.07.029

Skrajnowska, D., Bobrowska-Korczak, B., Tokarz, A., Bialek, S., Jezierska, E., & Makowska, J. (2013). Copper and resveratrol attenuates serum catalase,

glutathione peroxidase, and element values in rats with DMBA-induced mammary carcinogenesis. *Biological Trace Element Research*, *156*(1–3), 271–278. https://doi.org/10.1007/s12011-013-9854-x

Skrott, Z., Mistrik, M., Andersen, K. K., Friis, S., Majera, D., Gursky, J., Ozdian, T., Bartkova, J., Turi, Z., Moudry, P., Kraus, M., Michalova, M., Vaclavkova, J., Dzubak, P., Vrobel, I., Pouckova, P., Sedlacek, J., Miklovicova, A., Kutt, A., … Bartek, J. (2017). Alcohol-abuse drug disulfiram targets cancer via p97 segregase adaptor NPL4. *Nature*, *552*(7684), 194–199. https://doi.org/10.1038/nature25016

Smirnova, J., Kabin, E., Järving, I., Bragina, O., Tõugu, V., Plitz, T., & Palumaa, P. (2018). Copper(I)-binding properties of de-coppering drugs for the treatment of Wilson disease. α-Lipoic acid as a potential anti-copper agent. *Scientific Reports*, *8*(1). https://doi.org/10.1038/s41598-018-19873-2

Song, M., Song, Z., Barve, S., Zhang, J., Chen, T., Liu, M., Arteel, G. E., Brewer, G. J., & McClain, C. J. (2008). Tetrathiomolybdate protects against bile duct ligation-induced cholestatic liver injury and fibrosis. *Journal of Pharmacology and Experimental Therapeutics*, *325*(2). https://doi.org/10.1124/jpet.107.131227

Sonveaux, P., Copetti, T., De Saedeleer, C. J., Végran, F., Verrax, J., Kennedy, K. M., Moon, E. J., Dhup, S., Danhier, P., Frérart, F., Gallez, B., Ribeiro, A., Michiels, C., Dewhirst, M. W., & Feron, O. (2012). Targeting the Lactate Transporter MCT1 in Endothelial Cells Inhibits Lactate-Induced HIF-1 Activation and Tumor Angiogenesis. *PLoS ONE*, *7*(3), e33418. https://doi.org/10.1371/journal.pone.0033418

Spector, L. G., & Birch, J. (2012). The epidemiology of hepatoblastoma. *Pediatric Blood and Cancer*, *59*(5), 776–779. https://doi.org/10.1002/pbc.24215

Srivastava, S., Panda, S., Li, Z., Fuhs, S. R., Hunter, T., Thiele, D. J., Hubbard, S. R., & Skolnik, E. Y. (2016). Histidine phosphorylation relieves copper inhibition in the mammalian potassium channel KCa3.1. *ELife*, *5*(AUGUST). https://doi.org/10.7554/eLife.16093

Stelmashook, E. V., Isaev, N. K., Genrikhs, E. E., Amelkina, G. A., Khaspekov, L. G., Skrebitsky, V. G., & Illarioshkin, S. N. (2014). Role of zinc and copper ions in the pathogenetic mechanisms of Alzheimer's and Parkinson's diseases. *Biochemistry (Moscow)*, *79*(5), 391–396. https://doi.org/10.1134/S0006297914050022

Suzuki, K. T., Ogra, Y., & Ohmichi, M. (1995). Molybdenum and Copper Kinetics after Tetrathiomolybdate Injection in LEC Rats : Specific Role of Serum Albumin. *Topics in Catalysis*, *9*(3), 170–175. https://doi.org/10.1016/S0946-672X(11)80043-X

Syed, B. A., Beaumont, N. J., Patel, A., Naylor, C. E., Bayele, H. K., Joannou, C. L., Rowe, P. S. N., Evans, R. W., Kaila, S., & Srai, S. (2002). Analysis of the human hephaestin gene and protein: comparative modelling of the N-terminus ecto-domain based upon ceruloplasmin. *Protein Engineering*, *15*(3), 205–214. https://doi.org/10.1093/PROTEIN/15.3.205

Tacchini, L., Bianchi, L., Bernelli-Zazzera, A., & Cairo, G. (1999). Transferrin receptor

induction by hypoxia. HIF-1-mediated transcriptional activation and cell-specific post-transcriptional regulation. *Journal of Biological Chemistry*, *274*(34), 24142–24146. https://doi.org/10.1074/jbc.274.34.24142

Tai, W. T., Hung, M. H., Chu, P. Y., Chen, Y. L., Chen, L. J., Tsai, M. H., Chen, M. H., Shiau, C. W., Boo, Y. P., & Chen, K. F. (2016). SH2 domain-containing phosphatase 1 regulates pyruvate kinase M2 in hepatocellular carcinoma. *Oncotarget*, *7*(16), 22193–22205. https://doi.org/10.18632/oncotarget.7923

Tainer, J. A., Getzoff, E. D., Beem, K. M., Richardson, J. S., & Richardson, D. C. (1982). Determination and analysis of the 2 Å structure of copper, zinc superoxide dismutase. *Journal of Molecular Biology*, *160*(2), 181–217. https://doi.org/10.1016/0022-2836(82)90174-7

Tang, Z., Gasperkova, D., Xu, J., Baillie, R., Lee, J.-H., & Clarke, S. D. (2000). Nutrient-Gene Expression Copper Deficiency Induces Hepatic Fatty Acid Synthase Gene Transcription in Rats by Increasing the Nuclear Content of Mature Sterol Regulatory Element Binding Protein 1 1. *J. Nutr*, *130*, 2915–2921. https://academic.oup.com/jn/article-abstract/130/12/2915/4686233

Tanzi, R. E., Petrukhin, K., Chernov, I., Pellequer, J. L., Wasco, W., Ross, B., Romano, D. M., Parano, E., Pavone, L., & Brzustowicz, L. M. (1993). The Wilson disease gene is a copper transporting ATPase with homology to the Menkes disease gene. *Nature Genetics*, *5*(4), 344–350.

Tawari, P. E., Wang, Z., Najlah, M., Tsang, C. W., Kannappan, V., Liu, P., McConville, C., He, B., Armesilla, A. L., & Wang, W. (2015). The cytotoxic mechanisms of disulfiram and copper(II) in cancer cell. *Toxicology Research*, *4*(6), 1439–1442. https://doi.org/10.1039/c5tx00210a

Telianidis, J., Hung, Y. H., Materia, S., & Fontaine, S. La. (2013). Role of the P-Type ATPases, ATP7A and ATP7B in brain copper homeostasis. *Frontiers in Aging Neuroscience*, *5*(AUG), 44. https://doi.org/10.3389/fnagi.2013.00044

Télouk, P., Puisieux, A., Fujii, T., Balter, V., Bondanese, V. P., Morel, A. P., Clapisson, G., Lamboux, A., & Albarede, F. (2015). Copper isotope effect in serum of cancer patients. A pilot study. *Metallomics*, *7*(2), 299–308. https://doi.org/10.1039/c4mt00269e

Tennant, J., Stansfield, M., Yamaji, S., Srai, S. K., & Sharp, P. (2002). Effects of copper on the expression of metal transporters in human intestinal Caco-2 cells. *FEBS Letters*, *527*(1–3), 239–244. https://doi.org/10.1016/S0014-5793(02)03253-2

Terzi, E., Piscaglia, F., Forlani, L., Mosconi, C., Renzulli, M., Bolondi, L., & Golfieri, R. (2014). TACE performed in patients with a single nodule of hepatocellular carcinoma. *BMC Cancer*, *14*(1), 601. https://doi.org/10.1186/1471-2407-14-601

Thattil, R., & Dufour, J. F. (2013). Hepatocellular carcinoma in a non-cirrhotic patient with Wilson's disease. In *World Journal of Gastroenterology* (Vol. 19, Issue 13, pp. 2110–2113). Baishideng Publishing Group Inc. https://doi.org/10.3748/wjg.v19.i13.2110

Thompson, C. B. (2009). Metabolic enzymes as oncogenes or tumor suppressors. *New England Journal of Medicine*, *360*(8), 813–815. https://doi.org/10.1056/NEJMe0810213

Torre, L. A., Bray, F., Siegel, R. L., Ferlay, J., Lortet-Tieulent, J., & Jemal, A. (2015). Global cancer statistics, 2012. *CA: A Cancer Journal for Clinicians*, *65*(2), 87–108. https://doi.org/10.3322/caac.21262

Tosco, A., Fontanella, B., Danise, R., Cicatiello, L., Grober, O. M. V., Ravo, M., Weisz, A., & Marzullo, L. (2010). Molecular bases of copper and iron deficiency-associated dyslipidemia: A microarray analysis of the rat intestinal transcriptome. *Genes and Nutrition*, *5*(1), 1–8. https://doi.org/10.1007/s12263-009-0153-2

Totoki, Y., Tatsuno, K., Covington, K. R., Ueda, H., Creighton, C. J., Kato, M., Tsuji, S., Donehower, L. A., Slagle, B. L., Nakamura, H., Yamamoto, S., Shinbrot, E., Hama, N., Lehmkuhl, M., Hosoda, F., Arai, Y., Walker, K., Dahdouli, M., Gotoh, K., … Shibata, T. (2014). Trans-ancestry mutational landscape of hepatocellular carcinoma genomes. *Nature Genetics*, *46*(12), 1267–1273. https://doi.org/10.1038/ng.3126

Trumbull, K. A., & Beckman, J. S. (2009). A role for copper in the toxicity of zinc-deficient superoxide dismutase to motor neurons in amyotrophic lateral sclerosis. *Antioxidants and Redox Signaling*, *11*(7), 1627–1639. https://doi.org/10.1089/ars.2009.2574

Tsai, T. Y., & Lee, Y. H. W. (1998). Roles of copper ligands in the activation and secretion of Streptomyces tyrosinase. *Journal of Biological Chemistry*, *273*(30), 19243–19250. https://doi.org/10.1074/jbc.273.30.19243

Tsang, T., Posimo, J. M., Gudiel, A. A., Cicchini, M., Feldser, D. M., & Brady, D. C. (2020). Copper is an essential regulator of the autophagic kinases ULK1/2 to drive lung adenocarcinoma. *Nature Cell Biology*, *22*(4), 412–424. https://doi.org/10.1038/s41556-020-0481-4

Tsukihara, T., Aoyama, H., Yamashita, E., Tomizaki, T., Yamaguchi, H., Shinzawa-Itoh, K., Nakashima, R., Yaono, R., & Yoshikawa, S. (1995). Structures of metal sites of oxidized bovine heart cytochrome c oxidase at 2.8 Å. *Science*, *269*(5227), 1069–1074. https://doi.org/10.1126/science.7652554

Tsvetkov, P., Detappe, A., Cai, K., Keys, H. R., Brune, Z., Ying, W., Thiru, P., Reidy, M., Kugener, G., Rossen, J., Kocak, M., Kory, N., Tsherniak, A., Santagata, S., Whitesell, L., Ghobrial, I. M., Markley, J. L., Lindquist, S., & Golub, T. R. (2019). Mitochondrial metabolism promotes adaptation to proteotoxic stress. *Nature Chemical Biology*, *15*(7). https://doi.org/10.1038/s41589-019-0291-9

Tummala, K. S., Brandt, M., Teijeiro, A., Graña, O., Schwabe, R. F., Perna, C., & Djouder, N. (2017). Hepatocellular Carcinomas Originate Predominantly from Hepatocytes and Benign Lesions from Hepatic Progenitor Cells. *Cell Reports*, *19*(3), 584–600. https://doi.org/10.1016/j.celrep.2017.03.059

Turski, M. L., Brady, D. C., Kim, H. J., Kim, B.-E., Nose, Y., Counter, C. M., Winge, D.

R., & Thiele, D. J. (2012). A Novel Role for Copper in Ras/Mitogen-Activated Protein Kinase Signaling. *Molecular and Cellular Biology*, *32*(7), 1284–1295. https://doi.org/10.1128/mcb.05722-11

Turski, Michelle L, & Thiele, D. J. (2009). New roles for copper metabolism in cell proliferation, signaling, and disease. *J Biol Chem*, *284*(2), 717–721.

Uversky, V. N., Li, J., & Fink, A. L. (2001). Metal-triggered structural transformations, aggregation, and fibrillation of human α-synuclein: A possible molecular link between parkinson's disease and heavy metal exposure. *Journal of Biological Chemistry*, *276*(47), 44284–44296. https://doi.org/10.1074/jbc.M105343200

Vallet, S. D., Guéroult, M., Belloy, N., Dauchez, M., & Ricard-Blum, S. (2019). A Three-Dimensional Model of Human Lysyl Oxidase, a Cross-Linking Enzyme. *ACS Omega*, *4*(5), 8495–8505. https://doi.org/10.1021/acsomega.9b00317

Van Den Berghe, P. V. E., Folmer, D. E., Malingré, H. E. M., Van Beurden, E., Klomp, A. E. M., Van De Sluis, B., Merkx, M., Berger, R., & Klomp, L. W. J. (2007). Human copper transporter 2 is localized in late endosomes and lysosomes and facilitates cellular copper uptake. *Biochemical Journal*, *407*(1), 49–59. https://doi.org/10.1042/BJ20070705

Vander Heiden, M. G., Locasale, J. W., Swanson, K. D., Sharfi, H., Heffron, G. J., Amador-Noguez, D., Christofk, H. R., Wagner, G., Rabinowitz, J. D., Asara, J. M., & Cantley, L. C. (2010). Evidence for an alternative glycolytic pathway in rapidly proliferating cells. *Science*, *329*(5998), 1492–1499. https://doi.org/10.1126/science.1188015

Végran, F., Boidot, R., Michiels, C., Sonveaux, P., & Feron, O. (2011). Lactate influx through the endothelial cell monocarboxylate transporter MCT1 supports an NF-kB/IL-8 pathway that drives tumor angiogenesis. *Cancer Research*, *71*(7), 2550–2560. https://doi.org/10.1158/0008-5472.CAN-10-2828

Vendelboe, T. V., Harris, P., Zhao, Y., Walter, T. S., Harlos, K., El Omari, K., & Christensen, H. E. M. (2016). The crystal structure of human dopamine β-hydroxylase at 2.9 Å resolution. *Science Advances*, *2*(4), e1500980. https://doi.org/10.1126/sciadv.1500980

Vibert, E., Azoulay, D., Hoti, E., Iacopinelli, S., Samuel, D., Salloum, C., Lemoine, A., Bismuth, H., Castaing, D., & Adam, R. (2010). Progression of alphafetoprotein before liver transplantation for hepatocellular carcinoma in cirrhotic patients: A critical factor. *American Journal of Transplantation*, *10*(1), 129–137. https://doi.org/10.1111/j.1600-6143.2009.02750.x

Vogt, S., Maser, J., & Jacobsen, C. (2003). Data analysis for x-ray fluorescence imaging. *Journal De Physique. IV : JP*. https://doi.org/10.1051/jp4:20030156

Vulpe, C. D., Kuo, Y. M., Murphy, T. L., Cowley, L., Askwith, C., Libina, N., Gitschier, J., & Anderson, G. I. (1999). Hephaestin, a ceruloplasmin homologue implicated in intestinal iron transport, is defective in the sla mouse. *Nature Genetics*, *21*(2), 195–199. https://doi.org/10.1038/5979

Vyskočil, A., & Viau, C. (1999). Assessment of molybdenum toxicity in humans. *Journal of Applied Toxicology*, *19*(3), 185–192. https://doi.org/10.1002/(SICI)1099-1263(199905/06)19:3<185::AID-JAT555>3.0.CO;2-Z

Walker, J. M., Huster, D., Ralle, M., Morgan, C. T., Blackburn, N. J., & Lutsenko, S. (2004). The N-terminal Metal-binding Site 2 of the Wilson's Disease Protein Plays a Key Role in the Transfer of Copper from Atox1. *Journal of Biological Chemistry*, *279*(15), 15376–15384. https://doi.org/10.1074/jbc.M400053200

Walshe, J. M. (1969). Management of penicillamine nephropathy in Wilson's disease: a new chelating agent. *Lancet*, *294*(7635), 1401–1402. https://doi.org/10.1016/S0140-6736(69)90940-4

Wang, B., Hsu, S. H., Frankel, W., Ghoshal, K., & Jacob, S. T. (2012). Stat3-mediated activation of microRNA-23a suppresses gluconeogenesis in hepatocellular carcinoma by down-regulating Glucose-6-phosphatase and peroxisome proliferator-activated receptor gamma, coactivator 1 alpha. *Hepatology*, *56*(1), 186–197. https://doi.org/10.1002/hep.25632

Wang, W., McLeod, H. L., & Cassidy, J. (2003). Disulfiram-mediated inhibition of NF-κb activity enhances cytotoxicity of 5-fluorouracil in human colorectal cancer cell lines. *International Journal of Cancer*, *104*(4), 504–511. https://doi.org/10.1002/ijc.10972

Wang, X., Flores, S., Ha, J., Doguer, C., & Collins, J. F. (2016). Lack of intestinal divalent metal-ion transporter 1 (DMT1) perturbs copper homeostasis in mice. *The FASEB Journal*, *30*, 292.1-292.1. https://doi.org/10.1096/FASEBJ.30.1_SUPPLEMENT.292.1

Wang, Y., Kuramitsu, Y., Takashima, M., Yokoyama, Y., Iizuka, N., Tamesa, T., Sakaida, I., Oka, M., & Nakamura, K. (2011). Identification of four isoforms of aldolase B down-regulated in hepatocellular carcinoma tissues by means of two-dimensional western blotting. *In Vivo*, *25*(6).

Wardman, P., & Candeias, L. P. (1996). Fenton Chemistry: An Introduction. *Radiation Research*, *145*(5), 523. https://doi.org/10.2307/3579270

Wei, H., Frei, B., Beckman, J. S., & Zhang, W.-J. (2011). Copper chelation by tetrathiomolybdate inhibits lipopolysaccharide-induced inflammatory responses in vivo. *American Journal of Physiology-Heart and Circulatory Physiology*, *301*(3), H712–H720. https://doi.org/10.1152/ajpheart.01299.2010

Wei, H., Zhang, W. J., LeBoeuf, R., & Frei, B. (2014). Copper induces - And copper chelation by tetrathiomolybdate inhibits - Endothelial activation in vitro. *Redox Report*, *19*(1), 40–48. https://doi.org/10.1179/1351000213Y.0000000070

Wei, H., Zhang, W. J., McMillen, T. S., LeBoeuf, R. C., & Frei, B. (2012). Copper chelation by tetrathiomolybdate inhibits vascular inflammation and atherosclerotic lesion development in apolipoprotein E-deficient mice. *Atherosclerosis*, *223*(2), 306–313. https://doi.org/10.1016/j.atherosclerosis.2012.06.013

White, C., Kambe, T., Fulcher, Y. G., Sachdev, S. W., Bush, A. I., Fritsche, K., Lee, J.,

Quinn, T. P., & Petris, M. J. (2009a). Copper transport into the secretory pathway is regulated by oxygen in macrophages. *Journal of Cell Science*, *122*(9). https://doi.org/10.1242/jcs.043216

White, C., Kambe, T., Fulcher, Y. G., Sachdev, S. W., Bush, A. I., Fritsche, K., Lee, J., Quinn, T. P., & Petris, M. J. (2009b). Copper transport into the secretory pathway is regulated by oxygen in macrophages. *Journal of Cell Science*, *122*(9), 1315–1321. https://doi.org/10.1242/jcs.043216

White, D. L., Thrift, A. P., Kanwal, F., Davila, J., & El-Serag, H. B. (2017). Incidence of Hepatocellular Carcinoma in All 50 United States, From 2000 Through 2012. *Gastroenterology*, *152*(4), 812-820.e5. https://doi.org/10.1053/j.gastro.2016.11.020

Wong, C. C.-L., Au, S. L.-K., Tse, A. P.-W., Xu, I. M.-J., Lai, R. K.-H., Chiu, D. K.-C., Wei, L. L., Fan, D. N.-Y., Tsang, F. H.-C., Lo, R. C.-L., Wong, C.-M., & Ng, I. O.-L. (2014). Switching of Pyruvate Kinase Isoform L to M2 Promotes Metabolic Reprogramming in Hepatocarcinogenesis. *PLoS ONE*, *9*(12), e115036. https://doi.org/10.1371/journal.pone.0115036

Wong, C. C. L., Kai, A. K. L., & Ng, I. O. L. (2014). The impact of hypoxia in hepatocellular carcinoma metastasis. *Frontiers of Medicine in China*, *8*(1), 33–41. https://doi.org/10.1007/s11684-013-0301-3

Wu, G., Wu, J., Wang, B., Zhu, X., Shi, X., & Ding, Y. (2018). Importance of tumor size at diagnosis as a prognostic factor for hepatocellular carcinoma survival: A population-based study. *Cancer Management and Research*, *10*, 4401–4410. https://doi.org/10.2147/CMAR.S177663

Wu, H., Pan, L., Gao, C., Xu, H., Li, Y., Zhang, L., Ma, L., Meng, L., Sun, X., & Qin, H. (2019). Quercetin inhibits the proliferation of glycolysis-addicted HCC cells by reducing hexokinase 2 and Akt-mTOR pathway. *Molecules*, *24*(10). https://doi.org/10.3390/molecules24101993

Wu, X., Xue, X., Wang, L., Wang, W., Han, J., Sun, X., Zhang, H., Liu, Y., Che, X., Yang, J., & Wu, C. (2018). Suppressing autophagy enhances disulfiram/copper-induced apoptosis in non-small cell lung cancer. *European Journal of Pharmacology*, *827*, 1–12. https://doi.org/10.1016/j.ejphar.2018.02.039

Xiao, T., Ackerman, C. M., Carroll, E. C., Jia, S., Hoagland, A., Chan, J., Thai, B., Liu, C. S., Isacoff, E. Y., & Chang, C. J. (2018). Copper regulates rest-activity cycles through the locus coeruleus-norepinephrine system. *Nature Chemical Biology*, *14*(7), 655–663. https://doi.org/10.1038/s41589-018-0062-z

Xiao, Z., Brose, J., Schimo, S., Ackland, S. M., La Fontaine, S., & Wedd, A. G. (2011). Unification of the copper(I) binding affinities of the metallo-chaperones Atx1, Atox1, and related proteins: Detection probes and affinity standards. *Journal of Biological Chemistry*, *286*(13), 11047–11055. https://doi.org/10.1074/jbc.M110.213074

Xiao, Z., Loughlin, F., George, G. N., Howlett, G. J., & Wedd, A. G. (2004). C-Terminal Domain of the Membrane Copper Transporter Ctr1 from Saccharomyces cerevisiae Binds Four Cu(I) Ions as a Cuprous-Thiolate Polynuclear Cluster: Sub-femtomolar

Cu(I) Affinity of Three Proteins Involved in Copper Trafficking. *Journal of the American Chemical Society*, *126*(10), 3081–3090. https://doi.org/10.1021/ja0390350

Xie, L., & Collins, J. F. (2011). Transcriptional regulation of the Menkes copper ATPase (Atp7a) gene by hypoxia-inducible factor (HIF2α) in intestinal epithelial cells. *American Journal of Physiology - Cell Physiology*, *300*(6). https://doi.org/10.1152/ajpcell.00023.2011

Xie, L., & Collins, J. F. (2013). Transcription factors Sp1 and Hif2α mediate induction of the copper-transporting ATPase (Atp7a) gene in intestinal epithelial cells during hypoxia. *Journal of Biological Chemistry*, *288*(33), 23943–23952. https://doi.org/10.1074/jbc.M113.489500

Xu, W., Kwon, J. H., Moon, Y. H., Kim, Y. B., Yu, Y. S., Lee, N., Choi, K. Y., Kim, Y. S., Park, Y. K., Kim, B. W., & Wang, H. J. (2014). Influence of preoperative transcatheter arterial chemoembolization on gene expression in the HIF-1α pathway in patients with hepatocellular carcinoma. *Journal of Cancer Research and Clinical Oncology*, *140*(9), 1507–1515. https://doi.org/10.1007/s00432-014-1713-4

Xue, X., Ramakrishnan, S. K., Weisz, K., Brenner, D., Fearon, E. R., & Shah Correspondence, Y. M. (2016). Iron Uptake via DMT1 Integrates Cell Cycle with JAK-STAT3 Signaling to Promote Colorectal Tumorigenesis Graphical Abstract Highlights d Iron accumulation in CRC is dependent on HIF-2a-induced iron importer DMT1 d Genetic disruption or pharmacological inhi. *Cell Metabolism*, *24*, 447–461. https://doi.org/10.1016/j.cmet.2016.07.015

Yarze, J. C., Martin, P., Muñoz, S. J., & Friedman, L. S. (1992). Wilson's disease: Current status. *The American Journal of Medicine*, *92*(6), 643–654. https://doi.org/10.1016/0002-9343(92)90783-8

Yoshii, J., Yoshiji, H., Kuriyama, S., Ikenaka, Y., Noguchi, R., Okuda, H., Tsujinoue, H., Nakatani, T., Kishida, H., Nakae, D., Gomez, D. E., De Lorenzo, M. S., Tejera, A. M., & Fukui, H. (2001a). The copper-chelating agent, trientine, suppresses tumor development and angiogenesis in the murine hepatocellular carcinoma cells. *International Journal of Cancer*, *94*(6), 768–773. https://doi.org/10.1002/ijc.1537

Yoshii, J., Yoshiji, H., Kuriyama, S., Ikenaka, Y., Noguchi, R., Okuda, H., Tsujinoue, H., Nakatani, T., Kishida, H., Nakae, D., Gomez, D. E., De Lorenzo, M. S., Tejera, A. M., & Fukui, H. (2001b). The copper-chelating agent, trientine, suppresses tumor development and angiogenesis in the murine hepatocellular carcinoma cells. *International Journal of Cancer*, *94*(6), 768–773. https://doi.org/10.1002/ijc.1537

Yoshiji, H., Yoshii, J., Kuriyama, S., Ikenaka, Y., Noguchi, R., Yanase, K., Namisaki, T., Kitade, M., Yamazaki, M., & Fukui, H. (2005). Combination of copper-chelating agent, trientine, and methotrexate attenuates colorectal carcinoma development and angiogenesis in mice. *Oncology Reports*, *14*(1), 213–218. https://doi.org/10.3892/or.14.1.213

Yousef, E. N., & Angel, L. A. (2020). Comparison of the pH-dependent formation of His and Cys heptapeptide complexes of nickel(II), copper(II), and zinc(II) as determined

by ion mobility-mass spectrometry. *Journal of Mass Spectrometry*, *55*(3), e4489. https://doi.org/10.1002/jms.4489

Yu, Z., Zhao, X., Huang, L., Zhang, T., Yang, F., Xie, L., Song, S., Miao, P., Zhao, L., Sun, X., Liu, J., & Huang, G. (2013). Proviral insertion in murine lymphomas 2 (PIM2) oncogene phosphorylates pyruvate kinase M2 (PKM2) and promotes glycolysis in cancer cells. *Journal of Biological Chemistry*, *288*(49), 35406–35416. https://doi.org/10.1074/jbc.M113.508226

Zaitseva, I., Zaitsev, V., Card, G., Moshkov, K., Bax, B., Ralph, A., Lindley, P., Zaitseva, I., Zaitsev, V., Card, G., Ralph, A., Lindley, P., Bax, B., & Moshkov, K. (1996). The X-ray structure of human serum ceruloplasmin at 3.1 Å: nature of the copper centres. In *JBIC* (Vol. 1).

Zampino, R., Pisaturo, M. A., Cirillo, G., Marrone, A., Macera, M., Rinaldi, L., Stanzione, M., Durante-Mangoni, E., Gentile, I., Sagnelli, E., Signoriello, G., del Giudice, E. M., Adinolfi, L. E., & Coppola, N. (2015). Hepatocellular carcinoma in chronic HBV-HCV co-infection is correlated to fibrosis and disease duration. *Annals of Hepatology*, *14*(1), 75–82. https://doi.org/10.1016/s1665-2681(19)30803-8

Zhang, W. J., & Frei, B. (2003). Intracellular metal ion chelators inhibit TNFα-induced SP-1 activation and adhesion molecule expression in human aortic endothelial cells. *Free Radical Biology and Medicine*, *34*(6), 674–682. https://doi.org/10.1016/S0891-5849(02)01375-8

Zhang, X., Wang, Q., Wu, J., Wang, J., Shi, Y., & Liu, M. (2018). Crystal structure of human lysyl oxidase-like 2 (hLOXL2) in a precursor state. *Proceedings of the National Academy of Sciences of the United States of America*, *115*(15), 3828–3833. https://doi.org/10.1073/pnas.1720859115

Zhang, Z., Qiu, L., Lin, C., Yang, H., Fu, H., Li, R., & Kang, Y. J. (2014). Copper-dependent and -independent hypoxia-inducible factor-1 regulation of gene expression. *Metallomics*, *6*(10). https://doi.org/10.1039/c4mt00052h

Zhao, X., Zhao, L., Yang, H., Li, J., Min, X., Yang, F., Liu, J., & Huang, G. (2018). Pyruvate kinase M2 interacts with nuclear sterol regulatory element– binding protein 1a and thereby activates lipogenesis and cell proliferation in hepatocellular carcinoma. *Journal of Biological Chemistry*, *293*(17), 6623–6634. https://doi.org/10.1074/jbc.RA117.000100

Zhu, S., Shanbhag, V., Wang, Y., Lee, J., & Petris, M. (2017). A role for the ATP7A copper transporter in tumorigenesis and cisplatin resistance. *Journal of Cancer*, *8*(11), 1952–1958. https://doi.org/10.7150/jca.19029

Zimmermann, A. (2016). Invasion Patterns and Metastatic Patterns of Hepatocellular Carcinoma. In *Tumors and Tumor-Like Lesions of the Hepatobiliary Tract* (pp. 1–29). Springer International Publishing. https://doi.org/10.1007/978-3-319-26587-2_4-1

Zimnicka, A. M., Tang, H., Guo, Q., Kuhr, F. K., Oh, M. J., Wan, J., Chen, J., Smith, K. A., Fraidenburg, D. R., Choudhury, M. S. R., Levitan, I., Machado, R. F., Kaplan, J.

H., & Yuan, J. X. J. (2014). Upregulated copper transporters in hypoxia-induced pulmonary hypertension. *PLoS ONE*, *9*(3). https://doi.org/10.1371/journal.pone.0090544